Delft University of Technology

Formic acid-driven biocatalytic oxyfunctionalisation: The alchemy of ants, mushrooms and air

Willot, Sébastien

Important note
To cite this publication, please use the final published version (if applicable).
Please check the document version above.

Formic acid-driven biocatalytic oxyfunctionalisation: The alchemy of ants, mushrooms and air

Dissertation

for the purpose of obtaining the degree of doctor

at Delft University of Technology

by the authority of the Rector Magnificus, Prof.dr.ir. T.H.J.J. van der Hagen,

chair of the Board for Doctorates

to be defended publicly on

Wednesday 10th of June 2020 at 10:00 o'clock

By

Sébastien Jean-Paul WILLOT

Ingénieur diplômé de l'Ecole Nationale Supérieure de Chimie de Mulhouse, Université de Haute Alsace, France

Born in Mulhouse, France

This dissertation has been approved by the promotors.

Composition of the doctoral committee:

Rector Magnificus,	chairperson
Prof. dr. F. Hollmann	Delft University of Technology, promotor
Prof. dr. I.W.C.E. Arends	Utrecht University, promotor
Dr. C.E. Paul	Delft University of Technology, copromotor

Independent members:

Prof. dr. U. Hanefeld	Delft University of Technology
Prof. dr. A. Liese	Hamburg University of Technology, Germany
Prof. dr. M. Hofrichter	Dresden University of Technology, Germany
Dr. O. Thum	Evonik Industries AG, Germany
Prof. dr. W. Hagen	Delft University of Technology, reserve member

Table of Contents

SUMMARY

Summary

Selective oxyfunctionalisation of inert C-H bonds is an important but challenging transformation in organic synthesis. Enzymes excel in incorporating an oxygen atom into organic molecules selectively. The well described P450 monooxygenases in particular are extremely active thanks to their iron heme cofactor that can selectively oxidise non activated C-H bonds. These enzymes rely on a complex redox system, whereas peroxygenases utilise only peroxide as oxidant and therefore arise as a better alternative for synthetic chemistry. However, in presence of high concentration of peroxide, the heme cofactor is going through a self-destruction. An *in situ* generation system is consequently needed to mildly provide the peroxide to the enzyme for performing the catalysis efficiently. All systems are based on the reduction of O_2. They all have their own advantages and drawbacks, but have in common the use of rather complex molecules as reductant. The aim of this thesis was to apply formate as an atom efficient reductant for H_2O_2-dependent enzymes, peroxizymes. The overall system is then the oxyfunctionalisation of molecules using only formate and O_2 as reactant.

In chapter 2 we explore a simple, small molecule based method to transform a P450 monooxygenase into P450 peroxygenase. These small molecules, called also 'decoy molecules', facilitate the shunt pathway of P450 monooxygenases principally enabling simple, H_2O_2-driven reactions thereby circumventing the complicated natural electron transport chain of P450 monooxygenases. Because the P450 portfolio is enormous, a successful strategy for its conversion would lead to a broad substrate scope of our *in situ* system. Applied to the self-sufficient P450 BM-3, the TTN (Total Turn Over Number) of the enzyme could be increased by at least a factor of 2. The overall catalytic activity of the system, however, remained low with generally less than 1000 catalytic cycles of the biocatalyst. Therefore, the focus of the thesis became mainly on the unspecific peroxygenase from *Agrocybe aegerita* (r*Aae*UPO) that can reach times higher TTN 100.

In chapter 3, we proposed a photo-biocatalytic system to drive UPO-hydroxylation with formic acid and molecular oxygen. The system consists of the combination of

Summary

formate dehydrogenase from *Candida boidinii* (*Cb*FDH), NAD$^+$ and photocatalysts (methylene blue, phenosafranin and FMN). *Cb*FDH is catalysing the dehydrogenation of formic acid to CO_2 while reducing NAD$^+$ to NADH. The photocatalysts connect this to r*Aae*UPO with its photoreduction by NADH followed by its spontaneous oxidation by O_2. This system successfully promoted ethylbenzene hydroxylation by r*Aae*UPO. When a mix of photocatalysts is applied, a better use of light could be obtained. However, the photocatalytic systems are harmful for the enzyme itself, affecting the robustness of the system. Photo-produced reactive oxygen species such as singlet oxygen or radicals are most likely responsible for the poor robustness.

For these reasons, in chapter 4, we explored a recently re-studied formate oxidase from *Aspergillus oryzae* (*Ao*FOx), for the direct oxidation of formic acid with reduction of O_2. This enzyme is highly active because of its modified flavin cofactor, 8-formyl-FAD. The resulting r*Aae*UPO/*Ao*FOx enzyme mix was performing outstandingly with a TTN higher than 1,000,000 for *Ao*FOx in some cases. *Ao*FOx coupled with *Ci*VCPO performed well and 1.6 g of product could be isolated while keeping an impressive TTN of 1,500,000 for *Ci*VCPO and 150,000 for *Ao*FOx. The main limitation of the system identified is the pH dependency of formate binding.

While further characterising the *Ao*FOx/r*Aae*UPO system, we realised that *Ao*FOx had promiscuous activity for methanol and formaldehyde oxidation (chapter 5). We therefore wanted to exploit this activity to drive our biocascades. Full oxidation of methanol will lead to 3 equivalents of product per mol of methanol and as a result a high atom efficiency for the total reaction results. However, the poor binding capacity of *Ao*FOx to methanol, K_M in the molar range, is making the single use of *Ao*FOx for the 3 oxidations of MeOH practically unfeasible. This issue is circumvented by including the alcohol oxidase from *Pichia pastoris* *Pp*AOx in the enzyme mix. Up to 2.5 equivalents of (*R*)-1-phenylethanol could be obtained from methanol in this way. This new cascade simplifies a previous system from 6 to 3 components.

Overall, in this thesis, some novel approaches for biocatalytic oxyfunctionalisation have been established. Most promisingly, *Ao*FOx is considered as the catalyst for the future to promote preparatively relevant H_2O_2-dependent reactions.

Samenvatting

Samenvatting

De selectieve oxyfunctionalisatie van inerte C-H verbindingen is een belangrijke maar uitdagende transformatie in de organische synthese. Enzymen zijn zeer geschikt in het selectief incorporeren van een zuurstofatoom in een organisch molecuul. De welbekende P450 monooxygenases laten hoge activiteiten zien voor deze reacties. Dit, dankzij een ijzer heem cofactor die selectief niet-geactiveerde C-H verbindingen kan oxideren. Waar deze enzymen afhankelijk zijn van een complex redox systeem, maken peroxygenases gebruik van enkel peroxide als oxidant, wat hen een beter alternatief maakt voor de synthetische chemie. In aanwezigheid van hoge concentraties peroxide zal de heem cofactor zichzelf echter vernietigen. Daarom is er, om het enzym alsnog efficiënt te kunnen laten werken, een mild *in situ* regeneratiesysteem nodig voor de peroxide. Alle reeds bestaande methoden zijn gebaseerd op de reductie van zuurstof en hebben hun eigen voor- en nadelen. Een gemene deler is echter dat vaak vrij complexe moleculen moeten fungeren als reductant. Het doel van dit proefschrift was dan ook om methaanzuur te gebruiken als een atoom-efficiënte reductant voor H_2O_2 afhankelijke enzymen; de peroxizymen. Het uiteindelijke doel is de oxyfunctionalisatie van moleculen met enkel methaanzuur en zuurstof als reactanten.

In hoofdstuk 2 onderzoeken we een simpele methode, gebaseerd op kleine moleculen, om een P450 monooxygenase te transformeren tot een P450 peroxygenase. Zogenoemde "decoy molecules" maken het voor P450 monooxygenases mogelijk de "shunt pathway" te gebruiken waardoor H_2O_2 als reactant kan worden geaccepteerd. Hiermee kan het complexe natuurlijke elektron transportsysteem voor P450 monooxygenases worden omzeild. Omdat het aantal verschillende beschikbare P450 enorm is, zou deze methode kunnen leiden tot een groter aantal mogelijke substraten voor onze verschillende *in situ* methoden. Toevoeging van deze stof aan een zelfvoorzienende P450 MB-3 vergrootte de TTN (Total Turn Over Number) voor dit enzym met meer dan twee orden van grootte. De katalytische activiteit van het systeem bleef echter laag, met over het algemeen minder dan 1000 katalytische cycli voor de biokatalysator. Vandaar dat dit

Samenvatting

proefschrift zich vanaf dit punt voornamelijk richtte op de non-specifieke peroxygenase van *Agrocybe aegerita* (r*Aae*UPO) welke 100 keer grotere TTN kan behalen.

In hoofdstuk 3 stellen we een foto-biokatalytisch systeem voor UPO-hydroxylaties met methaanzuur en moleculaire zuurstof als reactanten. Het systeem bestaat uit een combinatie van formiaat dehydrogenase van Candida boidinii (*Cb*FDH), NAD^+ en verschillende fotokatalysatoren (methylene blue, phenosafranin en FMN). *Cb*FDH katalyseert de dehydrogenering van methaanzuur tot CO_2 waarbij NAD^+ wordt gereduceerd tot NADH. De fotokatalysator koppelt dit vervolgens aan r*Aae*UPO door middel van fotoreductie door het NADH, gevolgd door spontane oxidatie door O_2. Dit systeem maakte de hydroxylering van ethylbenzeen door rAaeUPO mogelijk. Wanneer een mix van de fotokatalysatoren werd gebruikt kon het licht efficiënter worden gebruikt. De fotokatalytische systemen bleken echter ook schadelijk voor het enzym zelf, wat de stabiliteit van het systeem beïnvloedde. Reactieve zuurstof componenten, zoals singletzuurstof en radicalen die ontstaan gedurende het fotochemische proces, zijn hoogst waarschijnlijk verantwoordelijk voor dit verlies in stabiliteit.

Om deze redenen bestudeerden we in hoofdstuk 4 de recent herbeschreven formiaat oxidase van *Aspergillus oryzae* (*Ao*FOx). Dit enzym katalyseert de directe oxidatie van methaanzuur gevolgd door de reductie van O_2. Dit enzym is zeer actief vanwege een gemodificeerde flavine cofactor, 8-formyl-FAD. De resulterende rAaeUPO/AoFOx enzym mix presteerde uitstekend met in sommige gevallen TTN van meer dan 1,000,000 voor AoFOx. AoFOx kon ook worden gekoppeld aan CiVCPO, waarna 1.6 gram product kon worden geïsoleerd met indrukwekkende TTN van 1,500,000 voor CiVCPO en 150,000 voor AoFOx. Dit systeem werd echter gelimiteerd door een afhankelijkheid van de pH van de oplossing, wat voortkwam uit de binding tussen het formiaat en het enzym.

Terwijl we het AoFOx/rAaeUPO systeem karakteriseerden realiseerden wij ons dat AoFOx promiscue activiteit had voor methanol en formaldehyde oxidatie (hoofdstuk 5). Deze activiteit wilden wij gebruiken voor onze cascade. Volledige oxidatie van

methanol leidt tot drie productequivalenten per mol methanol wat zal resulteren in een hogere atoomefficiëntie voor de totale reactie. Echter, door de lage affiniteit van AoFOx voor methanol, met een Km in de orde van een molair voor het substraat, zal de toepassing van AoFOx op zichzelf niet voldoende zijn om de methanol drie keer te oxideren. Deze kwestie werd verholpen doormiddel van toevoeging van de alcohol oxidase van *Pichia pastoris*, *Pp*AOx, aan het enzym mengsel. Omzettingen tot aan 2.5 equivalenten van (*R*)-1-phenylethanol ten opzichte van methanol konden op deze manier worden bereikt. Deze nieuwe cascade versimpelt een vorig systeem door het aantal gebruikte componenten te verlagen van zes naar drie.

Resumerend worden er verschillende nieuwe benaderingen voor biokatalytische oxyfunctionalisaties voorgesteld in dit proefschrift. AoFOx is hierin het meest veelbelovend als de katalysator voor de toekomst in de preparatieve bereiding van relevante H_2O_2-afhankelijke reacties.

Chapter 1. Introduction

Chapter 1. Introduction

1.1. Context

From plastics to fertilizers, chemistry holds a strong place in our life.[1] Our current living standard is highly dependent on the chemicals produced by industries. One clear example is the consumption of drugs on which modern medicine is mostly based. However, the state-of-the art industrial chemistry does not meet our current need: sustainability. Too many chemical productions are relying on processes that are not sustainable: energy demanding, fossil-based, creating waste, and using harmful materials. With challenges such as climate change and fossil energy depletion, solutions have to be found and applied to replace these processes.[2-4]

The concept of "green chemistry"/sustainable chemistry started in the late 80's.[5] R. Sheldon was one of its pioneers and introduced the concept of E-factor, which gives an order of magnitude of generated waste.[6] In the 90's, Anastas and Warner introduced the 12 principles of green chemistry as a guideline for sustainable chemistry.[7] From that moment on, the concept of sustainability in chemistry has been constantly growing.

The field of catalysis is an indispensable tool for sustainable chemistry, complying with the 12 principles of green chemistry.[8] In short, a catalyst is a compound that lowers the energy barrier of a targeted reaction, introducing selectivity. The catalyst is not consumed by the reaction but is regenerated through a catalytic cycle. Catalysis will accelerate reactions only when thermodynamically feasible. Because of the energy requirement, reactions generally occur under milder conditions (**Table 1**). The hydrolysis of cellulose into glucose, which is a valuable renewable feedstock, is a perfect example. In order to decompose cellulose without a catalyst, temperatures as high as 400 °C are required. At this temperature however, the formed glucose decomposes as well, and yield of the reaction is lower than 40%. By applying sulfuric acid as catalyst, the temperature can be lowered to 180 °C and the yield in glucose increases. With a solid acid such as amorphous functionalized carbon, the reaction occurs at even lower temperatures. Finally, by applying cellulase as enzymatic catalyst, the reaction occurs at very mild temperature (40 °C)

and the glucose yield goes up to 95%. Catalysis holds a strong place in chemistry, especially where lower energy barrier and selectivity is needed such as oxidation.

Table 1. Temperature and yield of cellulose hydrolysis to glucose with and without catalyst [9]

Catalyst	Temperature °C	Yield of glucose	Reference
None	250-400	<40	[10]
H_2SO_4	100-180	65	[10, 11]
Sulfonated carbon (amorphous)	110	64	[12]
Cellulase	40-125	75-95	[10, 13]

1.2. Oxidation and oxyfunctionalisation

One of the most challenging chemical transformations where there is a high need for better and more sustainable solutions is selective oxidation.[14-17] Non-selective reactions lead to the creation of waste and side products. As a result, atom efficiencies are low, and complex and costly downstream processes are required to isolate the product stream.

For oxidation, the use of molecular oxygen from air as the oxidant is the most convenient. Nevertheless, the reaction of the triplet ground state of molecular oxygen is spin forbidden with singlet organic molecules and thus its activation energy is very high.[18]

Different routes exist to circumvent this energy barrier. A singlet molecule can react with triplet oxygen to form two doublets (free radicals), which is a spin allowed reaction. In nature, reduced flavins perform this reaction through high delocalization of electrons.[19]

Singlet oxygen, an excited form of oxygen, can also react with organic molecules.[20-22] Quenching of a photoexcited compound by triplet oxygen can be used to produce it.[23, 24] Disproportionation of peroxide can also lead to singlet oxygen.[25]

Chapter 1. Introduction

Another possibility is through the reaction of oxygen *via* a paramagnetic metal to form a superoxometal complex to activate the oxygen. Iron,[26, 27] manganese,[28, 29] and ruthenium[30, 31] form oxo species. Osmium and ruthenium can form dioxo species.[32-34] In this case, other oxygen donors such as peroxide can be applied to form oxo species.[17, 35] In this thesis, molecular oxygen and hydrogen peroxide were the oxygen donors of choice.

One important aspect in metal oxidation catalysis is the design of the ligand.[36, 37] Firstly, the energy of the catalyst can be tuned. Secondly, chirality can be induced by bulky and complex ligands. Complexity of catalyst design results in complex synthesis pathway. This leads to expensive and laborious production processes. Nature's way is to use enzymes instead as highly performing and selective catalysts that contain these paramagnetic metals in their active site.

1.3. Biocatalysis

The field of biocatalysis consists of the application of enzymes, proteins, to catalyse reactions.[38, 39] Thanks to their long sequence of inherently chiral amino acids, enzymes hold a complex 3D structure. This complex scaffold then induces selectivity by steric effects.[38] This is often over-simplified as the rule of key and lock, postulated by Fischer.[40] This rule has been later expanded with the induced-fit theory that considers conformation changes during the catalysis.[41] Enzymes are classified and mostly named according to the type of reaction they catalyse. For instance, monooxygenases catalyse the insertion of a single oxygen atom into a molecule.

Enzymes are not only extremely catalytically active but also highly selective. Low catalyst loading is able to perform the reaction. For example, the unspecific peroxygenase (UPO, discussed later) enzyme amount applied to reactions is typically lower than 0.01 %(mol mol^{-1}).[42-44] Catalysis occurs thanks to the amino acids themselves or a cofactor such as a metal ion or complex.

Synthetic chemistry applying enzymes as catalysts has been feasible, because suitable enzymes are now becoming readily available. Moreover, they can be modified *via* mutation for substrate specificity and produced efficiently.[45]

In the laboratory, genetically modified host organisms are commonly used to produce these biocatalysts.[46] In principle, the host acts as a computer that will read an expression vector, the code, and will produced the enzyme(s) accordingly. During this thesis, two different organisms where used to produce the enzymes: the bacterium *Escherichia coli* (*E. coli*) and the yeast *Pichia pastoris* (*P. pastoris*). In this case, so-called recombinant DNA is introduced to the host organism through a transformation. The gene, encoding for the enzyme, inserted into the host plasmid, will be expressed.

Typically, specific antibiotic resistance is displayed thanks to a so-called marker coded in the plasmid. Broth supplemented with the corresponding antibiotic will thus ensure that only the GMO will grow and survive. The promotor, which initiates the transcription of the gene, is often induced by an external small molecule. In the case of *P. pastoris*, the promotor is alcohol oxidase 1 (AOX1), an enzyme part of the metabolism of *P. pastoris*.[47, 48] By switching the carbon source from glycerol to methanol, the need of AOX1 will increase. Therefore, the transcription of it will increase as for the DNA for the aimed protein attached to it within the expression vector.

Enzymes can be extra-cellularly secreted, as is the case for the recombinant rationally evolved unspecific peroxygenase from *Agrocybe aegerita* (r*Aae*UPO) produced by *P. pastoris*.[49] Alternatively, when it remains within the organism, as in the case for the formate oxidase from *Aspergillus oryzae* (*Ao*FOx) produced by *E. coli*,[50, 51] the cells need to be disrupted to release the enzyme in free solution. Further purification steps can be performed if high purity of the catalyst is required. In chapters 3 and 4, *Ao*FOx is used for its capacity to produce hydrogen peroxide. Its purification is needed to remove catalase activity, i.e. peroxide dismutation.[50]

1.3.1. Biocatalytic oxidation

Enzymes that catalyse oxidation reactions are part of the class I, oxidoreductases.[39] They can be further divided into different groups given in **Table 2**. In this thesis, at least one enzyme of every class has been used. A rather large part of oxidoreductases relies on nicotinamide cofactor (NAD(P)$^+$) as the primary redox

partner. Oxidases are an interesting class of enzymes that only rely on molecular oxygen to perform dehydrogenation of organic compounds. The catalytic origin of these enzymes varies but metals and flavins predominate.

Table 2. Simplified representation of the different classes of oxidoreductases

Dehydrogenase	Substrate-H_2 + NAD(P)$^+$ $\longrightarrow$ Substrate + NAD(P)H + H$^+$
Oxidase	Substrate-H_2 + O_2 $\longrightarrow$ Substrate + H_2O_2
Oxygenase	Substrate + NAD(P)H + O_2 + H$^+$ $\longrightarrow$ Substrate-O + NAD(P)$^+$ + H_2O
Peroxidase	Substrate-H_2 + O_2 $\longrightarrow$ Substrate + 2 H_2O Substrate + O_2 $\longrightarrow$ Substrate-O + H_2O

1.3.2. P450 monooxygenases

Oxygenases are enzymes that catalyse oxyfunctionalisations. Different redox-active cofactors can be found: heme-iron,[52] non-heme iron,[53-55] flavin[56] and copper.[57] As for all oxygenases, P450 monooxygenases catalyse the introduction of an oxygen atom from molecular oxygen into a molecule.[58-60] These enzymes rely on a highly oxidised iron IV complex, called compound I, to perform the reaction. Regioselectivity is possible here only thanks to the protein scaffold. These enzymes catalyse the selective oxidation of stable bonds, such as aliphatic sp^3 C-H bonds.[61] Moreover, hundreds of variations in nature have been described, making these enzymes' portfolio tremendous. For these reasons P450s have been widely studied, modified and applied for organic synthesis.[58, 61-63]

To activate the oxygen, reduction of the heme is first necessary prior to oxygen attack that forms compound I. However, P450s rely on a complex electron transport chain to reduce the heme.[64, 65] Molecular oxygen, needed for the reaction, can pull the electrons out at every step (**Figure 1**). These uncoupling reactions lead to the waste of the primary reductant.[65]

For this reason unspecific peroxygenases have grown recently as an alternative to P450 monooxygenases for *in vitro* biocatalysis.[43] These enzymes form the same

compound I and rely efficiently on hydrogen peroxide as the oxygen donor (**Figure 1**).[66]
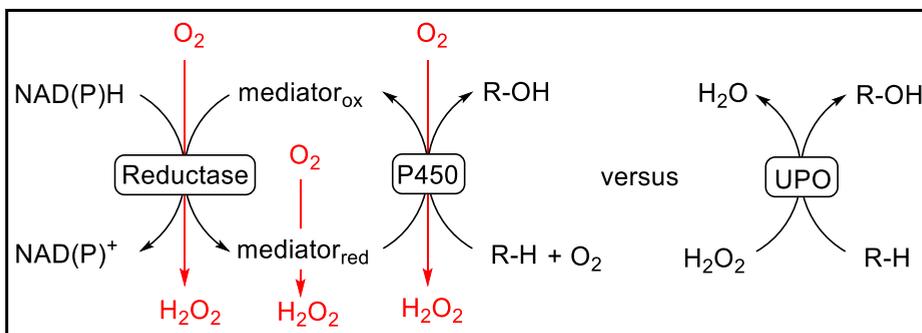
Figure 1. Oxidation by P450 (uncoupling reactions) versus UPO

1.4. Unspecific peroxygenases

1.4.1. Mechanism

Several enzymes, such as P450 monooxygenases and chloroperoxidases, have been reported to be able to use peroxide as the oxygen donor to perform similar reactions.[67, 68] However, the peroxygenase from *Agrocybe Aegerita* (*Aae*UPO) was one of the first reported to perform catalysis with high activity and stability. As said previously, less than 0.01% (mol mol^{-1}) of the enzyme is needed for reaction. Compound I can be formed from H_2O_2 because of a glutamate residue lying above the heme (**Figure 2**).[66] This glutamate deprotonates hydrogen peroxide that lies upon the heme. This first step facilitates the formation a double Fe-O bond while the O-O bond is broken to create a H-O bond and leads to the formation a water molecule.
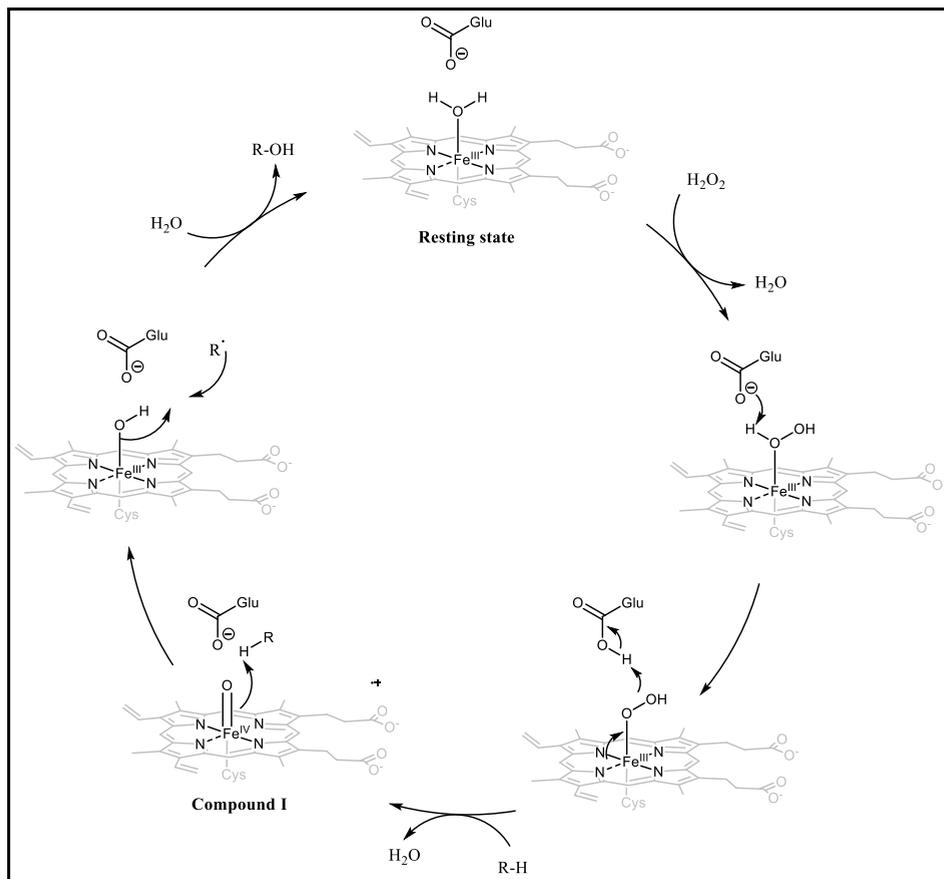
Figure 2. Simplified UPO-hydroxylation mechanism[66]

From compound I, peroxygenases can perform different types of reactions, hence their name "unspecific". For instance, *Aae*UPO catalyses radical formation under acidic conditions and oxyfunctionalisation (hydroxylation, epoxidation) under pH neutral conditions.[69] In a third case, in presence of chloride, UPO can catalyse chlorination.[70] In this thesis, we are interested in the oxyfunctionalisation of organic molecules by UPO. A description of different types of oxidation this enzyme catalyses is reported below.

1.4.2.   UPO-catalysed reactions

1.4.2.1. *sp*^{3} C-H-bonds hydroxylation

Hydroxylation of *sp*^{3} C-H bond is the most interesting reaction to perform with UPO (**Figure 3**).[71-75] Obtaining chemoselectivity is challenging due to difficult distinction between *sp*^{3} C-H bonds within a molecule. Another challenge is the over-oxidation of the product by the enzyme. The aliphatic compounds and the corresponding alcohol are often both substrates of UPO, if the concentration of the hydroxyproduct is too high, over-oxidation happens. For this reason, 100% yield is rarely obtained with UPO.
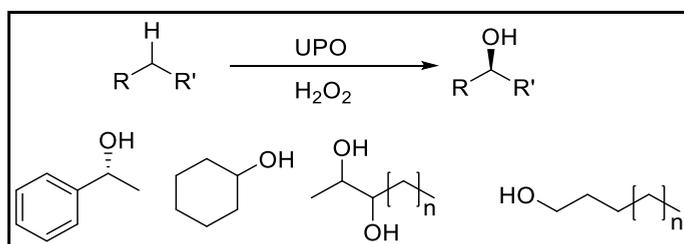
Figure 3. UPO-catalysed C-H bonds hydroxylation[71-75]

1.4.2.2. Epoxidation

UPO can also be applied to produce epoxides (**Figure 4**).[76, 77] Unfortunately, the reported reactions so far suffer from poor enantioselectivity. For instance, styrene oxide is produced as a racemate whereas *cis*-β-methylstyrene is one of the few examples with selectivity. These reactions are highly interesting for application. Propylene oxide is a building block for polyurethane and propylene carbonate. When *cis*-β-methylstyrene oxide is ring opened with a methylamine, pseudoephedrine can be synthesised. One side reaction that might occur here is oxidative cleavage of the epoxide by UPO.
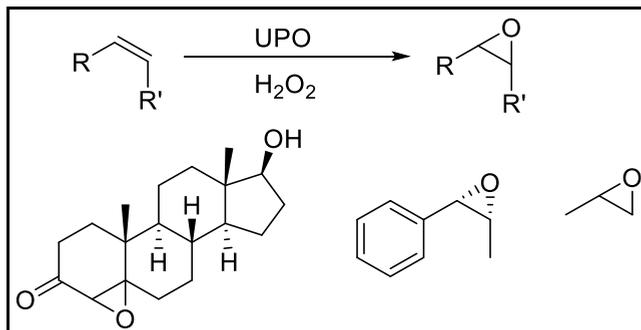
Figure 4. UPO-catalysed epoxidation[76, 77]

1.4.2.3. Sulfoxidation

UPOs are able to oxidise sulfide to form the corresponding sulfoxide (**Figure 5**),[78-85] without over-oxidation to sulfone. So far, only a few examples are available, thioanisole being the model substrate applied.
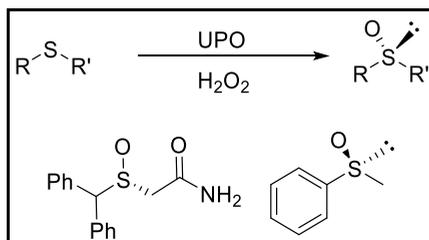
Figure 5. UPO-catalysed sulfoxidation[78-85]

1.4.2.4. Aromatic hydroxylation

Aromatic hydroxylation by UPO is possible and has been reported to occur in two steps.[86-90] First, an epoxide is formed on the aromatic ring. This arene oxide is highly unstable and will rearrange to reform the electronic delocalisation, forming an alcohol (**Figure 6**).
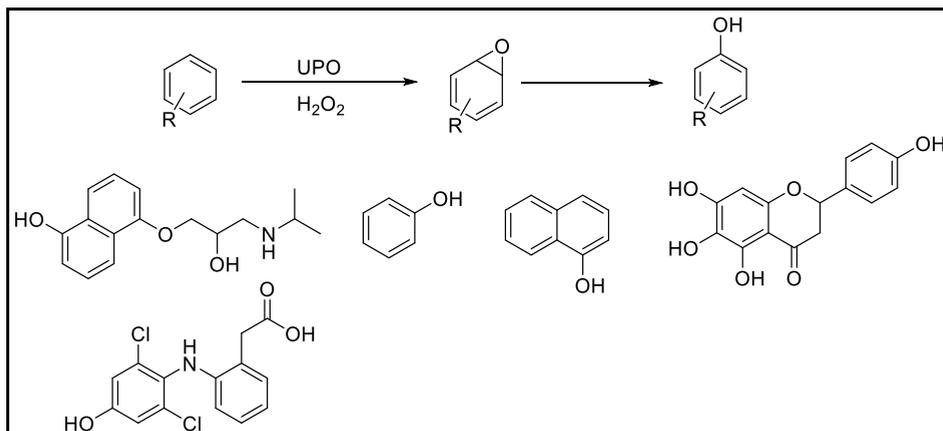
Figure 6. UPO-catalysed epoxidation/hydroxylation of aromatic compounds[85-90]

1.4.3.   UPO inactivation

In addition to these reactions, peroxide might be depleted into molecular oxygen by UPO (catalase activity).[91] Within this catalytic cycle, a malfunction may happen in presence of high concentration of peroxide (**Figure 7**). A multiple oxidative attack may lead to a putative compound III.[91, 92] This compound III further leads to the formation of a hydroxyl radical in a Haber-Weiss reaction. This highly reactive radical can oxidise a carbon atom on the porphyrin rings. This results in the formation of α-meso-hydroxy-heme that further leads to heme-bleaching and by consequence definite inactivation of the enzyme.[93] To avoid inactivation of UPO, the peroxide concentration should be kept at a suitable level for fast catalysis and low inactivation.[94]
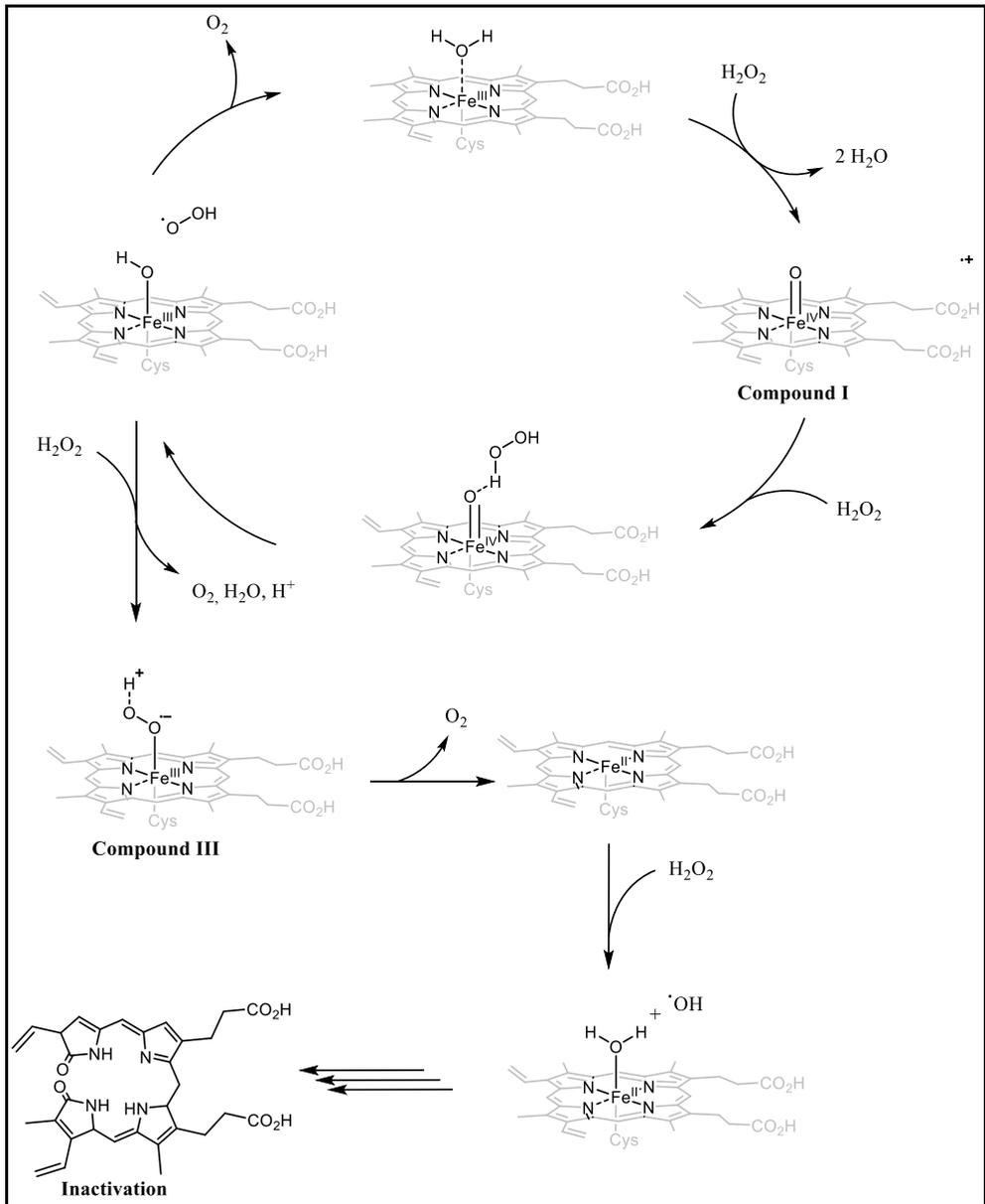
Figure 7. UPO inactivation mechanism within catalase activity[91, 92, 94]

1.5. *In situ* H_2O_2 generation systems

Table 3. Examples of *in situ* generation of H_2O_2

Cosubstrate	Coproduct	Catalyst(s)	reference
Glucose	D-glucono-δ-lactone	GOx	[95]
MeOH	CO_2	AOx/FDM/FDH/3HB6H/NAD	[44]
Alanine	Ammonium pyruvate	AAOx	[96]
choline chloride	Betaine hydrochloride	ChOx	[97]
formic acid	CO_2	FDH/NAD/YqjM	[42]
-	-	Cathode	[98-102]
H_2	-	Pd	[103]
photochemical			
EDTA	EDtriA/H_2CO/CO_2	Flavin	[104-106]
H_2O	-	Flavin-modified cathode	[107]
MeOH	CO_2	Au-TiO_2	[108]
H_2O	-	Au-TiO_2	[109]
MES	n.d.	Flavin	[110]
Methanol	CO_2	g-C_3N_4	[111]

As mentioned above, H_2O_2 needs to be slowly provided to UPO to avoid oxidative inactivation. One direct method consists of slowly feeding the reaction with a peroxide solution. This solution comes with two issues: dilution of the system and hot spots. Dilution might lead to lower enzymatic activity and the need of dealing with a higher volume during the process. Moreover, hot spots, i.e. localised high concentrations of peroxides, will still happen, leading to local enzyme inactivation.

Therefore, *in situ* generation of H_2O_2 is the most suitable solution for a mild homogeneous provision of the oxidant. All the reported systems are based on the reduction of molecular oxygen, coming from air. These systems can be biocatalytic, photocatalytic, electrochemical or a combination of them (**Table 3**). For clarity, we

will only describe the systems probed during this thesis: photo- and biocatalytic generation system of H_2O_2.

1.5.1. Photochemical generation of H_2O_2

In the last years, a wide range of photocatalytic systems to drive biocatalysis has been reported.[104-106, 108, 109, 111] All of them are based on a photocatalyst being excited by visible and/or near UV light. The photocatalyst state can vary from heterogeneous like metal nanoparticles or homogeneous like flavins. In both cases, the starting principle is similar. In this thesis, we have focused on the application of easily available flavins and alloxazine derivatives.[112]

In this case the photocatalyst absorbs one photon transferring one electron from the highest occupied molecular orbital (HOMO) to the lowest unoccupied molecular orbital (LUMO). With this electron the molecule resides in a higher energy state and the reduction of the photocatalyst by a weak reductant becomes possible. This reduced photocatalyst is spontaneously oxidised by molecular oxygen to produce hydrogen peroxide. The advantage of photocatalysis is the use of (sun)light as the driving force of the reaction, leading to a very energy sustainable system.

1.5.2. Enzymatic generation of H_2O_2

Enzymatic generation systems are preferred to delivering peroxide to peroxidases. Reaction conditions are more likely to be compatible between two enzymatic systems. Moreover, selectivity of the enzymes will minimize the occurrence of side reactions by the H_2O_2 generation system like over-oxidation. The co-expression of the enzymes in the same organism is also possible to lower the price of biocatalyst production and to open the possible use of whole cell catalyst that can further lower the price.[113, 114] The application of whole cell catalysis also avoids the use of an expensive extraction and/or purification process.

Among all H_2O_2 generation systems, the "golden standard" is glucose/glucose oxidase (GOx). GOx catalyses the oxidation of glucose to gluconolactone through the reduction of O_2.[95] The robustness of the system and the cheap cosubstrate are two valuable points for its application. A sugar environment is also usually beneficial

for stability of the enzyme.[115, 116] GOx has been discovered in 1928 and since then has been used for different applications: sensors, additives, etc.[95] Because of its use on industrial scale, GOx has the advantage of a low price.

Nevertheless, the use of the glucose/GOx system for chemical has its limitations. Glucose is a viscous aqueous miscible liquid and high loadings lead to high viscosity. The mixture will be difficult to handle, demanding high energy consumption for stirring. Moreover, one mole of peroxide requires one mole of glucose. The atom efficiency of the system is first rather low. Thus, the side product formation will be significant, resulting in a demanding downstream process and a high E factor.

1.5.3. Formic acid as sacrificial reductant for in situ H_2O_2 formation

One of the aims of the thesis is to established an *in situ* H_2O_2-generation system that uses formic acid (formate) as a suitable sacrificial reductant. Formic acid can be produced by oxidation of biomass,[117, 118] or CO_2 fixation.[119] Moreover, with technologies such as the formic acid based battery,[120-122] the need for, and thus availability of, sustainable formic acid will increase in the future.

The oxidation of formic acid by O_2 leads to carbon dioxide and H_2O_2 formation. The atom efficiency of this system is then higher compared to the GOx/glucose system. Only electrochemical and H_2/Pd systems show better atom efficiency. Nevertheless, these methods greatly suffer from diffusion limitations and difficult handling respectively. In our case, CO_2 will diffuse out of the reaction mixture, which simplifies the downstream processing. A small part will be in solution as carbonate which can be separated easily from the organic product(s). Moreover, the goal of this thesis is not only to prove the feasibility but also the viability of the system. In other words, the catalytic performances will have to be outstanding when compared with previous reported systems.[44]

1.6. Goal of the thesis

The overall idea of this thesis is to develop a new biocatalytic system to provide H_2O_2 from the reduction of molecular oxygen by formic acid (or formate). The primary targeted enzyme is UPO that needs mild continuous provision of peroxide to perform

its reactions in a robust way. In addition, UPO is not the only H_2O_2-dependent enzyme. Our formic acid system can be coupled to other enzymes even if in principle, *in situ* generation of peroxide is not highly needed. For instance, the vanadium dependent chloroperoxidase from *Curvularia inaequalis* outstandingly produces hypohalites from halides and hydrogen peroxide.[123] These hypohalites can react in different manners with organic compounds and for instance form halohydrin from C=C double bonds. However, if concentrations are too high, singlet oxygen can be formed from peroxides and hypohalites.[124] More than wasting the primary oxidant, this singlet oxygen might react with other components of the reaction.

By combining the *in situ* peroxide formation with H_2O_2-dependent enzymes, the oxidation of organic compounds can be performed with molecular oxygen and formic acid. By changing the H_2O_2-dependent enzyme, a wide range of oxidations will be accessible from formic acid and molecular oxygen (**Figure 8**).

During this thesis, we will first explore a newly proposed non-evolutionary strategy[125] to enhance peroxide shunt pathway of P450 monooxygenase (Chapter 2). By applying this strategy, the enzyme scope of the thesis could be highly increased. Two different biocatalytic systems will be then studied to produce H_2O_2 and coupled to peroxizymes (Chapter 3 and 4). Finally, the scope of the sacrificial reductant will be broadened to methanol and formaldehyde (Chapter 5).
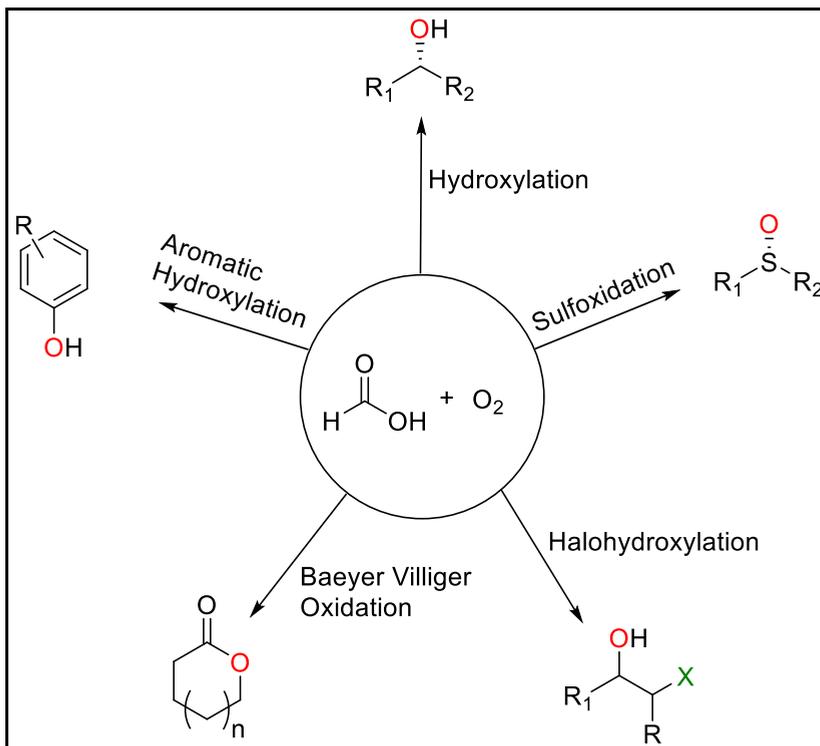
Figure 1. The goal of this thesis: Formic acid and molecular oxygen to drive (bio)oxidation reactions

Chapter 1. Introduction

1.7. References

1.   Andrady, A. L.; Neal, M. A., *Philos. Trans. R. Soc. B* **2009,** *364* (1526), 1977-1984.
2.   de Marco, B. A.; Rechelo, B. S.; Totoli, E. G.; Kogawa, A. C.; Salgado, H. R. N., *Saudi Pharm. J.* **2019,** *27* (1), 1-8.
3.   Sheldon, R. A., *Green Chem.* **2017,** *19* (1), 18-43.
4.   Sheldon, R. A., *ACS Sustain. Chem. Eng.* **2018,** *6* (1), 32-48.
5.   Linthorst, J. A., *Foundations of Chemistry* **2010,** *12* (1), 55-68.
6.   Sheldon, R. A., *Chem Ind-London* **1992,** (23), 903-906.
7.   Anastas, P. T.; Warner, J. C., Green Chemistry: Theory and Practice. Oxford University Press, Oxford: Oxford, 1998.
8.   Anastas, P. T.; Kirchhoff, M. M.; Williamson, T. C., *Appl. Catal. A.* **2001,** *221* (1-2), 3-13.
9.   Delidovich, I.; Palkovits, R., *Green Chem.* **2016,** *18* (3), 590-593.
10.   Yu, Y.; Lou, X.; Wu, H. W., *Energy Fuel* **2008,** *22* (1), 46-60.
11.   Negahdar, L.; Delidovich, I.; Palkovits, R., *Appl. Catal., B* **2016,** *184*, 285-298.
12.   Suganuma, S.; Nakajima, K.; Kitano, M.; Yamaguchi, D.; Kato, H.; Hayashi, S.; Hara, M., *J. Am. Chem. Soc.* **2008,** *130* (38), 12787-12793.
13.   Zhang, S.; Wolfgang, D. E.; Wilson, D. B., *Biotechnol. Bioeng.* **1999,** *66* (1), 35-41.
14.   Newhouse, T.; Baran, P. S., *Angew. Chem. Int. Edit.* **2011,** *50* (15), 3362-3374.
15.   White, M. C., *Science* **2012,** *335* (6070), 807-809.
16.   Reetz, M. T., *J. Am. Chem. Soc.* **2013,** *135* (34), 12480-12496.
17.   Sheldon, R. A.; Arends, I.; Hanefeld, U., *Green chemistry and catalysis.* John Wiley & Sons: 2007.
18.   Sawyer, D. T., *Oxygen chemistry.* Oxford University Press: New York, 1991; Vol. 26.
19.   Romero, E.; Gómez Castellanos, J. R.; Gadda, G.; Fraaije, M. W.; Mattevi, A., *Chem. Rev.* **2018,** *118* (4), 1742-1769.
20.   Flors, C.; Griesbeck, A. G.; Vassilikogiannakis, G., *Chemphotochem* **2018,** *2* (7), 510-511.
21.   Margaros, L.; Montagnon, T.; Tofi, M.; Pavlakos, E.; Vassilikogiannakis, G., *Tetrahedron* **2006,** *62* (22), 5308-5317.
22.   Punjabi, P. B.; Kabra, B. V.; Pitliya, R. L.; Vaidya, V. K.; Ameta, S. C., *J. Indian Chem. Soc.* **2001,** *78* (4), 175-184.
23.   Cote, C. D.; Schneider, S. R.; Lyu, M.; Gao, S.; Gan, L.; Holod, A. J.; Chou, T. H. H.; Styler, S. A., *Environ. Sci. Tech. Let.* **2018,** *5* (2), 92-97.
24.   Schweitzer, C.; Mehrdad, Z.; Noll, A.; Grabner, E.-W.; Schmidt, R., *J. Phys. Chem. A* **2003,** *107* (13), 2192-2198.
25.   Boehme, K.; Brauer, H. D., *Inorg. Chem.* **1992,** *31* (16), 3468-3471.
26.   Costas, M.; Mehn, M. P.; Jensen, M. P.; Que, L., *Chem. Rev.* **2004,** *104* (2), 939-986.
27.   Tshuva, E. Y.; Lippard, S. J., *Chem. Rev.* **2004,** *104* (2), 987-1011.

28.   Collins, T. J.; Gordonwylie, S. W., *J. Am. Chem. Soc.* **1989,** *111* (12), 4511-4513.

29.   Hill, C. L.; Brown, R. B., *J. Am. Chem. Soc.* **1986,** *108* (3), 536-538.

30.   Arends, I.; Kodama, T.; Sheldon, R., Oxidation using ruthenium catalysts. In *Ruthenium Catalysts and Fine Chemistry*, Springer: 2004; pp 277-320.

31.   Groves, J. T.; Bonchio, M.; Carofiglio, T.; Shalyaev, K., *J. Am. Chem. Soc.* **1996,** *118* (37), 8961-8962.

32.   Griffith, W. P., *Chem. Soc. Rev.* **1992,** *21* (3), 179-185.

33.   Ruthenium-Catalyzed Oxidation of Alkenes, Alcohols, Amines, Amides, β-Lactams, Phenols, and Hydrocarbons. In *Modern Oxidation Methods*, Wiley-VCH: pp 165-191.

34.   Schroder, M., *Chem. Rev.* **1980,** *80* (2), 187-213.

35.   Sheldon, R.; Cornils, B.; Herrmann, W., *Wiley-VCH Verlag GmbH, Weinheim* **2002,** *1*, 412-427.

36.   Kim, H.; Gerosa, G.; Aronow, J.; Kasaplar, P.; Ouyang, J.; Lingnau, J. B.; Guerry, P.; Farès, C.; List, B., *Nat. Commun.* **2019,** *10* (1), 770.

37.   Liao, S. H.; Coric, I.; Wang, Q. G.; List, B., *J. Am. Chem. Soc.* **2012,** *134* (26), 10765-10768.

38.   Illanes, A., *Principles and Applications. Editorial Springer-Verlag New York Inc., United States* **2008**.

39.   Faber, K., *Biotransformations in organic chemistry*. Springer: 2018; Vol. 5.

40.   Fischer, E., *Berichte der deutschen chemischen Gesellschaft* **1894,** *27* (3), 2985-2993.

41.   Fersht, A., *Structure and Mechanism in Protein Science*.

42.   Pesic, M.; Willot, S. J.; Fernandez-Fueyo, E.; Tieves, F.; Alcalde, M.; Hollmann, F., *Z. Naturforsch. C* **2019,** *74* (3-4), 101-104.

43.   Wang, Y.; Lan, D.; Durrani, R.; Hollmann, F., *Curr. Opin. Chem. Biol.* **2017,** *37*, 1-9.

44.   Ni, Y.; Fernandez-Fueyo, E.; Baraibar, A. G.; Ullrich, R.; Hofrichter, M.; Yanase, H.; Alcalde, M.; van Berkel, W. J. H.; Hollmann, F., *Angew. Chem. Int. Edit.* **2016,** *55* (2), 798-801.

45.   Bornscheuer, U. T.; Huisman, G. W.; Kazlauskas, R. J.; Lutz, S.; Moore, J. C.; Robins, K., *Nature* **2012,** *485* (7397), 185-194.

46.   Berg, J. M.; Tymoczko, J. L.; Stryer, L., *Biochemistry, Fifth Edition*. W.H. Freeman: 2002.

47.   Yang, J.; Cai, H.; Liu, J.; Zeng, M.; Chen, J.; Cheng, Q.; Zhang, L., *Sci. Rep.* **2018,** *8* (1), 1401.

48.   Portela, R. M. C.; Vogl, T.; Ebner, K.; Oliveira, R.; Glieder, A., *Biotechnol. J.* **2018,** *13* (3), 1700340.

49.   Molina-Espeja, P.; Ma, S.; Mate, D. M.; Ludwig, R.; Alcalde, M., *Enz. Microb. Tech.* **2015,** *73-74*, 29-33.

50.   Tieves, F.; Willot, S. J. P.; van Schie, M. M. C. H.; Rauch, M. C. R.; Younes, S. H. H.; Zhang, W. Y.; Dong, J. J.; de Santos, P. G.; Robbins, J. M.; Bommarius, B.; Alcalde, M.; Bommarius, A. S.; Hollmann, F., *Angew. Chem. Int. Edit.* **2019,** *58* (23), 7873-7877.

51.   Robbins, J. M.; Bommarius, A. S.; Gadda, G., *Arch. Biochem. Biophys.* **2018,** *643*, 24-31.

52.   Sligar, S. G.; Makris, T. M.; Denisov, I. G., *Biochem. Biophys. Res. Commun.* **2005,** *338* (1), 346-354.

53.   Kal, S.; Que, L., *Angew. Chem. Int. Edit.* **2019,** *58* (25), 8484-8488.

54.   Murray, L. J.; Garcia-Serres, R.; McCormick, M. S.; Davydov, R.; Naik, S. G.; Kim, S. H.; Hoffman, B. M.; Huynh, B. H.; Lippard, S. J., *Biochemistry* **2007,** *46* (51), 14795-14809.

55.   Foster, T. L.; Caradonna, J. P., *J. Am. Chem. Soc.* **2003,** *125* (13), 3678-3679.

56.   Eswaramoorthy, S.; Bonanno, J. B.; Burley, S. K.; Swaminathan, S., *Proc. Natl. Acad. Sci.* **2006,** *103* (26), 9832-9837.

57.   Ross, M. O.; MacMillan, F.; Wang, J. Z.; Nisthal, A.; Lawton, T. J.; Olafson, B. D.; Mayo, S. L.; Rosenzweig, A. C.; Hoffman, B. M., *Science* **2019,** *364* (6440), 566-+.

58.   Urlacher, V. B.; Girhard, M., *Trends Biotechnol.* **2012,** *30* (1), 26-36.

59.   Meunier, B.; de Visser, S. P.; Shaik, S., *Chem. Rev.* **2004,** *104* (9), 3947-3980.

60.   Denisov, I. G.; Makris, T. M.; Sligar, S. G.; Schlichting, I., *Chem. Rev.* **2005,** *105* (6), 2253-2278.

61.   Roduner, E.; Kaim, W.; Sarkar, B.; Urlacher, V. B.; Pleiss, J.; Glaser, R.; Einicke, W. D.; Sprenger, G. A.; Beifuss, U.; Klemm, E.; Liebner, C.; Hieronymus, H.; Hsu, S. F.; Plietker, B.; Laschat, S., *ChemCatChem* **2013,** *5* (1), 82-112.

62.   Nestl, B. M.; Hammer, S. C.; Nebel, B. A.; Hauer, B., *Angew. Chem. Int. Edit.* **2014,** *53* (12), 3070-3095.

63.   Jung, S. T.; Lauchli, R.; Arnold, F. H., *Curr. Opin. Biotech.* **2011,** *22* (6), 809-817.

64.   Holtmann, D.; Hollmann, F., *ChemBioChem* **2016,** *17* (15), 1391-1398.

65.   Holtmann, D.; Fraaije, M. W.; Arends, I. W. C. E.; Opperman, D. J.; Hollmann, F., *Chem. Commun.* **2014,** *50* (87), 13180-13200.

66.   Hofrichter, M.; Ullrich, R., *Curr. Opin. Chem. Biol.* **2014,** *19*, 116-125.

67.   Hu, S.; Dordick, J. S., *J. Org. Chem.* **2002,** *67* (1), 314-317.

68.   Lewis, J. C.; Coelho, P. S.; Arnold, F. H., *Chem. Soc. Rev.* **2011,** *40* (4), 2003-2021.

69.   Molina-Espeja, P.; Garcia-Ruiz, E.; Gonzalez-Perez, D.; Ullrich, R.; Hofrichter, M.; Alcalde, M., *Appl. Environ. Microbiol.* **2014,** *80* (11), 3496-3507.

70.   Hofrichter, M.; Kellner, H.; Pecyna, M. J.; Ullrich, R., *Adv Exp Med Biol* **2015,** *851*, 341-368.

71.   Peter, S.; Karich, A.; Ullrich, R.; Groebe, G.; Scheibner, K.; Hofrichter, M., *J. Mol. Catal. B: Enzym.* **2014,** *103*, 47-51.

72.   Kluge, M.; Ullrich, R.; Scheibner, K.; Hofrichter, M., *Green Chem.* **2012,** *14* (2), 440-446.

73.   Peter, S.; Kinne, M.; Wang, X.; Ullrich, R.; Kayser, G.; Groves, J. T.; Hofrichter, M., *FEBS J.* **2011,** *278* (19), 3667-3675.

74.   Gutierrez, A.; Babot, E. D.; Ullrich, R.; Hofrichter, M.; Martinez, A. T.; del Rio, J. C., *Arch. Biochem. Biophys.* **2011,** *514* (1-2), 33-43.

75.   Olmedo, A.; Aranda, C.; del Rio, J. C.; Kiebist, J.; Scheibner, K.; Martinez, A. T.; Gutierrez, A., *Angew. Chem. Int. Edit.* **2016,** *55* (40), 12248-12251.

76.   Peter, S.; Kinne, M.; Ullrich, R.; Kayser, G.; Hofrichter, M., *Enz. Microb. Tech.* **2013,** *52* (6-7), 370-376.
77.   Kiebist, J.; Schmidtke, K.-U.; Zimmermann, J.; Kellner, H.; Jehmlich, N.; Ullrich, R.; Zaender, D.; Hofrichter, M.; Scheibner, K., *ChemBioChem* **2017,** *18* (6), 563-569.
78.   van Bloois, E.; Pazmino, D. E. T.; Winter, R. T.; Fraaije, M. W., *Appl. Microbiol. Biotechnol.* **2010,** *86* (5), 1419-1430.
79.   Baciocchi, E.; Gerini, M. F.; Harvey, P. J.; Lanzalunga, O.; Mancinelli, S., *Eur. J. Biochem.* **2000,** *267* (9), 2705-2710.
80.   Ozaki, S.; Yang, H. J.; Matsui, T.; Goto, Y.; Watanabe, Y., *Tetrahedron: Asymmetry* **1999,** *10* (1), 183-192.
81.   ten Brink, H. B.; Schoemaker, H. E.; Wever, R., *Eur. J. Biochem.* **2001,** *268* (1), 132-138.
82.   Tuynman, A.; Schoemaker, H. E.; Wever, R., *Monatsh. Chem.* **2000,** *131* (6), 687-695.
83.   Bassanini, I.; Ferrandi, E. E.; Vanoni, M.; Ottolina, G.; Riva, S.; Crotti, M.; Brenna, E.; Monti, D., *Eur. J. Org. Chem.* **2017,** (47), 7186-7189.
84.   Gao, F.; Wang, L.; Liu, Y.; Wang, S.; Jiang, Y.; Hu, M.; Li, S.; Zhai, Q., *Biochem. Eng. J.* **2015,** *93*, 243-249.
85.   Bassanini, I.; Ferrandi, E. E.; Vanoni, M.; Ottolina, G.; Riva, S.; Crotti, M.; Brenna, E.; Monti, D., *Eur. J. Org. Chem.* **2017,** *2017* (47), 7186-7189.
86.   Karich, A.; Kluge, M.; Ullrich, R.; Hofrichter, M., *Amb Express* **2013,** *3*.
87.   Kluge, M.; Ullrich, R.; Scheibner, K.; Hofrichter, M., *J. Mol. Catal. B.: Enzym.* **2014,** *103*, 56-60.
88.   Gomez de Santos, P.; Canellas, M.; Tieves, F.; Younes, S. H. H.; Molina-Espeja, P.; Hofrichter, M.; Hollmann, F.; Guallar, V.; Alcalde, M., *ACS Cat.* **2018,** *8* (6), 4789-4799.
89.   Barkova, K.; Kinne, M.; Ullrich, R.; Hennig, L.; Fuchs, A.; Hofrichter, M., *Tetrahedron* **2011,** *67* (26), 4874-4878.
90.   Kinne, M.; Poraj-Kobielska, M.; Aranda, E.; Ullrich, R.; Hammel, K. E.; Scheibner, K.; Hofrichter, M., *Bioorg. Med. Chem. Lett.* **2009,** *19* (11), 3085-3087.
91.   Alexander, K.; Katrin, C.; Rene, U.; Martin, H., *J. Mol. Catal. B.: Enzym.* **2016,** *134*, 238-246.
92.   Valderrama, B.; Ayala, M.; Vazquez-Duhalt, R., *Chemistry & Biology* **2002,** *9* (5), 555-565.
93.   Ayala, M.; Batista, C. V.; Vazquez-Duhalt, R., *J. Biol. Inorg. Chem.* **2011,** *16* (1), 63-68.
94.   Burek, B. O.; Bormann, S.; Hollmann, F.; Bloh, J. Z.; Holtmann, D., *Green Chem.* **2019,** *21* (12), 3232-3249.
95.   Bankar, S. B.; Bule, M. V.; Singhal, R. S.; Ananthanarayan, L., *Biotechnol. Adv.* **2009,** *27* (4), 489-501.
96.   Okrasa, K.; Falcimaigne, A.; Guibe-Jampel, E.; Therisod, M., *Tetrahedron: Asymmetry* **2002,** *13* (5), 519-522.
97.   Ma, Y.; Li, P.; Li, Y.; Willot, S. J. P.; Zhang, W.; Ribitsch, D.; Choi, Y. H.; Verpoorte, R.; Zhang, T.; Hollmann, F.; Wang, Y., *ChemSusChem* **2019,** *12* (7), 1310-1315.

Chapter 1. Introduction

98.   Getrey, L.; Krieg, T.; Hollmann, F.; Schrader, J.; Holtmann, D., *Green Chem.* **2014,** *16* (3), 1104-1108.

99.   Holtmann, D.; Krieg, T.; Getrey, L.; Schrader, J., *Catal. Commun.* **2014,** *51*, 82-85.

100.   Krieg, T.; Huettmann, S.; Mangold, K.-M.; Schrader, J.; Holtmann, D., *Green Chem.* **2011,** *13* (10), 2686-2689.

101.   Kohlmann, C.; Lutz, S., *Eng. Life Sci.* **2006,** *6* (2), 170-174.

102.   Lutz, S.; Steckhan, E.; Liese, A., *Electrochem. Commun.* **2004,** *6* (6), 583-587.

103.   Karmee, S. K.; Roosen, C.; Kohlmann, C.; Luetz, S.; Greiner, L.; Leitner, W., *Green Chem.* **2009,** *11* (7), 1052-1055.

104.   Churakova, E.; Kluge, M.; Ullrich, R.; Arends, I.; Hofrichter, M.; Hollmann, F., *Angew. Chem. Int. Edit.* **2011,** *50* (45), 10716-10719.

105.   Churakova, E.; Arends, I. W. C. E.; Hollmann, F., *ChemCatChem* **2013,** *5* (2), 565-568.

106.   Perez, D. I.; Grau, M. M.; Arends, I. W. C. E.; Hollmann, F., *Chem. Commun.* **2009,** (44), 6848-6850.

107.   Choi, D. S.; Ni, Y.; Fernandez-Fueyo, E.; Lee, M.; Hollmann, F.; Park, C. B., *ACS Cat.* **2017,** *7* (3), 1563-1567.

108.   Zhang, W.; Burek, B. O.; Fernandez-Fueyo, E.; Alcalde, M.; Bloh, J. Z.; Hollmann, F., *Angew. Chem. Int. Edit.* **2017,** *56* (48), 15451-15455.

109.   Zhang, W.; Fernandez-Fueyo, E.; Ni, Y.; van Schie, M.; Gacs, J.; Renirie, R.; Wever, R.; Mutti, F. G.; Rother, D.; Alcalde, M.; Hollmann, F., *Nat. Catal.* **2018,** *1* (1), 55-62.

110.   Seel, C. J.; Kralik, A.; Hacker, M.; Frank, A.; Konig, B.; Gulder, T., *ChemCatChem* **2018,** *10* (18), 3960-3963.

111.   van Schie, M. M. C. H.; Zhang, W.; Tieves, F.; Choi, D. S.; Park, C. B.; Burek, B. O.; Bloh, J. Z.; Arends, I. W. C. E.; Paul, C. E.; Alcalde, M.; Hollmann, F., *ACS Cat.* **2019,** *9* (8), 7409-7417.

112.   Massey, V.; Hemmerich, P., *Biochemistry* **1978,** *17* (1), 9-16.

113.   Tufvesson, P.; Lima-Ramos, J.; Nordblad, M.; Woodley, J. M., *Org. Process Res. Dev.* **2011,** *15* (1), 266-274.

114.   Tufvesson, P.; Lima-Ramos, J.; Al Haque, N.; Gernaey, K. V.; Woodley, J. M., *Org. Process Res. Dev.* **2013,** *17* (10), 1233-1238.

115.   Brennan, J. D.; Benjamin, D.; DiBattista, E.; Gulcev, M. D., *Chem. Mater.* **2003,** *15* (3), 737-745.

116.   Mensink, M. A.; Frijlink, H. W.; van der Voort Maarschalk, K.; Hinrichs, W. L. J., *Eur. J. Pharm. Biopharm.* **2017,** *114*, 288-295.

117.   Wolfel, R.; Taccardi, N.; Bosmann, A.; Wasserscheid, P., *Green Chem.* **2011,** *13* (10), 2759-2763.

118.   Albert, J.; Wolfel, R.; Bosmann, A.; Wasserscheid, P., *Energ. Environ. Sci.* **2012,** *5* (7), 7956-7962.

119.   Jessop, P. G.; Joo, F.; Tai, C. C., *Coord. Chem. Rev.* **2004,** *248* (21-24), 2425-2442.

120.   Aslam, N. M.; Masdar, M. S.; Kamarudin, S. K.; Daud, W. R. W., *Apcbee Proc* **2012,** *3*, 33-39.

121.   Singh, A. K.; Singh, S.; Kumar, A., *Catal. Sci. Technol.* **2016,** *6* (1), 12-40.

122.   Ha, S.; Larsen, R.; Masel, R. I., *J. Power Sources* **2005,** *144* (1), 28-34.
123.   Dong, J. J.; Fernández-Fueyo, E.; Li, J.; Guo, Z.; Renirie, R.; Wever, R.; Hollmann, F., *Chem. Commun.* **2017,** *53* (46), 6207-6210.
124.   Maetzke, A.; Knak Jensen, S. J., *Chem. Phys. Lett.* **2006,** *425* (1), 40-43.
125.   Xu, J. K.; Wang, C. L.; Cong, Z. Q., *Chem. Eur. J.* **2019,** *25* (28), 6853-6863.

Chapter 2. Transforming actual P450 monooxygenase to peroxygenase

Chapter based on:

Chapter 2. Transforming actual P450 monooxygenase to peroxygenase

2.1. Introduction

Cytochrome P450 monooxygenases (P450 or CYP) catalyse a broad range of oxyfunctionalisation reactions of non-activated C–H- and C=C-bonds.[1-6] Especially, the frequently observed regio- and enantioselectivity of this transformation makes P450s potentially very useful tools in preparative biocatalysis.[7]

The catalytic cycle of P450 monooxygenases comprises the reductive activation of molecular oxygen to form the catalytically active oxyferryl species (i.e., a highly oxidized iron-oxo-complex). The reducing equivalents needed for this reaction are generally derived from reduced nicotinamide cofactors *via* more or less complex electron transport chains[8], adding complexity to the reaction schemes.[9]

In 1999, Arnold and co-workers proposed to preparatively exploit the well-known hydrogen peroxide shunt pathway.[10] Here, the catalytically active compound is formed directly from H_2O_2 thereby drastically simplifying the regeneration scheme of P450 monooxygenases (**Scheme 1**).
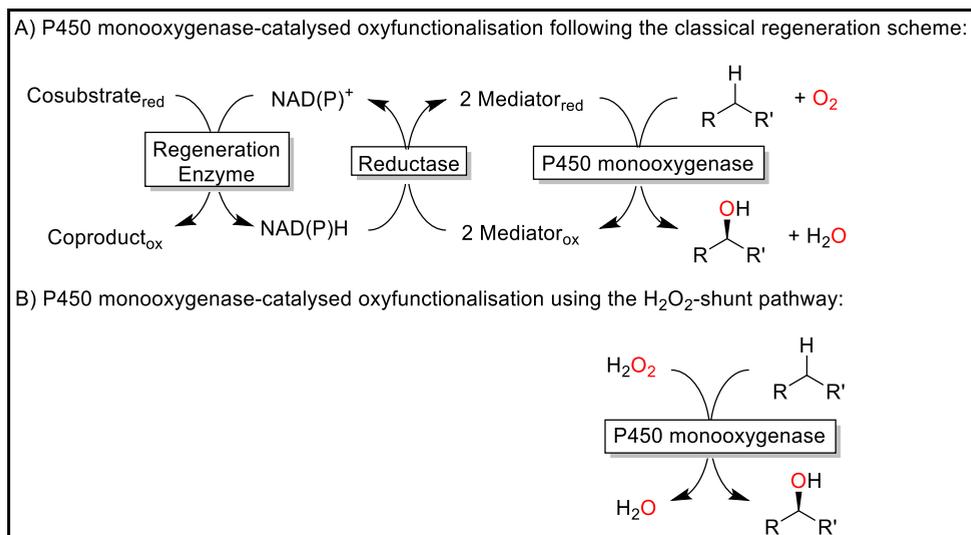
Scheme 1. Comparison of the classical regeneration and the H_2O_2-shunt pathway to drive P450 monooxygenase-catalysed oxyfunctionalisation reactions.

Unfortunately, the majority of the known P450s are rapidly inactivated by H_2O_2 making the H_2O_2 shunt pathway practically irrelevant. Some exceptions are known, in which P450s can efficiently use H_2O_2 through a substrate-assisted reaction mechanism for the hydroxylation or decarboxylation of fatty acids.[11-15]

Recently, Cong and co-workers reported an elegant possible solution to the H_2O_2-related inactivation of P450 monooxygenases.[16, 17] By comparing the catalytic mechanism and active sites of P450 monooxygenases with those of H_2O_2-dependent heme enzymes, peroxygenases, these authors reasoned that a base (glutamate) present in peroxygenases but missing in the active site of P450 monooxygenases may account for the poor activity of P450 monooxygenases with H_2O_2 (**Scheme 2**).
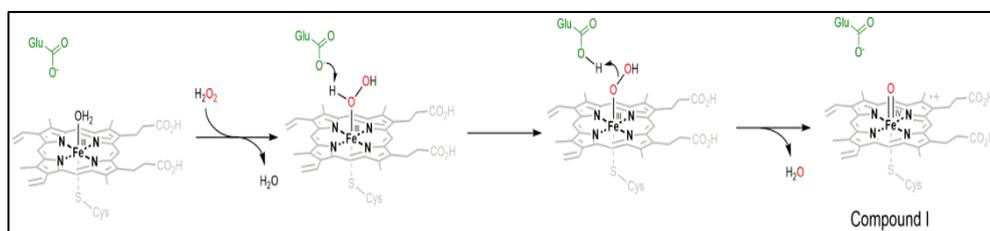
Scheme 2. Formation of Compound I from H_2O_2 in peroxygenases. The active-site base glutamate (Glu, green) facilitates the reaction by first deprotonating the primary H_2O_2-adduct and by re-protonation of the peroxo-intermediate.

To alleviate this shortcoming, a range of base-modified decoy molecules was suggested. In essence, these dual functional small molecules (DFSMs) comprise an imidazole-base coupled *via* a linker moiety to an amino acid anchoring part in order to position the base within the P450 monooxygenases' active sites, thereby enabling peroxygenase-like reactions.[18, 19] By doing so, the use of P450 *in vitro* could be greatly simplified.

2.2. Results

2.2.1. Preparation of the dual functional small molecules (DFSMs)

Imidazole-based DFSMs were synthesized following a literature-known four-step procedure.[16, 20] Overall, seven DFSMs comprising different amino acids and different

spacer lengths were synthesized (**Scheme 3**). Amongst the seven DFSMs synthesized only 3 (Im-C5-Ile, Im-C6-Phe and Im-C6-Ile) showed significant activity with the enzyme tested.
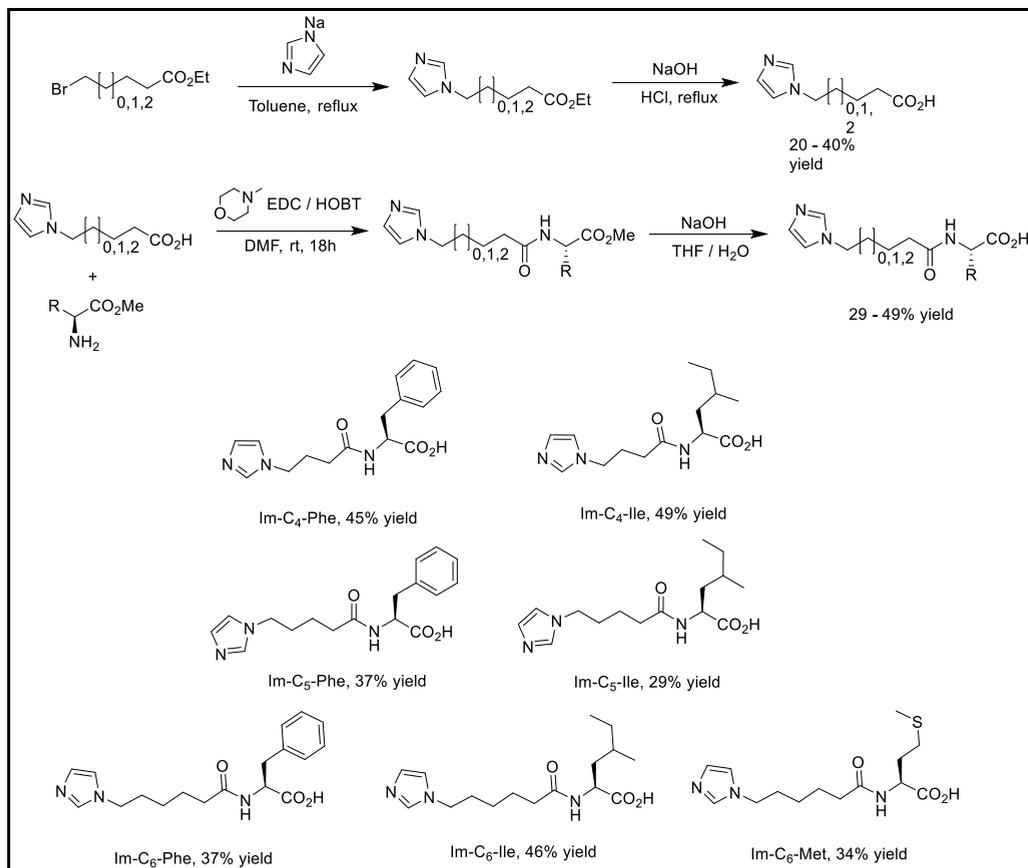
Scheme 3. Dual functional small molecules (DFSMs) synthesized for the P450BM3-catalyzed oxidations.

For the P450 monooxygenase we chose the well-known CYP102A1 (P450BM3) from *Bacillus megaterium*. More specifically, three variants P450BM3 F87A, P450BM3 V78A/F87A and P450BM3 A74E/F87V/P386S were recombinantly expressed in *Escherichia coli* and purified following literature methods.[21, 22] All variants contained a mutation at position 87, which had previously been reported to broaden the substrate scope of P450BM3.[23] The side-chain of phenylalanine 87 extends into the lumen of the substrate access channel close to the heme iron and

thus residues with less bulky side-chains, such as mutations to alanine or valine, widen the access channel by creating incremental space in the vicinity of the heme iron.[23] The mutation V78A has a similar effect, making the hydrophobic pocket that encloses the heme iron more capacious than in the wild type.[23] The variant P450BM3 A74E/F87V/P386S has previously been shown to possess 2 or 2.5 fold increased catalytic activity for the oxidation of β-ionone compared to the F87A or F87V single variants, respectively, and was therefore also included here.[21]

2.2.2. Biocatalytic transformations using the DFSMs/P450BM3 system

Having all components in hands, we first investigated the influence of the DFSMs on the P450BM3-catalyzed and H_2O_2-driven epoxidation of styrene (**1**) to obtain optically active styrene oxide (**2**). As shown in **Table 1**, only three of the seven DFSMs enabled H_2O_2-driven reactions with P450BM3.

Pleasingly, the presence of DFSMs significantly improved the catalytic performance of all P450BM3 variants. In the case of the F87A variant for example, Im-C6-Phe increased the product formation almost 20-fold. Other combinations gave similar improvements. Currently, we are unable to rationalize the improvements in light of DFSM binding to the enzyme active site and/or positioning of the substrates. Further studies will be necessary to obtain a quantitative structure–activity relationship. In line with the pH optimum of P450BM3,[24] the highest turnover numbers were observed at slightly alkaline pH values (**Table 1**, entries 1 vs. 5 and 6; entries 9 vs. 12). Decreasing the H_2O_2 concentration appeared to have a positive effect on the product formation (**Table 1**, entries 1 vs. 7), which we attribute to a lower inactivation rate at lower peroxide concentrations.

Interestingly, the DFSMs also influenced the enantioselectivity of the epoxidation reaction, which is in line with the original report by Cong and coworkers.[16] Possibly, this is due to a more stringent positioning of the starting material in the enzyme active site. However, again, no obvious structure–activity relationship was observed.

Chapter 2. Transforming actual P450 monooxygenase to peroxygenase

Table 1. Epoxidation of styrene (1) catalysed by DFSM/P450BM3 using H_2O_2 as the oxidant.[a]
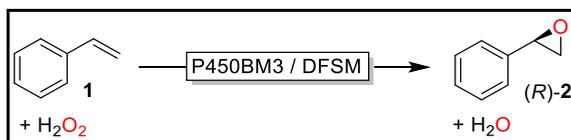
Entry	DFSM	pH	[2] (µM)	ee (%) [b]
F87A variant				
1	Im-C6-Phe	8	117	72
2	Im-C6-Ile	8	94	59
3	Im-C5-Ile	8	58	54
4	None [c]	8	6	10
5	Im-C6-Phe	7	68	65
6	Im-C6-Phe	6	≤2	-
7	Im-C6-Phe [d]	8	133	77
V78A/F87A variant				
8	Im-C6-Phe	8	54	6
9	Im-C6-Ile	8	97	22
10	Im-C5-Ile	8	80	19
11	None	8	11	n.d.
12	Im-C6-Ile	6	≤ 2	n.d.
A74E/F87V/P376S variant				
13	Im-C6-Phe	8	≤ 2	n.d.
14	Im-C6-Ile	8	17	4 (S)
15	Im-C5-Ile	8	17	6 (S)
16	None	8	≤ 2	n.d.

[a] Reaction conditions: [P450BM3] = 0.5 µM, [styrene] = 4 mM, [H_2O_2] = 20 mM; except entry 7, [DFSM] = 0.5 mM, KPi buffer, reaction time: 30 min; [b] Determined by gas chromatography; [c] No reaction was observed in absence of DFSM or biocatalyst; [d] [H_2O_2] = 5 mM; n.d. not determined.

Similarly, P450BM3-catalyzed sulfoxidation of thioanisole (**3**) was positively influenced by DFSMs (**Table 2**). Compared to the epoxidation reaction, rate accelerations were somewhat lower; the enantioselectivity of the sulfoxidation reaction, however, was significantly improved by the DFSMs. Both observations can

42

be rationalised by the spontaneous (non-enantioselective) oxidation of thioanisole by H_2O_2.[25] Quite interestingly, the P450BM3 A74E/F87V/P386S variant, which in the epoxidation reaction gave rather poor results compared to the other two variants, excelled in the sulfoxidation reaction.

As mentioned above, H_2O_2-related inactivation of the heme enzyme appeared to be a major limitation of the proposed H_2O_2-shunt pathway reaction of P450BM3. We therefore also investigated the effect of controlled *in situ* H_2O_2 generation *via* reductive activation of O_2 using an oxidase.[26] Thus, employing the commercially available alcohol oxidase from *Pichia pastoris* (*Pp*AOx), H_2O_2 was generated *in situ* from O_2 at the expense of methanol (which was oxidized to formaldehyde). When this system was applied (**Table 3**), reaction rates were significantly decreased (reaction times 18 h), while at the same time the turnover numbers of the biocatalyst were improved, compared to the use of H_2O_2 they were five times greater. The low concentration of H_2O_2 available slowed down both the reaction rate and the oxidative inactivation. We expect that further optimized reaction schemes may provide optimal H_2O_2 generation rates, ensuring maximized enzymatic sulfoxidation while minimizing the H_2O_2-related inactivation of the heme enzyme. Again, in the absence of any DFSM, near racemic product was observed, indicating predominant spontaneous sulfoxidation.

One major drawback of classic P450 monooxygenation reactions is that, due to the exclusive water solubility of the nicotinamide cofactors, they have to be performed in aqueous reaction media. As the majority of the reagents of interest for P450 monooxygenase-catalysed oxyfunctionalisations are rather hydrophobic, reagent concentrations tend to be in the lower millimolar range, reducing the preparative attractiveness of these reactions from an economic and environmental point-of-view.[27] In this respect, the proposed peroxide-driven reaction offers some interesting possibilities for non-aqueous reactions using P450 monooxygenases.

To test this hypothesis, we evaluated the epoxidation of styrene using precipitated P450BM3 F87A suspended in neat styrene as the reaction medium; the stoichiometric oxidant was ^{t}BuOOH (**Scheme 4**).

Table 2. P450BM3-catalyzed sulfoxidation of thioanisole (3) using H_2O_2 as the oxidant.
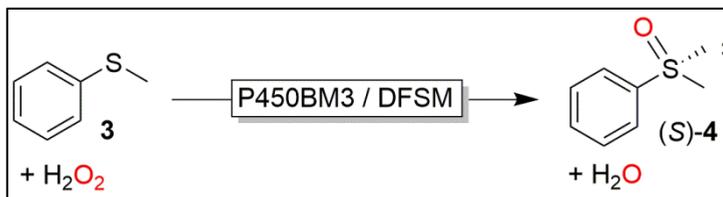
Entry	DFSM	[4] (μM)	ee (%)
F87A variant			
1	Im-C6-Phe	232	40
2	Im-C6-Ile	178	38
3	Im-C5-Ile	151	35
4	None	78	6
V78A/F87A variant			
5	Im-C6-Phe	103	41
6	Im-C6-Ile	75	40
7	Im-C5-Ile	77	44
8	None	53	4
A74E/F87V/P376S variant			
9	Im-C6-Phe	129	47
10	Im-C6-Ile	98	51
11	Im-C5-Ile	108	53
12	None	65	8

Conditions: [P450BM3] = 0.5 μM, [thioanisole] = 4 mM, [H_2O_2] = 20 mM, [DFSM] = 0.5 mM, 100 mM potassium phosphate buffer pH 8.0, reaction time = 30 min.

Table 3. P450BM3 F87A-catalyzed sulfoxidation of 3 using *in situ* generation of H_2O_2 by the *Pp*AOx-catalyzed oxidation of methanol.[a.]
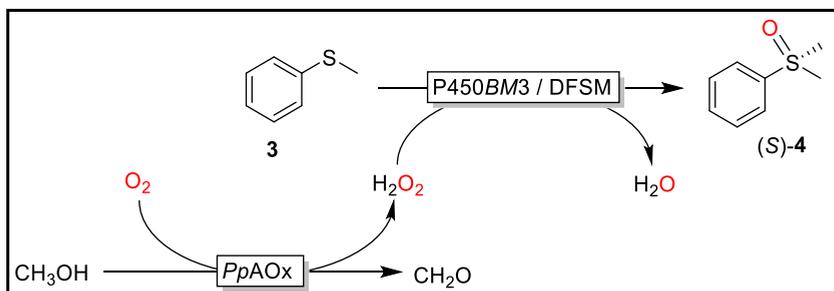
Entry	DFSM	[4] (µM)	ee (%)
1	Im-C6-Phe	381	31
2	Im-C6-Ile	359	33
3	Im-C5-Ile	320	30
4	None	248	≤3

[a] Reaction were stopped after 18 h at room temperature. For further details, see Materials and Methods section; determined by gas chromatography.
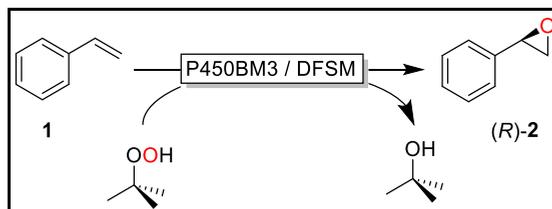
Scheme 4. P450BM3-catalyzed epoxidation in neat styrene using *t*BuOOH as stoichiometric oxidant.

Under these conditions, epoxidation of styrene was observed in the presence of Im-C5-Ile (TON$_{P450BM3}$ = 178, TON = [Styrene oxide]/[P450BM3]), while in the absence of Im-C5-Ile, 100 turnovers were still observed for the biocatalyst. (*R*)-**2** was obtained with optical purities around 15% for both reactions. In the absence of the P450BM3 F87A variant, no product formation was observed, even upon prolonged reaction times. To the best of our knowledge, this is the first example of a P450 monooxygenase reaction under neat conditions.

Chapter 2. Transforming actual P450 monooxygenase to peroxygenase

2.3. Conclusions

Overall, we have confirmed Cong's approach, turning P450 monooxygenases into peroxygenases by using DFSMs. The results shown in this study suggest specific interactions of the DFSMs with P450BM3 influencing their performance as catalysts. Further studies with a broader set of DFSMs will be necessary to establish quantitative structure–activity relationships and further optimize the reaction system. It will also be interesting to investigate possible match/mismatch combinations of the (chiral) amino acid anchoring groups. *In silico* studies might be relevant to perform in that case.

2.4. Materials and Methods

Unless otherwise noted, analytical grade solvents and commercially available reagents were used without further purification.

Dual functional small molecules (DFSMs) were synthesized according to the methodology described in the literature.[16] Compounds Im-C5-Ile, Im-C5-Phe, Im-C6-Ile, Im-C6-Phe and Im-C6-Met exhibited physical and spectral properties in accordance with those reported.[16]

GC (gas chromatography) analyses were performed on a Shimadzu GC-2010 Plus (Shimadzu, Kyoto, Japan). For the oxidation of styrene (**1**) to styrene oxide (**2**), a Chirasil Dex CB (Agilent, Santa Clara, CA, USA, 25 m × 0.32 mm × 0.25 μm) column was employed: Carrier gas He, 100 °C hold 12.50 min, 20 °C min^{-1} to 225 °C, hold 1 min. Retention times: **1**: 3.0 min; (*R*)-**2**: 7.5 min; (*S*)-**2**: 7.9 min and dodecane (internal standard): 9.8 min. For the oxidation of thioanisole (**3**) to methyl phenyl sulfoxide (**4**) a Lipodex E (Agilent, 50 m × 0.25 mm × 0.25 μm) column was used: Carrier gas He, 130 °C hold 6.0 min, 20 °C min^{-1} to 200 °C, hold 5.0 min, 25 °C min^{-1} to 220 °C hold 1.0 min. Retention times: **3**: 4.2 min; dodecane (internal standard): 4.9 min; (*S*)-**4**: 11.8 min, and (*R*)-**4**: 12.4 min.

NMR Spectra were recorded (^{1}H NMR 300 MHz; ^{13}C NMR 75 MHz) with the solvent peak used as the internal reference (7.26 and 77.0 ppm for ^{1}H and ^{13}C, respectively) using an Agilent 400 (400 MHz, Santa Clara, CA, USA)

P450BM3 F87A and P450BM3 V78A/F87A were produced according to a previously reported protocol.[22]

2.4.1. Preparation of P450BM3 A74E/F87V/P386S

pET28a P450BM3 A74E F87V P386S was expressed in *E. coli* BL21 (DE3). First, 5 mL Lysogeny Broth (LB) medium supplemented with 30 µg mL^{-1} kanamycin was inoculated with single colonies and grown overnight at 37 °C, 180 rpm for preculture. Then 1 L medium (900 mL Terrific Broth (TB) + 100 mL potassium phosphate buffer pH 7.5) supplemented with kanamycin (30 µg mL^{-1}) was inoculated with the 5 mL preculture and incubated at 37 °C, 180 rpm. When OD_{600} reached 0.8 (OD_{600}: Absorbance at 600 nm), induction was obtained by adding isopropyl β-D-1-thiogalactopyranoside (100 µmol L^{-1}); at this time point 5-aminolevulinic acid (500 µmol L^{-1}) and $FeSO_4$ (100 µmol L^{-1}) were also added. Cultures were then stirred at 30 °C, 180 rpm overnight. Cells were harvested by centrifugation (10,000 g, 30 min, 4 °C) and resuspended in 50 mM phosphate buffer pH 7.5 supplemented with RNase and DNase. After 30 min on ice, cells were disrupted with a French press. The cells debris was removed by centrifugation (14,000 rpm, 30 min, 4 °C). Purification was performed by nickel affinity chromatography using a 60 mL His-Trap FF crude column (GE Healthcare, Chicago, IL, USA) applying a gradient of imidazole. The enzyme was then desalted with a PD-10 column and concentrated with an Amicon filter with a cut-off of 30 kDa.

2.4.2. General Procedure for the Preparation of Im-C4-Phe and Im-C4-Ile

Im-C4-Phe and Im-C4-Ile were prepared starting from 4-(1*H*-imidazol-1-yl)butanoic acid: A DMF (dimethylformamide) solution (10 mL) containing HOBt (150 mg, 1.1 mmol), EDC (170 mg, 1.1 mmol), and 4-(1*H*-imidazol-1-yl)butanoic acid (154 mg, 1.0 mmol) was stirred at room temperature for 1 h. A solution of L-phenylalanine methyl ester or L-isoleucine methyl ester (1.1 mmol) and 4-methylmorpholine (202

mg, 2.0 mmol) dissolved in 10 mL of DMF was then added to the reaction mixture. After 18 h, the reaction mixture was partitioned between dichloromethane (50 mL) and H_2O (50 mL). The organic layer was washed with H_2O (3 × 50 mL) and dried over $MgSO_4$. The solution was concentrated under reduced pressure. The crude product was then dissolved in 2 mL NaOH aqueous solution (1.0 M) and 1 mL THF and stirred overnight. The THF was removed under reduced pressure and the solution was acidified to pH 2.0 with HCl (1.0 M). Water was then removed under reduced pressure and the residue was dissolved in ethanol. NaCl was separated by filtration and ethanol was evaporated to give the final products.

(*S*)-2-(4-(1*H*-imidazol-1-yl)butanamido)-3-phenylpropanoic acid (Im-C4-Phe): Colourless oil (135.4 mg, 45% yield). ^{1}H-NMR (300 MHz, d_6-DMSO): δ (ppm) 8.97 (s, 1H), 8.13 (d, 1H, J = 8.0 Hz), 7.91 (s, 1H), 7.62 (s, 1H), 7.31–7.14 (m, 5H). 4.37–4.29 (m, 1H), 4.13 (t, 2 H, J = 7.5 Hz), 3.07–3.01 (m, 1H), 2.82–2.74 (m, 1H), 2.07-1.96 (m, 4H). ^{13}C-NMR (75.4 MHz, d_6-DMSO): δ (ppm) 174.2, 172.6, 138.3, 135.6, 129.2 (2C), 128.7, 126.6 (2C), 124.8, 121.2, 54.1, 48.9, 37.1, 35.2, 25.3. HRMS: m/z calculated for $C_{16}H_{19}N_3O_3$ (M$^+$): 302.1499; found: 302.1498.

(*S*)-2-(4-(1*H*-imidazol-1-yl)butanamido)-3-methylpentanoic acid (Im-C4-Ile): Colourless oil (137.7 mg, 49% yield). ^{1}H-NMR (300 MHz, d_6-DMSO): δ (ppm) 9.12 (s, 1H), 8.19 (s, 1H), 7.95 (s, 1H), 7.67 (s, 1H), 4.16–4.11 (m, 1H), 3.92 (t, 2H, J = 7.9 Hz), 2.14–2.07 (m, 4H), 1.93-1.87 (m, 2H), 1.21–1.13 (m, 3H), 0.89–0.80 (m, 6H). ^{13}C-NMR (75.4 MHz, d_6-DMSO): δ (ppm) 174.1, 171.3, 137.6, 128.6, 119.8, 57.2, 49.0, 36.2, 34.4, 32.1, 31.9, 25.2, 16.1, 11.8. HRMS: m/z calculated for $C_{14}H_{23}N_3O_3$ (M$^+$): 281.1739; found: 281.1734.

2.4.5. General procedure for the biocatalyzed oxidation of styrene and thioanisole employing the P450BM3/DFSM system

Unless otherwise stated, the corresponding variant of P450BM3 (0.5 µM) was transferred to a glass sample bottle containing 0.1 M, pH 8.0 potassium phosphate buffer (0.36 mL), styrene (**1**) or thioanisole (**3**) (4 mM in methanol) and the DFSM (0.5 mM, dissolved in pH 8.0 phosphate buffer). H_2O_2 (20 mM, dissolved in pH 8.0 phosphate buffer) was added and the reaction was shaken at room temperature and

300 rpm for 30 min. The reaction was then extracted using ethyl acetate containing 5.0 mM of dodecane as the external standard (0.4 mL) and dried over anhydrous sodium sulfate. The conversion and the optical purity of styrene oxide (**2**) or methyl phenyl sulfoxide (**4**) was analysed by gas chromatography.

3.4. General method for the biocatalyzed oxidations employing the H$_2$O$_2$ *in situ* generation system

P450BM3 F87A (0.5 μM) was transferred to a glass sample bottle containing 0.1 M, pH 8.0 potassium phosphate buffer (0.36 mL), methanol (100 mM), thioanisole (**3**) (4 mM in methanol) and the DFSM (0.5 mM, dissolved in pH 8.0 phosphate buffer). A solution of the alcohol oxidase from *Pichia pastoris* (5 nM, dissolved in pH 8.0 phosphate buffer) was added and the reaction was shaken at room temperature and 300 rpm for 18 h. The reaction was then extracted using ethyl acetate containing 5 mM of dodecane as the external standard (0.4 mL) and dried over anhydrous sodium sulfate. The conversion and the optical purity of methyl phenyl sulfoxide (**4**) was analysed by gas chromatography.

2.4.6. General method for the epoxidation of styrene using precipitated P450BM3 F87A with DFSMs,

P450BM3 F87A was precipitated with acetone dried (30 mg) and transferred to a glass sample bottle containing styrene (**1**) (200 μL) and the DFSM (0.5 mM, dissolved in pH 8.0 potassium phosphate buffer). *t*BuOOH (20 mM, 70% in H$_2$O) was added and the reaction was shaken at room temperature and 300 rpm for 30 min. The reaction was then extracted using ethyl acetate containing 5.0 mM of dodecane as the external standard (0.4 mL) and dried over anhydrous sodium sulfate. The conversion and the optical purity of styrene oxide (**2**) was analysed by gas chromatography.

2.5. References

1.   Bornscheuer, U. T.; Huisman, G. W.; Kazlauskas, R. J.; Lutz, S.; Moore, J. C.; Robins, K., *Nature* **2012,** *485* (7397), 185-194.
2.   Fasan, R., *ACS Cat.* **2012,** *2* (4), 647-666.
3.   Wang, J. B.; Reetz, M. T., *Nature Chem.* **2015,** *7* (12), 948-949.

4.   Dong, J. J.; Fernandez-Fueyo, E.; Hollmann, F.; Paul, C. E.; Pesic, M.; Schmidt, S.; Wang, Y. H.; Younes, S.; Zhang, W. Y., *Angew. Chem. Int. Edit.* **2018,** *57* (30), 9238-9261.

5.   Rudroff, F.; Mihovilovic, M. D.; Groger, H.; Snajdrova, R.; Iding, H.; Bornscheuer, U. T., *Nat. Catal.* **2018,** *1* (4), 306-306.

6.   Urlacher, V. B.; Girhard, M., *Trends Biotechnol.* **2019,** *37* (8), 882-897.

7.   Schulz, S.; Girhard, M.; Urlacher, V. B., *ChemCatChem* **2012,** *4* (12), 1889-1895.

8.   Hannemann, F.; Bichet, A.; Ewen, K. M.; Bernhardt, R., *Bba-Gen Subjects* **2007,** *1770* (3), 330-344.

9.   Strohle, F. W.; Kranen, E.; Schrader, J.; Maas, R.; Holtmann, D., *Biotechnol. Bioeng.* **2016,** *113* (6), 1225-1233.

10.   Joo, H.; Lin, Z. L.; Arnold, F. H., *Nature* **1999,** *399* (6737), 670-673.

11.   Matsunaga, I.; Ueda, A.; Sumimoto, T.; Ichihara, K.; Ayata, M.; Ogura, H., *Arch. Biochem. Biophys.* **2001,** *394* (1), 45-53.

12.   Girhard, M.; Schuster, S.; Dietrich, M.; Durre, P.; Urlacher, V. B., *Biochem. Biophys. Res. Commun.* **2007,** *362* (1), 114-119.

13.   Rude, M. A.; Baron, T. S.; Brubaker, S.; Alibhai, M.; Del Cardayre, S. B.; Schirmer, A., *Appl. Environ. Microbiol.* **2011,** *77* (5), 1718-1727.

14.   Hrycay, E. G.; Bandiera, S. M., *Arch. Biochem. Biophys.* **2012,** *522* (2), 71-89.

15.   Munro, A. W.; McLean, K. J.; Grant, J. L.; Makris, T. M., *Biochem. Soc. Trans.* **2018,** *46*, 183-196.

16.   Ma, N. N.; Chen, Z. F.; Chen, J.; Chen, J. F.; Wang, C.; Zhou, H. F.; Yao, L. S.; Shoji, O.; Watanabe, Y.; Cong, Z. Q., *Angew. Chem. Int. Edit.* **2018,** *57* (26), 7628-7633.

17.   Xu, J. K.; Wang, C. L.; Cong, Z. Q., *Chem-Eur J* **2019,** *25* (28), 6853-6863.

18.   Chen, Z. F.; Chen, J.; Ma, N. N.; Zho, H. F.; Cong, Z. Q., *J. Porphyrins Phthalocyanines* **2018,** *22* (9-10), 831-836.

19.   Li, F. L.; Kong, X. D.; Chen, Q.; Zheng, Y. C.; Xu, Q.; Chen, F. F.; Fan, L. Q.; Lin, G. Q.; Zhou, J. H.; Yu, H. L.; Xu, J. H., *ACS Cat.* **2018,** *8* (9), 8314-8317.

20.   Haines, D. C.; Chen, B. Z.; Tomchick, D. R.; Bondlela, M.; Hegde, A.; Machius, M.; Peterson, J. A., *Biochemistry* **2008,** *47* (12), 3662-3670.

21.   Urlacher, V. B.; Makhsumkhanov, A.; Schmid, R. D., *Appl. Microbiol. Biotechnol.* **2006,** *70* (1), 53-59.

22.   Le-Huu, P.; Heidt, T.; Claasen, B.; Laschat, S.; Urlacher, V. B., *ACS Cat.* **2015,** *5* (3), 1772-1780.

23.   Whitehouse, C. J. C.; Bell, S. G.; Wong, L. L., *Chem. Soc. Rev.* **2012,** *41* (3), 1218-1260.

24.   Narhi, L. O.; Fulco, A. J., *J. Biol. Chem.* **1986,** *261* (16), 7160-7169.

25.   Pereira, P. C.; Arends, I. W. C. E.; Sheldon, R. A., *Process Biochem.* **2015,** *50* (5), 746-751.

26.   Burek, B. O.; Bormann, S.; Hollmann, F.; Bloh, J. Z.; Holtmann, D., *Green Chem* **2019,** *21* (12), 3232-3249.

27.   Ni, Y.; Holtmann, D.; Hollmann, F., *ChemCatChem* **2014,** *6* (4), 930-943.

Chapter 3. Expanding the spectrum of light-driven peroxygenase reactions.

Chapter 3. Expanding the spectrum of light-driven peroxygenase reactions

3.1. Introduction

Heme-dependent peroxygenases are receiving tremendous interest as catalysts for selective oxidation reactions.[1-3] These enzymes often show high catalytic performances. Moreover, they rely only on hydrogen peroxide (H_2O_2) to form the catalytically active Compound I, representing a simpler system than their homologue P450. Nevertheless, peroxygenases are prone to oxidative inactivation in presence of high amount of the oxidant.[4]

Therefore, for high catalytic performances, mild feeding of peroxide has to be applied. One way is the direct feeding of oxidant in the reaction. Two issues then arise: dilution of the reaction and hot spot of H_2O_2 still occurring in the solution. Thus, *in situ* generation systems of H_2O_2 seem the best solution for a homogenous feeding. A tremendous number of systems have been reported based on the reduction of molecular oxygen.[5-8] Among these systems, photocatalysis holds the promise of being "green" by utilizing sunlight as the driving force. [9-11]

Nevertheless, the reported systems at the beginning of this project were using photocatalysts with narrow absorption. For instance, flavin mononucleotide (FMN) absorbance range peak is at 450 nm which leaves all the photons >500 nm unutilized (**Figure 1**).[12-14] Considering the application of sunlight as energy source, a large part of the photons are then unexploited.
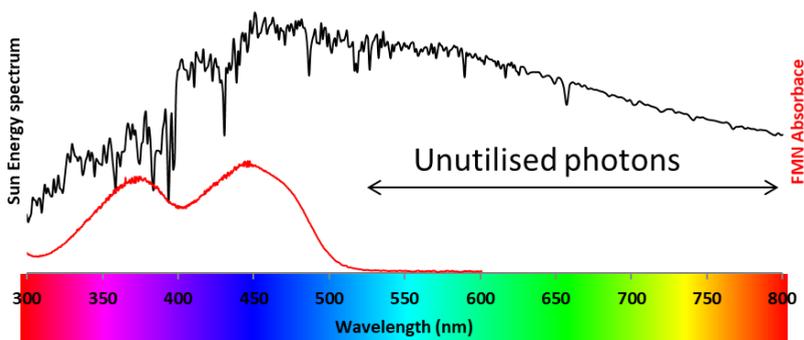
Figure 2. Comparison of FMN absorbance and sunlight spectrum

Therefore, this chapter aims at providing a solution for better use of sunlight. The strategy applied here is to mix photocatalysts with different absorbance maxima to cover a broad range of wavelengths. If the photocatalysts are compatible then the resulting cooperative effect could enhance the performances of the system. An atom efficient electron donor has to be applied in order to stay in line with the sustainability view of the study. Usually, ethylenediaminetetraacetic acid (EDTA), a rather large molecule is applied as the sacrificial electron donor.[12, 13] For this reason, formate has been chosen as reducing agent. Its oxidation leads to carbon dioxide (CO_2) which is simpler to handle in downstream process (*in situ* removal of CO_2). Also, this system could be, at a later stage, introduce within a cascade for full methanol oxidation.[6]

To couple formate oxidation to photocatalytic H_2O_2 generation, an enzymatic relay system comprising formate dehydrogenase from *Candida boidinii* (*Cb*FDH) to mediate the hydride transfer from formate to nicotinamide adenine dinucleotide (NAD$^+$)[15] has been envisioned. The advantage of this system comes from the resulting NADH that has been already reported to be photo-oxidisable.[16, 17] The peroxygenase used in this study was the recombinant, evolved peroxygenase from *Agrocybe aegerita* (r*Aae*UPO) that catalysed the hydroxylation of ethylbenzene towards (*R*)-1-phenylethanol (**Scheme 1**).
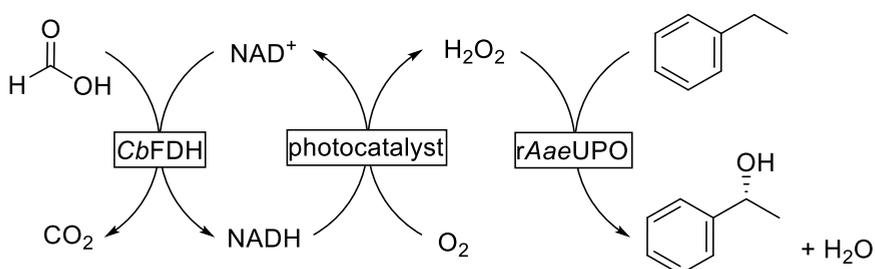
Scheme 1. Proposed photoenzymatic system for *in situ* generation of H_2O_2 to promote peroxygenase-catalysed hydroxylation reactions

Chapter 3. Expanding the spectrum of light-driven peroxygenase reactions

3.2. Results & Discussions

3.2.1. Screening of photocatalyst

First, 23 commercially available organic dyes were tested for their capability of oxidizing NADH and delivering the reducing equivalents to O_2 to yield H_2O_2. The screening assay was composed of 2 steps. First, each dye was incubated with NADH and irradiated with the proper LEDs (450 nm, 520 nm or 630 nm) in anaerobic conditions. Then if spectral change is observed by UV-Vis spectroscopy, the system is flushed with air. If the initial spectrum is recovered, the best hypothesis is that O_2 was able to oxidise the dye, resulting in H_2O_2 formation. Details of the recorded spectra can be found in **Table 2**.

Among the tested organic dyes, all the dyes sensitive to light in presence of NADH were polysubstituted anthracene rings (**Figure 2**). More precisely, in the superfamily of fluorone dyes, fluorescein derivatives were photoreducible by NADH whereas their reduced form were highly stable in aerobic conditions. These dyes are not relevant for this study but are highly interesting when anaerobic application is envisioned.[16] In the same time, rhodamine derivatives were not photoreduced in presence of NADH. All the dyes photoreduced by NADH and oxygen sensitive were all acridine derivatives, as such as FMN. Neutral red is the only molecule not included in this trend. Spectral changes could be observed but were extremely slow compared to the other acridine derivatives. One drawback of this screening assay is the use of LEDs from which the emission spectrum might not overlap perfectly with the absorption spectrum of each dye.

Photoreducible and O$_2$ sensitive

Methylene blue   Safranin O   Phenosafranin

Proflavin   Acridine Orange

Photosensitive

Eosin Y   Fluorescein   Rose Bengal

Rezasurin   Neutral Red

No sensitive effect

Alizarin red   Amido Black   Serva blue G

Rhodamine 110   Rhodamine 101   Rhodamine B

Coomassie blue   Cibracon 3G-A   Bromophenol blue

Indigo Carmin   Rhodamine 6G
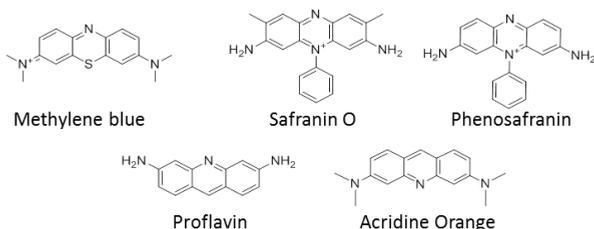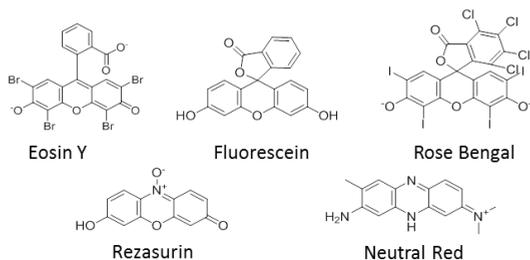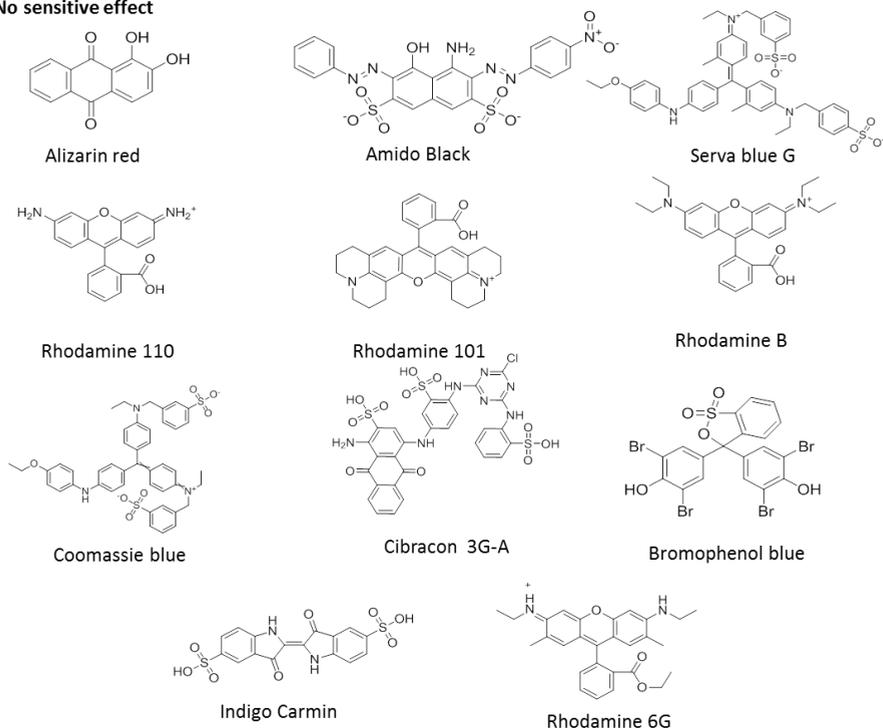
Figure 3. Screened dyes for H$_2$O$_2$ photoproduction. Detailed chromatograms can be found in Table 2 General conditions: [NADH] >300 µm, 50 mM potassium phosphate buffer pH 7.0, 30 °C, anaerobic conditions (100% N$_2$), 300 rpm.

3.2.2. Photoreduction of acridine derivatives and H_2O_2 production

The remaining candidates were investigated further with respect to their activity in photochemical reduction and H_2O_2 generation. First, different reported reducing agent of flavins were tested on the acridine derivatives (**Figure 3**). Astonishingly, 3-(*N*-morpholino)propanesulfonic acid, tris(hydroxymethyl)aminomethane and ascorbic acid (not shown) were poor electron donors for the tested photocatalysts while being reported as efficient for flavins and deazaflavins.[18] For instance, acridine orange could only be reduced by NADH with rates order of magnitude lower than FMN and the other tested photocatalysts. Methylene blue stands out with high rates of reduction with NADH. Overall, all compounds show quantitative rates for the first step of the photocascade.
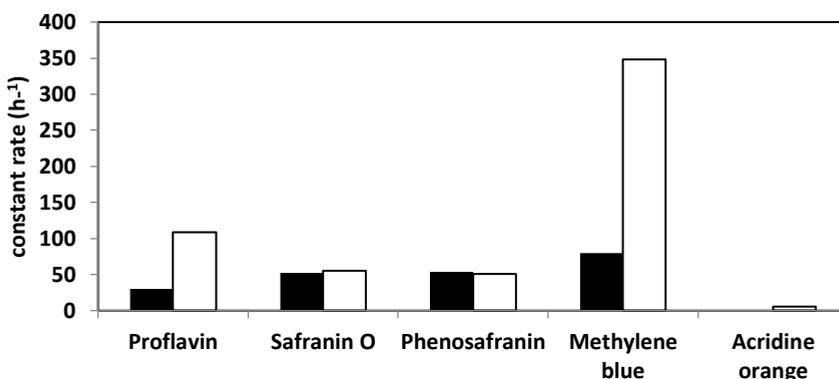
Figure 4. Photoreduction constant rates (first order) of the dyes with NADH (white) or EDTA (black) as reductant. Conditions: R.T. (22- 24 °C),50 mM potassium phosphate buffer pH 7, [reductant] = 1 mM, anaerobic conditions, blue LEDs (proflavin, acridine orange) or green LEDs (safranin O and phenosafranin), red LEDs (methylene blue).

Then, the production rate of H_2O_2 has been investigated. Drawing correlations between the physicochemical and structural properties of the photocatalysts and their activity (**Figure 4**) is difficult as factors such as redox potential, photo-excitability, light energy and reactivity of the reduced form with O_2 contribute to the macroscopically observed H_2O_2 generation rate. All the catalysts show interesting rates in the same order of magnitude than FMN. Only proflavin shows higher rates

than FMN in these conditions. Overall, all the compound can be tested in the *Cb*FDH/r*Aae*UPO biocascade.
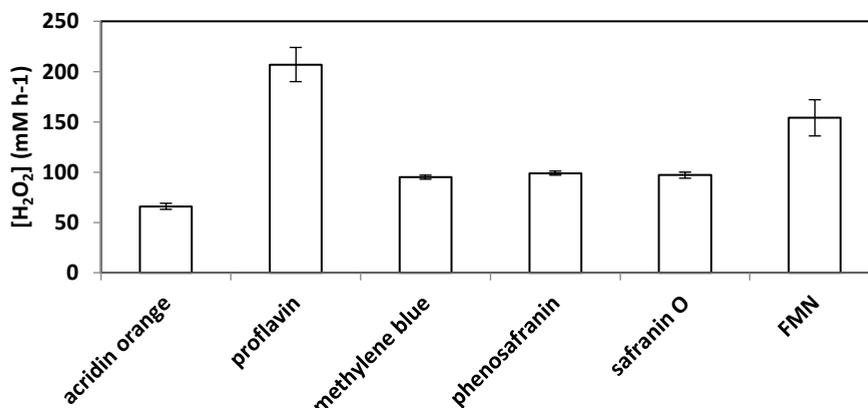
Figure 5. H_2O_2 production rates by the different photocatalysts. Conditions: [photocatalyst] = 50 µM, [NADH]= 1 mM, 30 °C, 300 rpm, 50 mM potassium phosphate buffer pH 7.0, λ (acridine orange, proflavin, FMN) = 450 nm, λ (phenosafranin, safranin O) = 512 nm, λ (methylene blue) = 662 nm.

3.2.3. *Cb*FDH/r*Aae*UPO photocascade

All the tested photocatalysts were applied and were able to promote r*Aae*UPO ethylbenzene hydroxylation when monochromatic light is applied. Proflavin that exhibits previously the best kinetics is on the other hand the less robust than FMN when promoting the r*Aae*UPO/*Cb*FDH system. Then, we focused on phenosafranin, methylene blue, and FMN, because this combination offers a broad coverage of the visible light and shows the best results when applied individually (**Figure 5**).
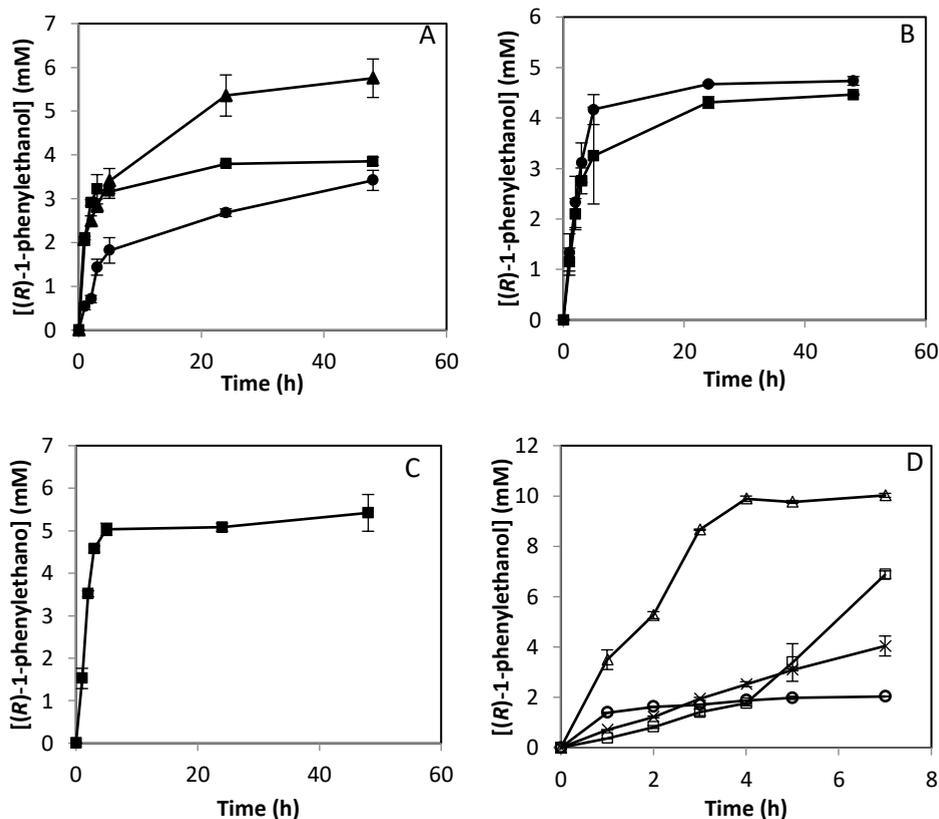
Figure 6. Photoenzymatic hydroxylation of ethylbenzene to 1-(R)-phenylethanol. (A) (▲) FMN, (■) proflavin, (●) acridine orange blue λ_{LED} **= 450 nm ; (B) (●) phenosafranin, (■) safranin O** λ_{LED} **= 512 nm ; (C) (■) methylene blue** λ_{LED} **= 662 nm ; (D) using 5 µM FMN (○), 10 µM methylene blue (□), 5 µM phenosafranin (x), or 10 µM methylene blue + 5 µM phenosafranin + 5 µM FMN (Δ) as photocatalysts** λ_{LED} **= 450 + 520 + 630 nm.** Conditions: aerobic atmosphere, 30°C, 50 mM potassium phosphate buffer pH 7.0, 0.8 %(v/v) methanol, [NaHCO$_2$] = 75 mM (A,B,C) [CbFDH] = 2.4 µM, [NAD$^+$]= 200 µM,[photosensitizer] = 50 µM, [ethylbenzene] = 50 mM, [rAaeUPO] = 50 nM, (D) [rAaeUPO] = 100 nM, [CbFDH] = 4.8 µM, [NAD$^+$] = 400 µM, [ethylbenzene] = 10 mM, N.B.: using a broad spectrum (sunlight-imitating) light source (Lightincure LC8 L9566, Hamamatsu) gave comparable results (**Figure 17**)

These photocatalysts could promote when mixed the rAaeUPO-catalysed stereospecific hydroxylation of ethylbenzene to 1-phenylethanol (**Figure 5D**). The relative rates observed with the individual photocatalysts qualitatively correspond to the photocatalytic H$_2$O$_2$ generation rates. The turnover numbers calculated for the

catalytic components (r*Aae*UPO, photocatalysts, NAD⁺, and *Cb*FDH) are 100 000, 500, 25, and 1785, respectively.

In the absence of either photocatalyst or r*Aae*UPO, no product formation is observed (**Figure 6A**). The same is true for experiments performed in the dark with the exception of methylene blue where upon prolonged reaction times some product traces is found (0.4 mM after 48 h, **Figure 6B**). This is in line with previous observations that methylene blue is capable of a "dark-reaction" with NADH.[17, 19] Some product formation (approximately 5−20% of the "normal" product formation rate) is observed in the absence of either component of the NADH regeneration system (i.e., in the absence of formate, CbFDH, or NAD⁺). The latter observation most likely can be attributed to an undesired reductive quenching of the excited photocatalysts by oxidizable components in the reaction mixture (i.e., proteins, amino acids, etc.).[20]
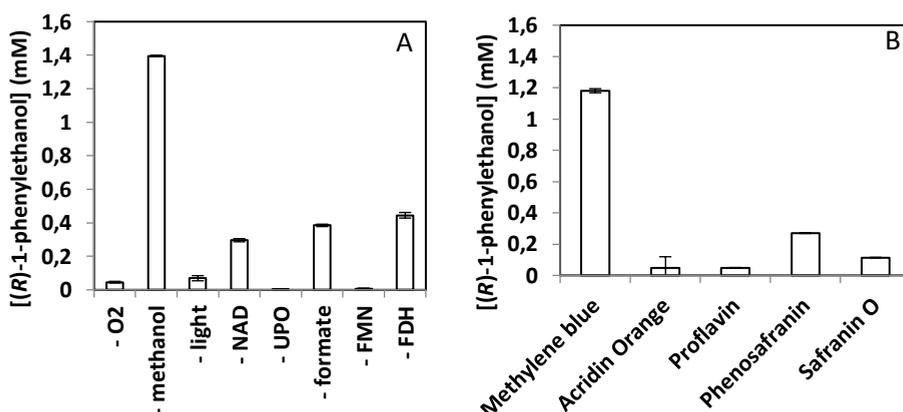
Figure 7. Negative control of the *Cb*FDH/r*Aae*UPO photocascade (A) system applying FMN as photocatalyst (B) cascade in dark conditions. Conditions: 300 rpm, 30 °C, 75 mM [formate], 50 mM potassium phosphate buffer (pH 7, 0.8% methanol (v/v)) , (A) [FDH] = 2.4 μM, 200 μM [NAD⁺],50 μM [FMN], 50 mM [ethylbenzene], 50 nM [UPO], λ_LED = 450 nm (B) [FDH] = 4.8 μM,[UPO] = 100 nM, [NAD⁺] = 400 μM [photocatalyst] = 50 μM, λ_LED = 450 + 520 + 630 nm

Next, the influence of different reaction parameters on the rate of the photoenzymatic hydroxylation has been examined in more details (**Figure 7**). In these conditions, the concentration of the photocatalysts directly influences the rate of the overall system

(**Figure 7A**). While this correlation is linear with methylene blue over the entire concentration range investigated, a saturation-type behaviour is observed with phenosafranin and FMN, which most likely can be attributed to the decreasing optical transparency of the reaction mixture at elevated concentrations of the latter photocatalysts. The overall reaction rate also directly correlates with the intensity of the light source (**Figure 7B**). Varying the concentration of either NAD$^+$ (**Figure 7E**) or *Cb*FDH (**Figure 7D**) directly influence the reaction rate while the concentration of r*Aae*UPO (**Figure 7C**) has no clear influence.

Overall, we conclude that the photochemical oxidation of NADH (being influenced by the *in situ* concentration of NADH and the concentration of the photoexcited catalyst(s) is overall rate-limiting under the conditions investigated. Interestingly, with methylene blue, an acceleration of the reaction rate is observed over time (**Figure 5D**). This acceleration could be assigned to a photochemical activation of the photocatalyst as a similar observation is made upon pre-incubation of methylene blue alone by red light (**Figure 16**); blue light does not induce this acceleration. It can also be attributed to side reaction/reactant(s) quenching the photoactivity of methylene blue. Currently, both hypotheses are still envisioned. One major challenge observed, especially using FMN as photocatalyst (**Figure 5D**), was the poor long-term stability of the overall reaction. Particularly, the NADH regeneration reaction was impaired.

Reaction Conditions (unless indicated otherwise): [rAaeUPO] = 50 nM, [CbFDH] = 2.4 µM, [NAD$^+$] = 0.2 mM, [NaHCO$_2$] = 75 mM, [ethylbenzene] = 10 mM, 50 mM potassium phosphate buffer (pH 7, 0.8% methanol (v/v)), T = 30 °C.
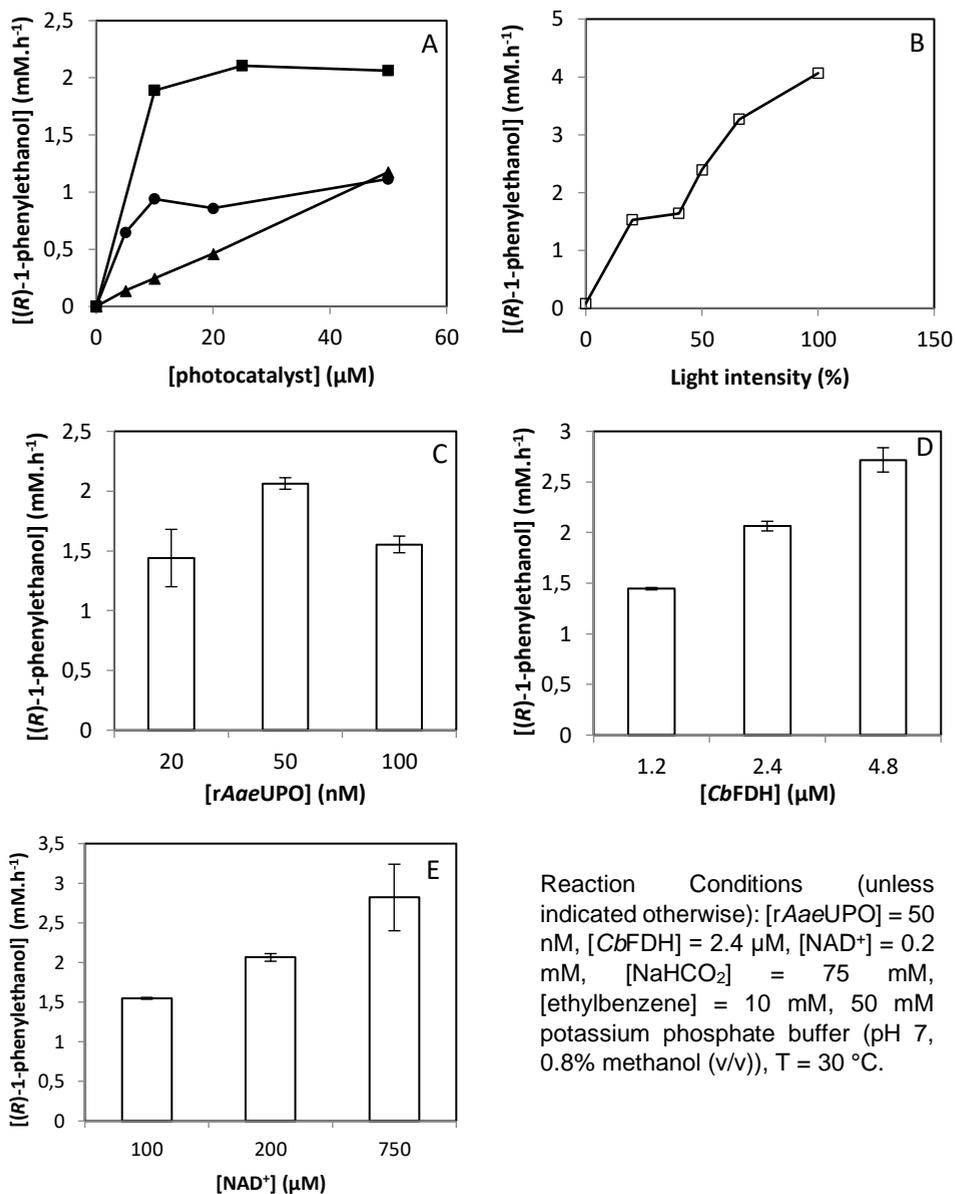
Figure 8. Influence of different parameters on rate of the hydroxylation of ethylbenzene. (A) Concentration of the photocatalyst (▲: methylene blue; ●: phenosafranin; ■: FMN); (B) intensity of broadband light source [rAaeUPO] = 100 nM, [CbFDH] = 4.8 µM, [NAD$^+$] = 0.4 mM); concentration of rAaeUPO (C), CbFDH (D), or NAD$^+$ (E).

3.2.4. Photostability

Therefore, the stability of *Cb*FDH in the presence of the photocatalysts upon illumination has been investigated (**Figure 8**). Especially, the flavin derived photocatalysts rapidly inactivates *Cb*FDH. The stability of *Cb*FDH decreases by a factor of 10 when exposed to light in presence of photocatalyst (half-life of 433 min in dark conditions). Especially flavins (riboflavin and FMN) are highly efficient towards enzyme inactivation.
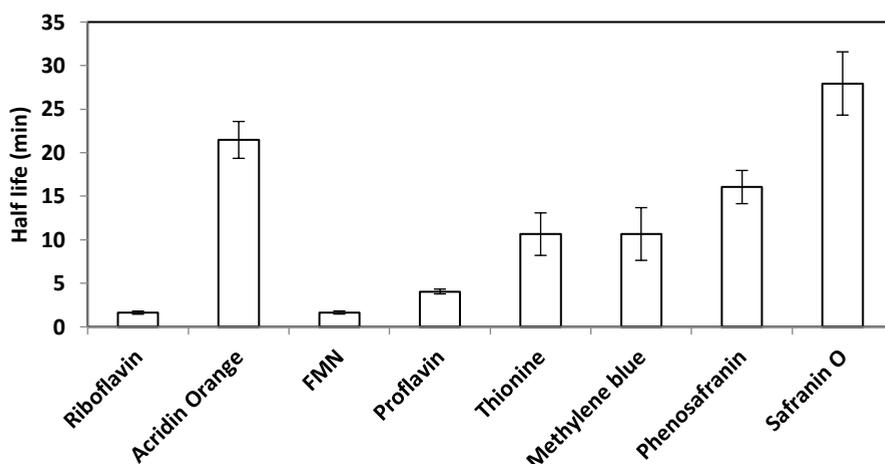
Figure 9. Stability of CbFDH in the presence of photocatalysts upon illumination. General conditions: [CbFDH] = 2.4 µM, [photocatalyst] = 50 µM, 50 mM potassium phosphate buffer (pH 7.0), 300 rpm, 30 °C.

To investigate the potential causes of this inactivation, methylene blue has been chosen as a model photocatalyst. *Cb*FDH was incubated with methylene blue in different conditions (**Figure 9**). *Cb*FDH activity is entirely lost after 40 min when mixed with methylene blue solution and is illuminated in aerobic conditions. Adding catalase to prevent accumulation of H_2O_2 does not influence this activity loss. In the meantime, the activity remains stable when: illumination is carried in anaerobic conditions, in aerobic conditions without methylene blue, or when no illumination is performed. Clearly, the combination of light, methylene blue and oxygen is causing the inactivation of *Cb*FDH. At that point, our best hypothesis was the formation of reactive oxygen species (ROS) that are known to form and/or be detrimental

radicals.[21] Based on these results, incubation of the enzyme has been repeated with the addition of Trolox (6-Hydroxy-2,5,7,8-tetramethylchroman-2-carboxylic acid, $C_{14}H_{18}O_4$), methionine or dithiothreitol. All these compounds have been reported to be radicals scavenger and oxygen singlet quencher.[22, 23] By addition of these compounds, the stability of *Cb*FDH is improved. More precisely, the activity decay is delayed (**Figure 10A**). Moreover, increasing scavenger concentration also increases the stability of *Cb*FDH (**Figure 10B**). Thus, ROS is likely responsible of the poor robustness. This might occur due to oxidative modification of surface-bound amino acids leading to enzyme inactivation/denaturation. On the basis of this, *Cb*FDH mutants exhibiting increased robustness in the presence of the excited photocatalysts can be conceived. In similar cases, this strategy resulted in significant stabilizations of the overall reaction.[24-27] Another already proposed solution for a similar case is to separate photo-and bio-catalysts.[21]

Another issue of the photoenzymatic reaction is photobleaching of the organic photocatalysts.[28, 29] Particularly, the flavin-based photocatalysts exhibit a modest stability upon illumination with 450 nm (**Figure 11**). Safranin derivatives excel in this respect by more than 100-fold longer half-life times as compared to, e.g., FMN. These findings also were confirmed in photo-enzymatic reactions using FMN, phenosafranin, or methylene blue, respectively in limiting concentration (**Table 2**). Compared to the first, the latter two give significantly higher turnover numbers.
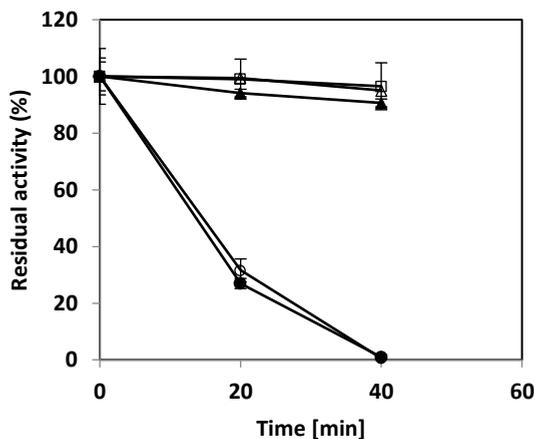
Figure 10. Stability of *Cb*FDH in the presence of methylene blue upon illumination in different conditions (○) reference, (Δ) anaerobic conditions, (□) without methylene blue, (●) with catalase, (▲) in dark conditions. Conditions: [*Cb*FDH] = 2.4 µM, [methylene blue] = 50 µM, 50 mM potassium phosphate buffer (pH 7.0), 30 °C, aerobic conditions, λ_{LED} = 630 nm
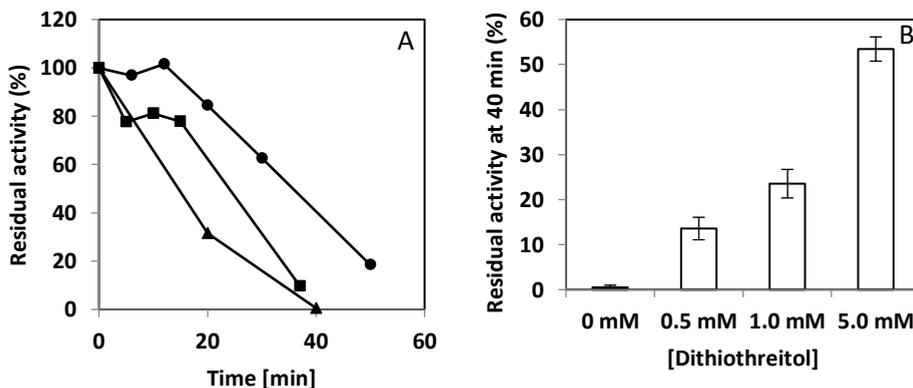
Figure 11. Influence of (A)Trolox (●) and methionine (■) (▲ no quencher)and (B) dithiothreitol concentration on *Cb*FDH stability upon illumination with methylene blue. Conditions: [*Cb*FDH] = 2.4 µM, [methylene blue] = 50 µM, 50 mM potassium phosphate buffer (pH 7.0), 30 °C, aerobic conditions, λ_{LED} = 630 nm, [Trolox] or [methionine] = 5 Mm
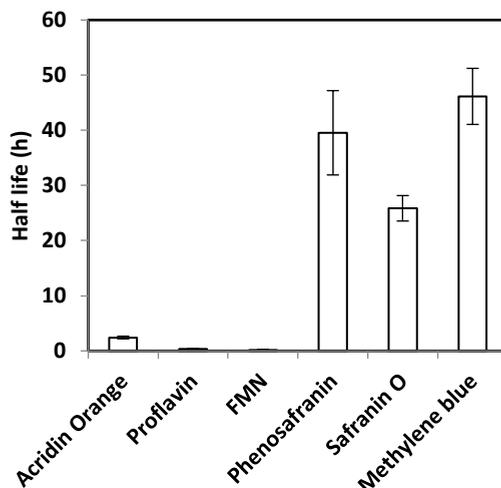
Figure 12. Stability of the photocatalysts upon illumination in presence of photocatalyst. Conditions: [CbFDH] = 2.4 µM, [photocatalyst] = 100 µM, 50 mM potassium phosphate buffer (pH 7), 300 rpm, 30 °C, , λ_{LED} = 450 nm (acridine orange, proflavin, FMN), 520 nm (phenosafranin, safranin) or 630 nm (methylene blue)

Table 1. Comparison of the turnover numbers (TON) of the different catalysts.

	$TON_{Photocatalyst}$	$TON_{rAaeUPO}$	TON_{CbFDH}
FMN	649	6490	135
phenosafranin	2500	25000	520
methylene blue	3992	39920	832

Conditions: [rAaeUPO] =100 nM, [CbFDH] = 4.8 µM, [NAD$^+$] = 0.4 mM, [NaHCO$_2$] = 75 mM, [ethylbenzene] = 10 mM, [photocatalyst] = 1 µM, 50 mM potassium phosphate buffer (pH 7, 0.8% methanol (v/v)), T= 30 °C, polychromatic light source.

3.3. Conclusion

Overall, mixing different photocatalysts has a beneficial effect when exposed to a polychromatic light source. Moreover, methylene blue and phenosafranin shows overall better performances than the previously reported FMN. In addition, if a system is sensitive to a specific wavelength, for instance blue light, another photocatalysts that absorb red light could be applied. This project was focused on applying photocatalysis for peroxide formation. Nevertheless, the scope of the system could be broadened. For instance, by applying the photocatalyst in other system in anaerobic conditions as previously reported for FMN.[16]

One promising way to further improve the light harvest is to apply a catalyst that converts infrared light (IR) into visible light that the other photocatalysts can then use. IR energy represents also a large part of the photo energy received on earth. Different systems have been reported that enable the conversion of IR up to visible light.[30, 31]

Nevertheless, this system is, at this stage, order of magnitude away from application. It does not represent a better solution concerning the formate oxidation of the full oxidation of methanol previously reported.[6] The possible generation of ROS, harmful for enzymes, is the greatest challenge regarding coupling photocatalysis and biocatalysis. One possibility to deal with this challenge is to supply the system with radical scavengers. But the addition of a new component in stoichiometric amount is not suitable. Also, engineering solutions such as physical separation is possible to prevent direct contact of the two catalytic systems but will affect greatly the rate of the reaction due to mass transfer limitation.[21] In view of direct application, it would be more suitable to find an enzyme that oxidize directly formate, a formate oxidase (FOx).

3.4. Materials & Methods

3.4.1.　Reaction conditions

Ethylbenzene, (R)-1-phenylethanol, (S)-1-phenylethanol, acetophenone, β-NAD$^+$ were purchased from Sigma–Aldrich in the highest purity available and used without

further purification. Formate dehydrogenase from *Candida boidinii* and the peroxygenase form *Agrocybe aegerita* were produced and purified according to previously published procedures.[32, 33]

3.4.2. Reaction conditions

Unless mentioned otherwise, reactions were performed at 30 °C in 50 mM potassium phosphate buffer pH 7.0, 300 rpm, 200 mM methanol, 400 µL reaction volume in 4 mL glass vials.

The reactions were performed in a jacketed beaker with commercial LEDs (24 W) winded around (**Figure 12** and **Figure 13**). The reactions vessels were placed in a homemade holder to ensure an equidistance between the reaction vessels and the light source (**Figure 12**).

For the reactions using a broad-spectrum light source, a LIGHTINGCURE LC8 L9566 (Hamamatsu) was used. The optic fibre of the light source was placed on top of a water bath.

Anaerobic reactions were performed in a glovebox with an atmosphere consisting in 98% N_2 and 2% H_2.

At different time intervals, aliquots were extracted with ethyl acetate (containing 5 mM 1-octanol as an internal standard). The organic phase was dried with magnesium sulfate, centrifuged and analyzed by GC.

Figure 13. In-house light set up consisting in a jacketed beaker with LEDs winded around (left) and white light set-up consisting on a water bath light beam coming from the top via an optic fibre (right).
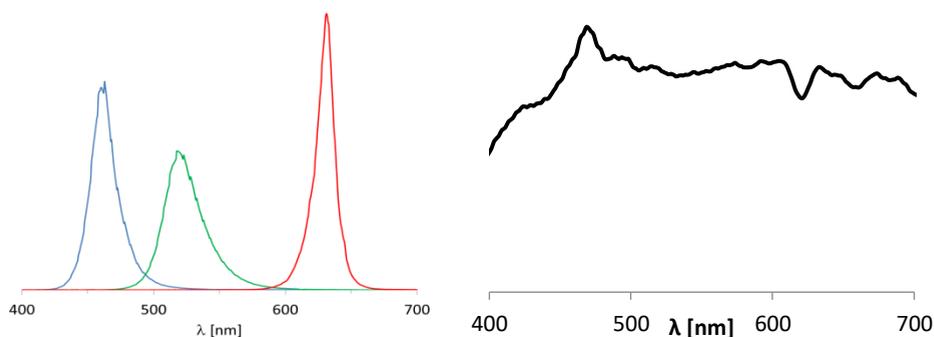
Figure 13. Emission spectra of the LEDs(left) and of the Hamamatsu LIGHTINGCURE LC8 L9566 (right).

3.4.3. Analytical procedures

3.4.3.1 Activity assays

Activity measurements were performed spectrophotometrically using the Agilent Technologies Cary 60 UV-Vis spectrophotometer (equipped with a single cell Peltier accessory) by monitoring the NADH consumption or generation, for FDH, respectively, at 340 nm in 1 mL plastic cuvettes.

The activity of FDH was measured in potassium phosphate buffer (50 mM) at 30 ˚C using NAD$^+$ (0.5 mM) and sodium formate (150 mM). The volumetric activities were calculated using an extinction coefficient of ε=6.3 mM^{-1}cm^{-1}.

3.4.3.2. GC measurements

GC measurements were performed using a GC-214 Gas Chromatograph (Shimadzu) equipped with a FID-Detector and a AOC-20i auto injector. Quantification of ethylbenzene, 1-phenylethanol and acetophenone were performed using a CP Wax 52CB column from Agilent (25m x 0.25mm x 1.2 µm); temp. program 150 °C hold 2.2 min; 25 °C/min to 210 °C hold 4.2 min, 30 °C/min to 250 °C hold 1 min. Retention times: ethylbenzene 1.60 min; 1-phenylethanol 7.15 min; acetophenone 5.90 min; 1-octanol (internal standard) 4.65 min (**Figure 14**). The enantiomeric excess for 1-phenylethanol was measured on a CP Chirasil Dex CB column from Agilent (25 m x 0.32 mm x 0.25 µm); temp. program 120 °C hold 2.6 min; 15 °C/min to 135 °C hold 3.3 min, 25 °C/min to 225 °C hold 1 min. Retention times: ethylbenzene 2.40 min; (*R*)-1-phenylethanol 6.20 min, (*S*)-1-phenylethanol 6.47 min; acetophenone 4.20 min (**Figure 15**).

All measurements have been performed at least as duplicates. Numbers shown are always based on calibration curves with authentic standards of the reagents (using internal standards). Error bars shown represent the standard deviation.
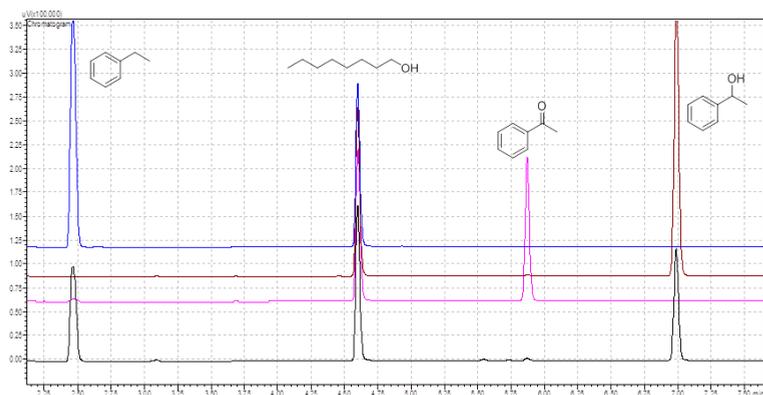
Figure 14. Example of chromatograms to quantify product formation. blue: ethylbenzene standard with octanol, brown: phenylethanol standard with octanol, pink: acetophenone standard with octanol, black: example of reaction
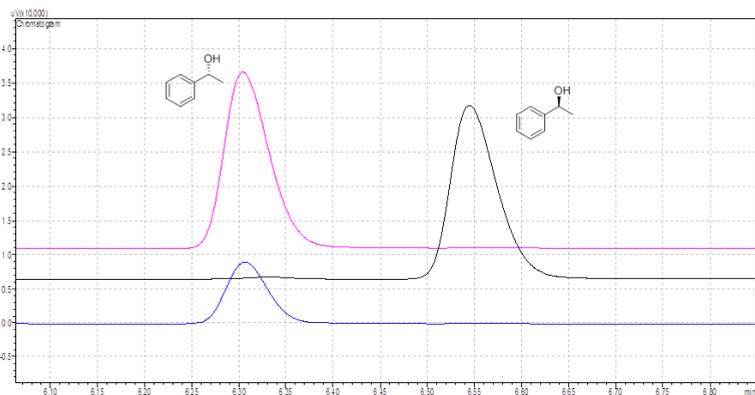
Figure 15. Exemplary chiral GC chromatograms of authentic (*R*)-1-phenylethanol and (*S*)-1-phenylethanol as well as one exemplary reaction product.

3.4.3.3. H_2O_2 concentration measurement

H_2O_2 concentration measurements were performed using an ABTS assay. Aliquots were mixed with 5 U (µmol. min^{-1}) of horseradish peroxidase and 1 mM 2,2'-azino-bis (3-ethylbenzothiazoline-6-sulphonic acid) (ABTS) in 50 mM phosphate buffer pH 7.0 at room temperature. The corresponding reaction will lead to the formation of an

absorbance peak at 420 nm which can be connected to the concentration of H_2O_2 with a calibration curve.

3.4.4. Additional Data

3.4.4.1. Photocatalyst screening

Several commercially available dyes have been screened. First, a reaction mixture of the photocatalyst and NADH were illuminated with the best overlapping LEDs light mode (blue, red or green) for 5 or 10 minutes. Then, if a significant change in the UV-Visible spectrum could be recorded, O_2 is introduced in the reaction mixture by bulling pure oxygen through it. The reaction is then placed in the dark and the UV-Visible spectrum is recorded again later on. The photocatalysts were successful if the initial spectrum could be partially recovered within a few minutes.

Table 2. UV-Visible spectra and conditions of the screened compounds.

Reaction steps	UV-Visible spectrum recorded
Acridine Orange 1. Initial spectrum 2. 5 minutes blue light illumination 3. 5 minutes in the dark with O_2	
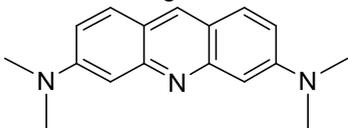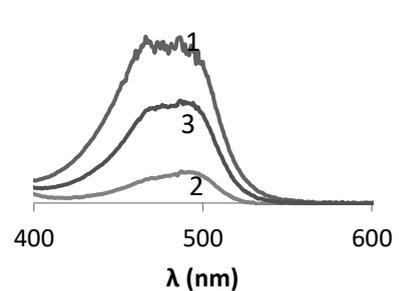
Proflavin
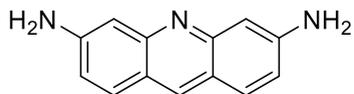
1. Initial spectrum
2. 5 minutes blue light illumination
3. 5 minutes in the dark with O_2
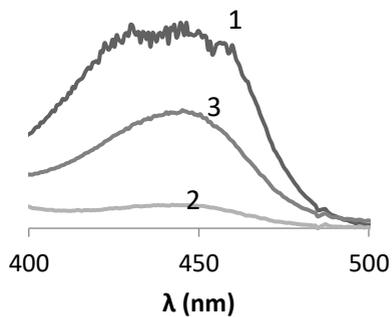
Alizarin yellow
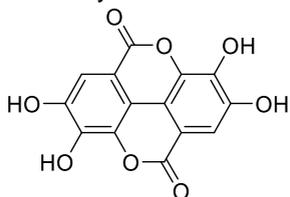
1. Initial spectrum
2. 5 minutes blue light illumination
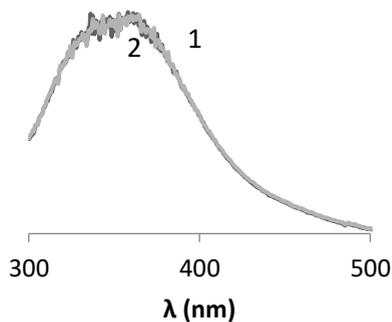
Alizarin red
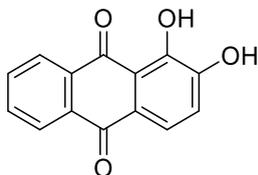
1. Initial spectrum
2. 5 minutes green light illumination
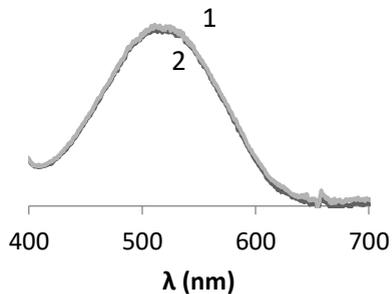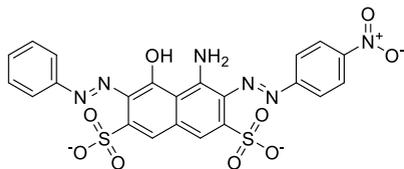
Amido Black 1. Initial spectrum 2. 5 min red light illumination	
Eosin Y 1. Initial spectrum 2. 5 min green light illumination 3. 30 min in the dark with O_2 4. 60 min in the dark with O_2	
Fluorescein 1. Initial spectrum 2. 10 min blue light illumination 3. 60 min in the dark with O_2 4. 180 min in the dark with O_2	
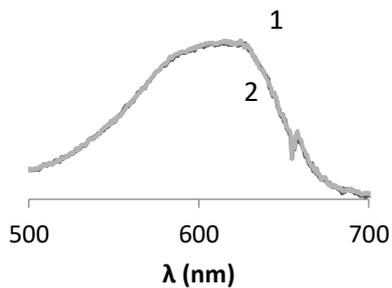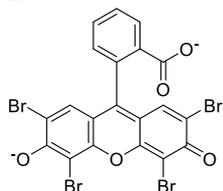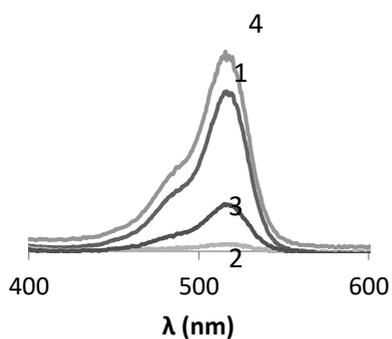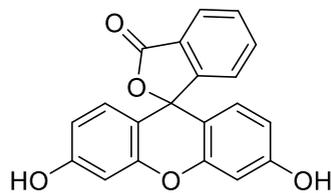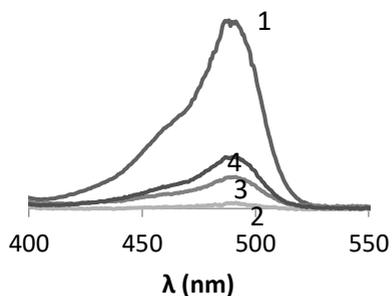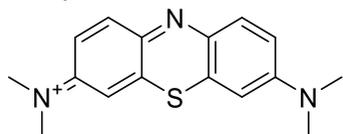
Methylene blue 1. Initial spectrum 2. 5 min red light illumination 3. 5 min in the dark with O_2	
Serva blue G 1. Initial spectrum 2. 5 min red light illumination	
Safranin O 1. Initial spectrum 2. 5 min green light illumination 3. 5 min in the dark with O_2	
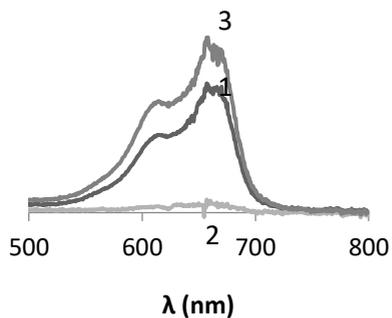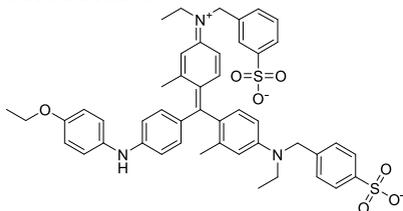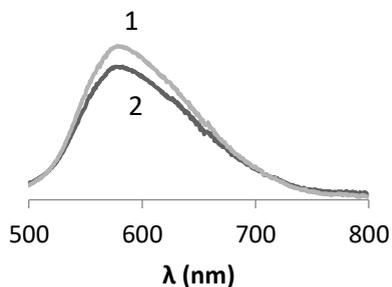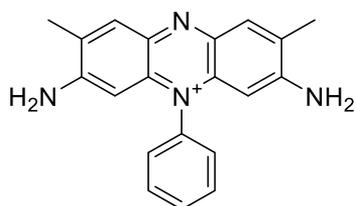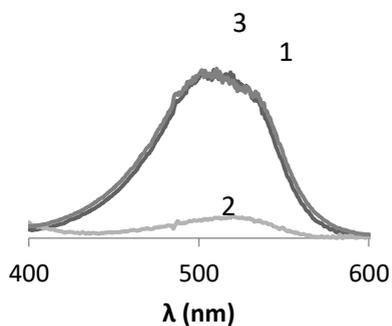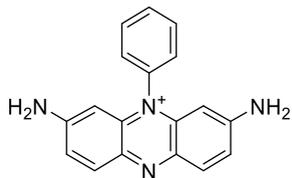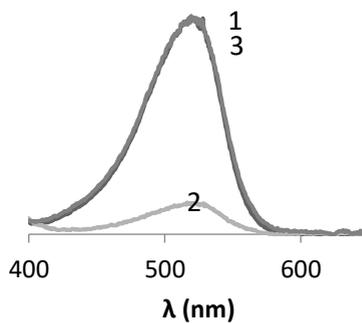
Phenosafranin	
Phenosafranin H_2N ... N^+ (phenyl) ... NH_2 N 1. Initial spectrum 2. 5 min green light illumination 3. 5 min in the dark with O_2	
Rose Bengal (structure with Cl, Cl, Cl, Cl, I, I, I, I, ^-O, O^-, O) 1. Initial spectrum 2. 5 min green light illumination 3. 24 h in the dark with O_2	
Rhodamine 6G (structure) 1. Initial spectrum 2. 10 min green light illumination	
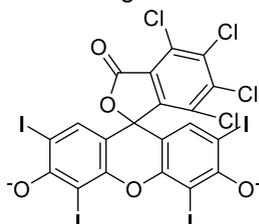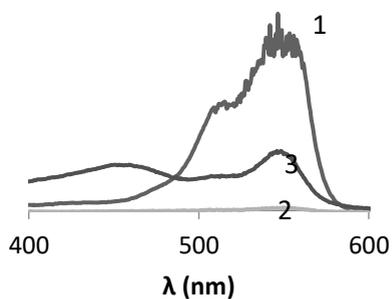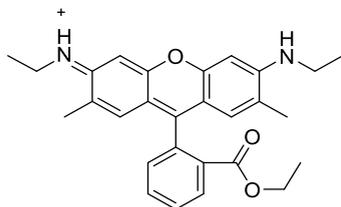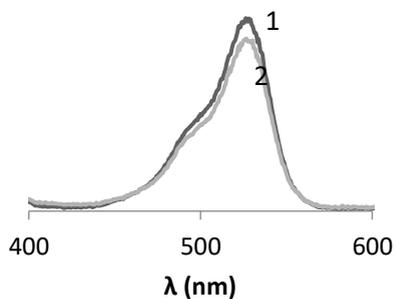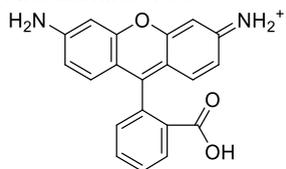
Rhodamine 110

1. Initial spectrum
2. 10 min green light illumination
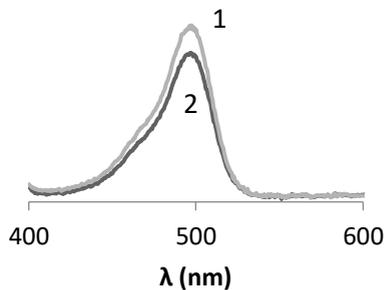
Rhodamine 101
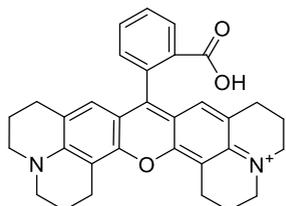
1. Initial spectrum
2. 10 min green light illumination
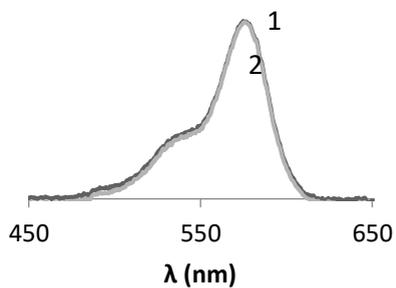
Rhodamine B
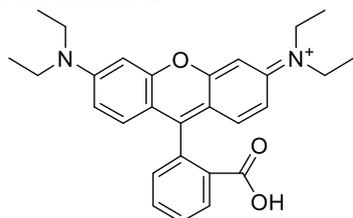
1. Initial spectrum
2. 10 min green light illumination
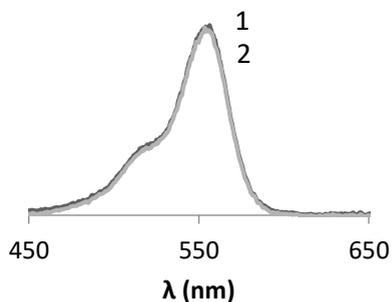
Rezasurin
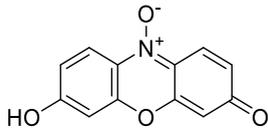
1. Initial spectrum
2. 10 min green light illumination
3. 24 h in the dark with O_2
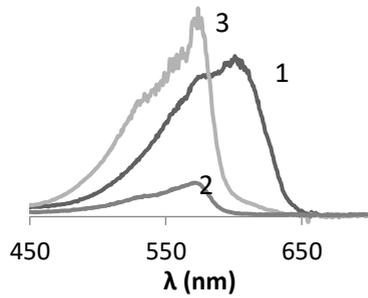
Neutral Red
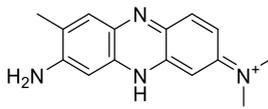
1. Initial spectrum
2. 5min red light illumination
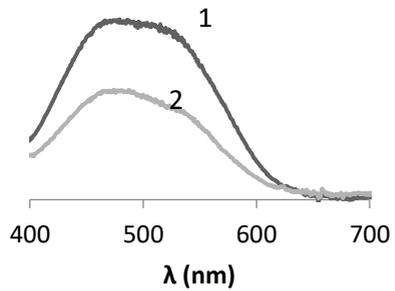
Indigo Carmin
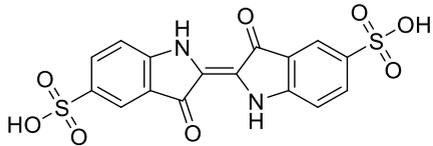
1. Initial spectrum
2. 5min red light illumination
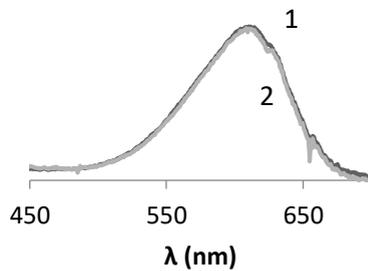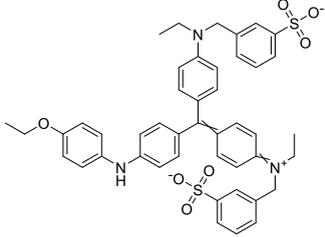
Coomassie blue 1. Initial spectrum 2. 5min red light illumination	
Cibracon 3G-A 1. Initial spectrum 2. 5min red light illumination	
Bromophenol blue 1. Initial spectrum 2. 5min red light illumination	
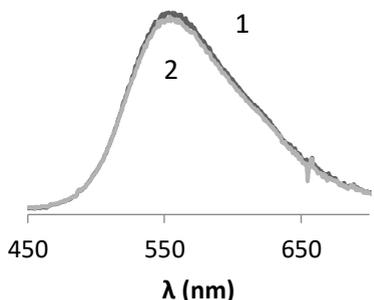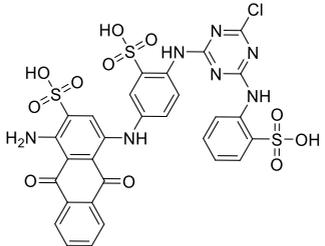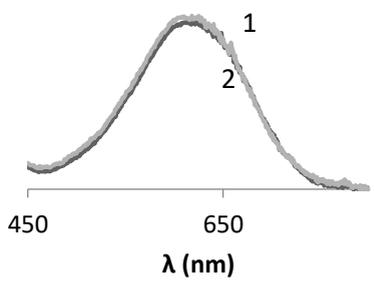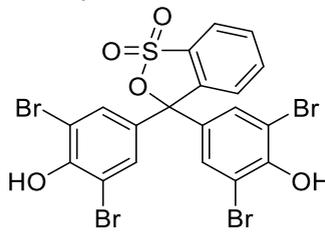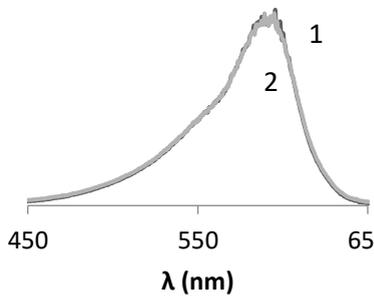
General conditions: [NADH] >300µm, 50 mM potassium phosphate buffer pH 7.0, 30 °C, anaerobic conditions (100% N_2), 300 rpm.

3.4.4.2. Methylene blue pre-illumination with red light

A lag phase could be noticed when methylene blue was applied in little amount. Thus, we decided to incubated methylene blue in light prior to the reaction to verify if light was the cause of this activation.
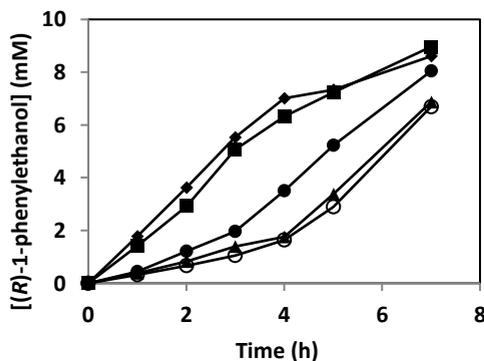
Figure 16. Phenylethanol production by the photoenzymatic cascade using methylene blue as photocatalyst. Prior the actual reaction methylene blue was illuminated with red light for (●) 20 min red light, (■) 60 min red light, (♦)120 min. For comparison: illuminations with blue light for (▲) 0 min or (○) 60 min. Conditions: [NaHCO$_2$] = 75 mM, 0.4 mM [NAD$^+$], [CbFDH] = 4.8 µM, 0.8%(v/v) methanol, [rAaeUPO]= 100 nM, 50 mM potassium phosphate buffer pH 7.0, 30 ˚C.

3.4.4.3. Experiments using a polychromatic (sun light-simulating) light source
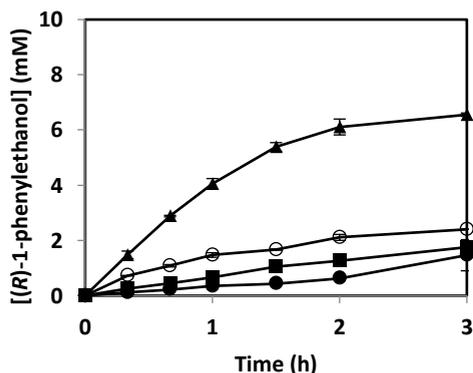
Figure 17. Time courses of some photoenzymatic transformations using a polychromatic light source, (○) ethylbenzene, (▲) phenylethanol). (▲): 5 µM phenosafranin + 10 µM methylene blue + 5 µM FMN, (■) 5 µM phenosafranin, (●) 10 µM methylene blue, (○) 5 µM FMN. Conditions: [NaHCO$_2$] = 75 mM, [NAD$^+$] = 0.4 mM, [FDH] = 4.8 µM, [rAaeUPO] = 100 nM, 50 mM potassium phosphate buffer (pH 7.0, 0.8%$_{(v/v)}$ methanol), 30 ˚C

3.5. References

1. Wang, Y.; Lan, D.; Durrani, R.; Hollmann, F., *Curr. Opin. Chem. Biol.* **2017,** *37*, 1.
2. Hofrichter, M.; Ullrich, R., *Curr. Opin. Chem. Biol.* **2014,** *19*, 116.
3. Dong, J.; Fernández-Fueyo, E.; Hollmann, F.; Paul, C.; Pesic, M.; Schmidt, S.; Wang, Y.; Younes, S.; Zhang, W., *Angew. Chem., Int. Ed.* **2018,** *57*, 9238.
4. Lutz, S.; Steckhan, E.; Liese, A., *Electrochem. Commun.* **2004,** *6*, 583.
5. Bankar, S. B.; Bule, M. V.; Singhal, R. S.; Ananthanarayan, L., *Biotechnol. Adv.* **2009,** *27*, 489.
6. Ni, Y.; Fernández-Fueyo, E.; Baraibar, A. G.; Ullrich, R.; Hofrichter, M.; Yanase, H.; Alcalde, M.; van Berkel, W. J. H.; Hollmann, F., *Angew. Chem., Int. Ed.* **2016,** *55*, 798.
7. Pesic, M.; Willot, S. J. P.; Fernández-Fueyo, E.; Tieves, F.; Alcalde, M.; Hollmann, F., *Z. Naturforsch., C: J. Biosci.* **2018**.
8. Pereira, P. C.; Arends, I.; Sheldon, R. A., *Process Biochem.* **2015,** *50*, 746.
9. Zhang, W.; Burek, B. O.; Fernández-Fueyo, E.; Alcalde, M.; Bloh, J. Z.; Hollmann, F., *Angew. Chem., Int. Ed.* **2017,** *56*, 15451.
10. Zhang, W.; Fernández-Fueyo, E.; Ni, Y.; van Schie, M.; Gacs, J.; Renirie, R.; Wever, R.; Mutti, F. G.; Rother, D.; Alcalde, M.; Hollmann, F., *Nat. Catal.* **2018,** *1*, 55.
11. Krieg, T.; Huttmann, S.; Mangold, K. M.; Schrader, J.; Holtmann, D., *Green Chem.* **2011,** *13*, 2686.
12. Churakova, E.; Arends, I. W. C. E.; Hollmann, F., *Chemcatchem* **2013,** *5*, 565.
13. Churakova, E.; Kluge, M.; Ullrich, R.; Arends, I.; Hofrichter, M.; Hollmann, F., *Angew. Chem., Int. Ed.* **2011,** *50*, 10716.
14. Perez, D. I.; Mifsud Grau, M.; Arends, I. W. C. E.; Hollmann, F., *Chem. Commun.* **2009**, 6848.
15. Popov, V. O.; Lamzin, V. S., *Biochem. J.* **1994,** *301*, 625.
16. Rauch, M.; Schmidt, S.; Arends, I. W. C. E.; Oppelt, K.; Kara, S.; Hollmann, F., *Green Chem.* **2017,** *19*, 376.
17. Kochius, S.; Ni, Y.; Kara, S.; Gargiulo, S.; Schrader, J.; Holtmann, D.; Hollmann, F., *ChemPlusChem* **2014,** *79*, 1554.
18. van Schie, M. M. C. H.; Younes, S. H. H.; Rauch, M. C. R.; Pesic, M.; Paul, C. E.; Arends, I. W. C. E.; Hollmann, F., *Mol Catal* **2018,** *452*, 277-283.
19. Könst, P.; Kara, S.; Kochius, S.; Holtmann, D.; Arends, I. W. C. E.; Ludwig, R.; Hollmann, F., *ChemCatChem* **2013,** *5*, 3027.
20. Frisell, W. R.; Chung, C. W.; Mackenzie, C. G., *J. Biol. Chem.* **1959,** *234*, 1297.
21. van Schie, M. M. C. H.; Zhang, W.; Tieves, F.; Choi, D. S.; Park, C. B.; Burek, B. O.; Bloh, J. Z.; Arends, I. W. C. E.; Paul, C. E.; Alcalde, M.; Hollmann, F., *Acs Catal* **2019**, 7409-7417.

22.   Alberto, M. E.; Russo, N.; Grand, A.; Galano, A., *Phys. Chem. Chem. Phys.* **2013,** *15* (13), 4642-4650.
23.   Banasova, M.; Valachova, K.; Juranek, I.; Soltes, L., *Chem. Pap.* **2014,** *68* (10), 1428-1434.
24.   Hildebrand, F.; Lütz, S., *Chem. - Eur. J.* **2009,** *15*, 4998.
25.   Rudroff, F.; Mihovilovic, M. D.; Gröger, H.; Snajdrova, R.; Iding, H.; Bornscheuer, U. T., *Nature Catal.* **2018,** *1*, 12.
26.   Sato, H.; Hummel, W.; Gröger, H., *Angew. Chem., Int. Ed.* **2015,** *54*, 4488.
27.   Zhang, W.; Fernandez Fueyo, E.; Hollmann, F.; Leemans Martin, L.; Pesic, M.; Wardenga, R.; Höhne, M.; Schmidt, S., *Eur. J. Org. Chem.* **2018**.
28.   Insinska-Rak, M.; Golczak, A.; Sikorski, M., *J. Phys. Chem. A* **2012,** *116*, 1199.
29.   Holzer, W.; Shirdel, J.; Zirak, P.; Penzkofer, A.; Hegemann, P.; Deutzmann, R.; Hochmuth, E., *Chem. Phys.* **2005,** *308*, 69.
30.   Wu, M. F.; Congreve, D. N.; Wilson, M. W. B.; Jean, J.; Geva, N.; Welborn, M.; Van Voorhis, T.; Bulovic, V.; Bawendi, M. G.; Baldo, M. A., *Nat. Photonics* **2016,** *10* (1), 31-34.
31.   Ravetz, B. D.; Pun, A. B.; Churchill, E. M.; Congreve, D. N.; Rovis, T.; Campos, L. M., *Nature* **2019,** *565* (7739), 343-346.
32.   Kara, S.; Schrittwieser, J. H.; Gargiulo, S.; Ni, Y.; Yanase, H.; Opperman, D. J.; van Berkel, W. J. H.; Hollmann, F., *Adv. Synth. Catal.* **2015,** *357* (8), 1687-1691.
33.   Molina-Espeja, P.; Ma, S.; Mate, D. M.; Ludwig, R.; Alcalde, M., *Enz. Microb. Tech.* **2015,** *73-74*, 29-33.

Chapter 4. Formate oxidase (FOx) from *Aspergillus oryzae*: one catalyst enables diverse H$_2$O$_2$-dependent biocatalytic oxidation reaction

Chapter based on:

Chapter 4. Formate oxidase (FOx) from *Aspergillus oryzae*: one catalyst enables diverse H$_2$O$_2$-dependent biocatalytic oxidation reaction

4.1. Introduction

As discussed in chapter 3, connecting formic oxidation and H$_2$O$_2$ production by a photo-enzymatic cascade is not trivial. The use of photocatalysis seems to engender poor robustness, mainly coming from the enzymatic activity loss. This tendency has been also reported for other similar systems. At this stage, applying photocatalyst(s) directly with enzyme seems to bring more challenges than solutions. Thus, the most suitable system might be only enzymatically based.

Today, glucose oxidase (GOx) is the catalyst of choice for *in situ* H$_2$O$_2$ generation.[1] It couples the oxidation of glucose to the reductive activation of O$_2$ to form H$_2$O$_2$ in a highly efficient and robust fashion. The GOx system, however, suffers from high levels of waste generation (196 g of gluconate waste per mol H$_2$O$_2$ equivalent are generated).[2] Additionally, practical issues such as the high viscosity of the reaction medium have to be dealt with at larger reaction scales. Formate would be a more suitable reductant for the reductive activation of O$_2$ (generating only 44 g of volatile and therefore not accumulating CO$_2$ waste per mol H$_2$O$_2$ equivalent). The systems available today, however, either rely on bioincompatible transition-metal catalysts,[3] or are too complex[2, 4] or too elaborate[5, 6] to be practical.

Recently, a formic acid oxidase from *Aspergillus oryzae* (*Ao*FOx) has been reported as the first member of the glucose-methanol-choline (GMC) oxidoreductase superfamily that oxidizes formic acid instead of simple alcohols.[7-11] This enzyme features a wide pH activity range from 2.8–6.8 and a k$_{cat}$ value of 82 s^{-1} over that range. It contains an unusual 8-formyl flavin adenine dinucleotide (FAD) cofactor, which is formed *in situ* from FAD through self-oxidation. Its unique catalytic properties render *Ao*FOx a promising candidate for H$_2$O$_2$-dependent enzymatic reactions. We therefore set out to evaluate the potential of *Ao*FOx as a catalyst to promote H$_2$O$_2$-dependent biocatalytic oxidation reactions (**Scheme 1**).

Chapter 4. Formate oxidase (FOx) from *Aspergillus oryzae*: one catalyst enables diverse H₂O₂-dependent biocatalytic oxidation reaction
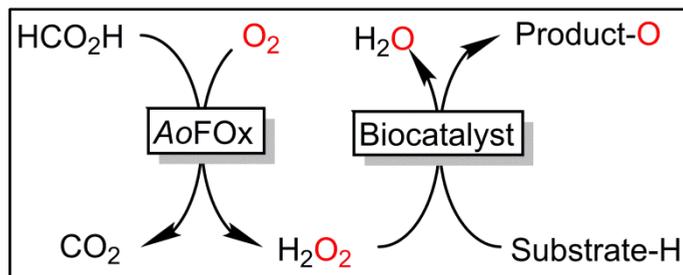
Scheme 2. The formate oxidase from *Aspergillus oryzae* (*Ao*FOx) enables *in situ* H₂O₂ generation from formate and ambient oxygen to promote a broad range of biocatalytic oxidation reactions.

4.2. Benchmark *Ao*FOx with r*Aae*UPO hydroxylation

*Ao*FOx was prepared according to a previously published procedure.[12] In short, *Ao*FOx was produced in recombinant *E. coli* and partially purified to remove catalase activity. Overall, from 1 L culture broth, 38 mg of purified enzyme were obtained within 1 day (see section 4.6.1.).

Having *Ao*FOx in hand, we decided to first apply this enzyme for some selective oxyfunctionalisation reactions catalysed by the recombinant evolved unspecific peroxygenase from *Agrocybe aegerita* (r*Aae*UPO) produced by *Pichia pastoris*.[13-15] As a model reaction, we first focused on the selective hydroxylation of ethyl benzene into (*R*)-1-phenylethanol. A preliminary optimisation of the reaction conditions (**Figure 1**) revealed that the bienzymatic cascade operates optimally in slightly acidic reaction media (pH 6, **Figures 1 and 9**), which is in line with the reported preferences of the enzymes and its stability (**Figure 17**).[16] An apparent optimal temperature of 25 °C was determined (**Figures 1**). Between 20 and 35 °C, the initial rates of the overall system were largely temperature independent (**Figure 10**) but the reaction ceased sooner at elevated temperatures. At 40 °C for example, no further product formation was observed after 2 h. In contrast, steady product accumulation occurred at 30 °C or lower. This behaviour can be attributed to the poor thermal stability of *Ao*FOx (**Figure 18**).

Chapter 4. Formate oxidase (FOx) from *Aspergillus oryzae*: one catalyst enables diverse H_2O_2-dependent biocatalytic oxidation reaction
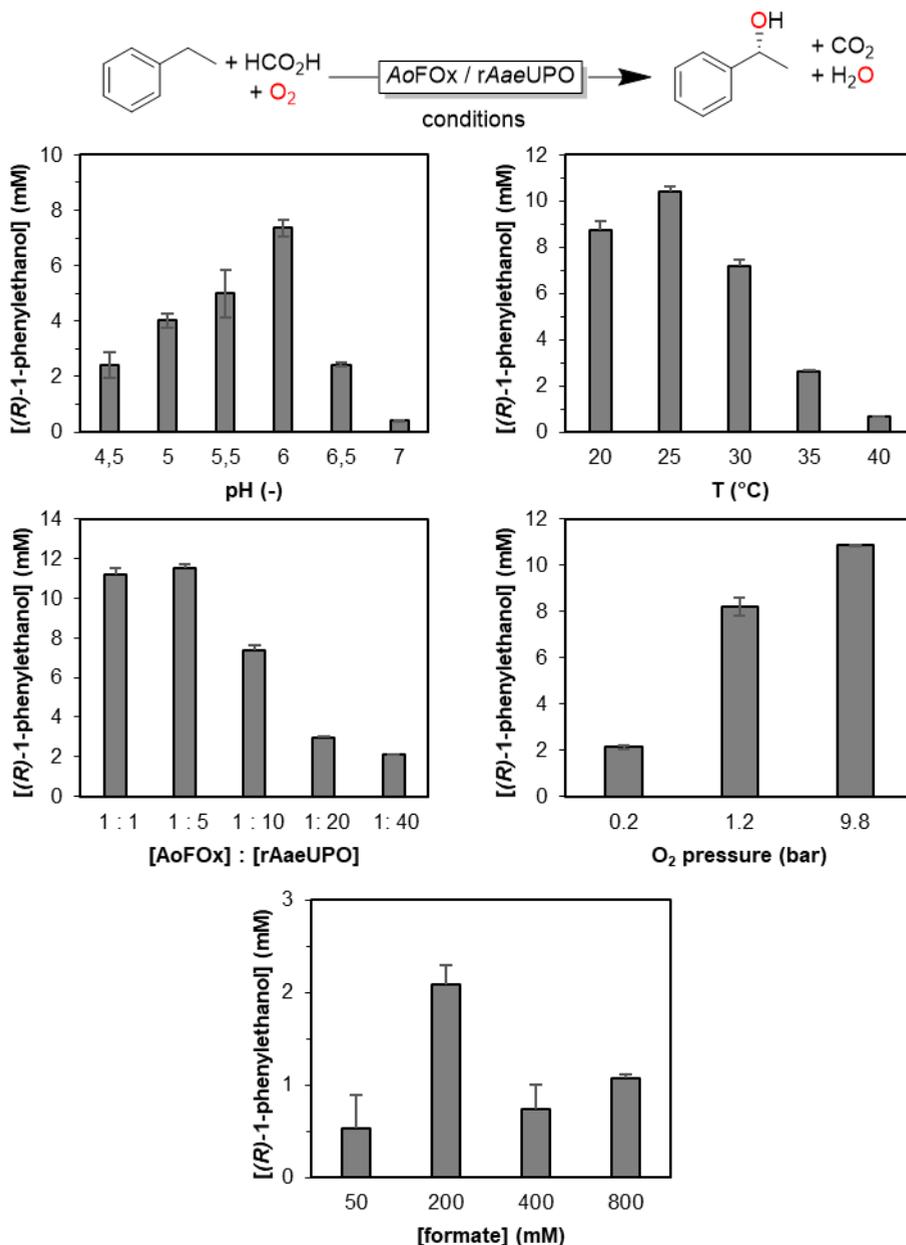
Figure 14. Characterisation of the reaction parameters that influence the efficiency of the bienzymatic hydroxylation of ethyl benzene. Individual reaction conditions are given in Figures 2, 9-12.

We determined an apparent optimal formate concentration of 200 mM (**Figures 1 and 12**), which represents a compromise between the relatively high K_M value of

86

*Ao*FOx at this pH and the decreasing peroxygenase activity of UPOs at higher formate concentrations.[17]

The relative ratio of (H_2O_2-generating) *Ao*FOx and (H_2O_2-consuming) r*Aae*UPO had a very pronounced effect on the efficiency of the overall reaction system (**Figures 1 and 11**). The highest initial rate was observed at an equimolar ratio of the two enzymes, albeit at the expense of poor long-term stability of the overall system (after 5 h, no further product formation was observed; **Figure 11**). Lower ratios of *Ao*FOx to r*Aae*UPO gave lower productivity but significantly greater robustness. At a ratio of 1:5, stable product formation for at least 24 h was observed.

The availability of molecular oxygen had a significant influence on the overall reaction (**Figure 1**). Previous studies on *Ao*FOx[10] show that K_M towards molecular oxygen is 240 µM, which is approximatively the solubility of O_2 in water at room temperature. Under ambient atmosphere without stirring, an O_2 transfer rate of 0.84 ± 0.03 mM h^{-1} was estimated, which limits the productivity of the overall system. Increasing the O_2 availability by increasing the O_2 partial pressure in the headspace of the reaction dramatically increased the productivity of the overall reaction more than ten-fold (**Figure 1 and 2**).

All negative controls (i.e. reactions leaving out either one of the enzymes or reactions in the absence of formate) were performed for all of the reactions reported. With the sole exception of Cytochrome C (CytC) catalysed sulfoxidation, where traces of sulfoxide were also observed in the absence of CytC, the control reactions gave no product formation.
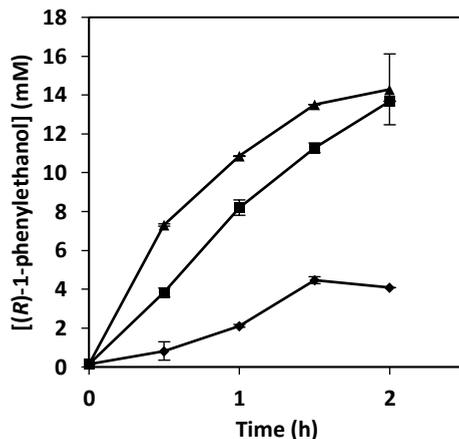
Figure 15. Effect of oxygen pressure on AoFOx-driven oxidation of ethylbenzene by rAaeUPO. Conditions: 100 mM potassium phosphate buffer (pH 6.0), 25 °C, [ethylbenzene] = 100 mM, [r*Aae*UPO] = 1 µM, [*Ao*FOx] = 100 nM and [NaHCO₂] = 200 mM.0 (squares), 2.0 (circles) or 10.6 bar.
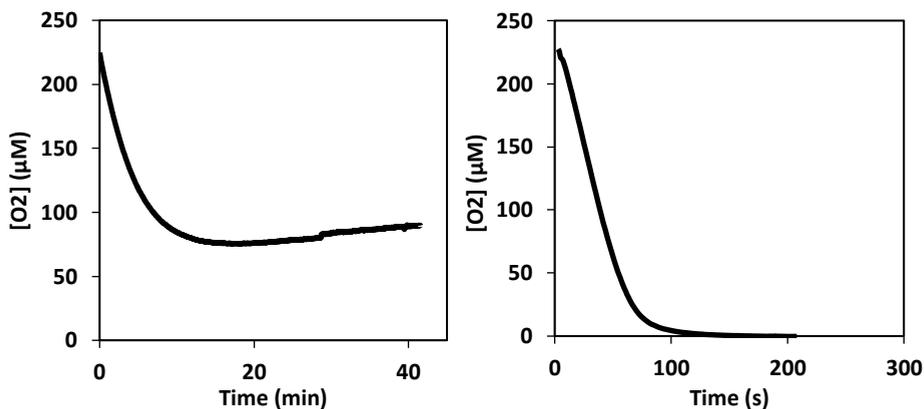
Figure 16. Oxygen consumption measured with a Clark electrode[18] during rAaeUPO/AoFOx cascade applying either 10 (left) or 100 (right) nM *Ao*FOx. Conditions: 100 mM potassium phosphate buffer (pH 6.0), 25 °C, [ethylbenzene] = 100 mM, [r*Aae*UPO] = 100 nM, [*Ao*FOx] = 10-100 nM and [NaHCO₂] = 200 mM.

4.3. Peroxizyme scope

Next, we explored the enzyme and product scope of the *Ao*FOx-catalysed H$_2$O$_2$ generation system to promote various H$_2$O$_2$-dependent biocatalytic oxidation reactions (**Figures 4-7**). First, we investigated some peroxygenase-catalysed hydroxylation and epoxidation reactions. The proposed H$_2$O$_2$-generation system enabled excellent catalytic performance of the peroxygenase used. Both product concentrations and r*Aae*UPO-turnover numbers were at least as high as for previous methods using more complicated H$_2$O$_2$ generation systems.[2, 19-22]

The stereospecific hydroxylation of ethyl benzene was performed on a semi-preparative scale, yielding 434 mg of *(R)*-1-phenylethanol (see 4.5.4.). A very satisfactory turnover number for the *Ao*FOx of more than 300,000 was achieved, which suggests that this in situ H$_2$O$_2$ generation system is potentially economically feasible. It is also worth mentioning that up to 31.3 mM (*R*)-1-phenylethanol was produced (**Figure 13**), which is one of the highest numbers observed so far using r*Aae*UPO.[2] It should be mentioned here that in case of volatile reagents, imperfect mass balances were observed upon prolonged reaction times. We believe that this is a technical issue that will be overcome in future scale-up experiments.

Cytochrome C, another heme-containing protein capable of catalysing H$_2$O$_2$-driven oxygen transfer reactions, especially sulfoxidation,[23] was evaluated next (**Figure 5**). Compared with the turnover numbers observed with r*Aae*UPO, the numbers achieved with CytC appear rather low. However, these numbers are still significantly higher than those achieved previously using other H$_2$O$_2$-generation systems.[23] The lack of enantioselectivity in the sulfoxidation of thioanisole is in accordance with previous reports.[23] It should be kept in mind here that the natural role of CytC is not that of an enzyme but rather that of an electron-transport protein.

Chapter 4. Formate oxidase (FOx) from *Aspergillus oryzae*: one catalyst enables diverse H$_2$O$_2$-dependent biocatalytic oxidation reaction

4.2 ± 0.1 mM (42%)
TON$_{AoFox}$ = 420,000
TON$_{rAaeUPO}$ = 83,000

7.3 ± 0.1 mM (89%) 99.3 % ee
TON$_{AoFox}$ = 146,300
TON$_{rAaeUPO}$ = 36,600

31 ± 0.6 mM (31%) 99% ee
TON$_{AoFox}$ = 318,000
TON$_{rAaeUPO}$ = 31,800
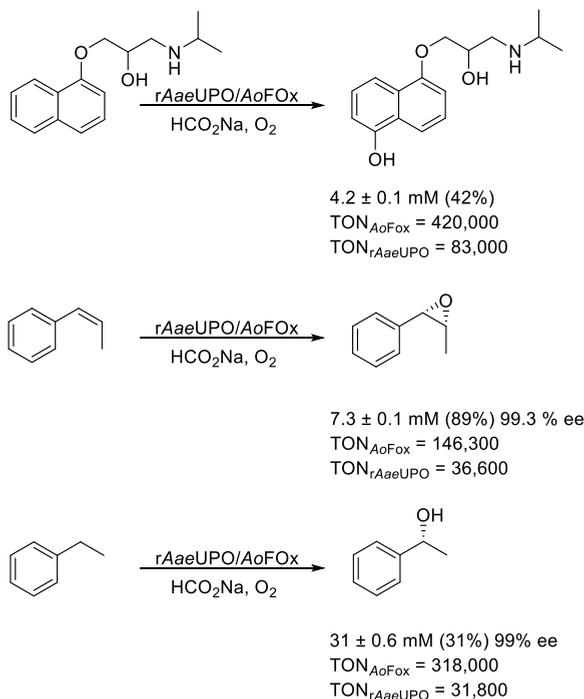
Figure 17. Oxyfunctionalization catalysed by r*Aae*UPO/*Ao*FOx cascade: hydroxylation of propranolol to 5'-hydroxypropanolol epoxidation of *cis*-β-methylstyrene to *cis*-methylstyrene oxide hydroxylation of ethylbenzene to *(R)*-1-phenylethanol. See section 4.5.2. for conditions and time courses.

7.2 ± 0.1 mM (72%) <5 % ee
TON$_{AoFox}$ = 716,000
TON$_{CytC}$ = 360
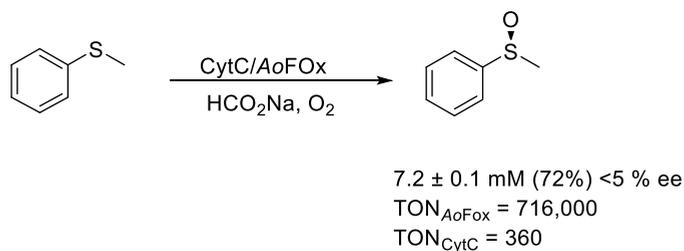
Figure 18. Sulfoxidation of thioanisole into methyl phenyl sulfoxide catalysed by CytC/*Ao*FOx cascade. See section 4.5.2. for conditions and time courses.

Another important H_2O_2-driven reaction is the so-called perhydrolase reaction of lipases.[24, 25] In short, a lipase catalyses the perhydrolysis of carboxylic (esters) to yield a reactive peracid, which in turn can undergo Baeyer–Villiger oxidations of ketones or Prilezhaev oxidations of C=C-double bonds. Our proposed *Ao*FOx H_2O_2-generation system proved to be applicable in principle to drive these reactions (**Figure 6**). Using the lipase B from *Candida antarctica*, *Ca*lB) together with octanoic acid as co-catalyst gave catalytic turnover in the chemoenzymatic Baeyer–Villiger oxidation of cyclohexanone as well as the chemoenzymatic epoxidation of styrene. However, compared to the other systems investigated here, rather low turnover numbers for the biocatalyst were observed. This can be attributed to the low affinity of *Ca*lB towards H_2O_2 in aqueous systems[26-28] resulting in low *Ca*lB activity under the conditions chosen. Further investigations aiming at higher *in situ* H_2O_2 concentrations are currently ongoing.

2.1 ± 0.2 mM (21%), *rac.*
TON_{AoFox} = 22,100
TON_{CalB} = 110

1.4 ± 0.2 mM (14%) *rac.*
TON_{AoFox} = 14,200
TON_{CalB} = 71
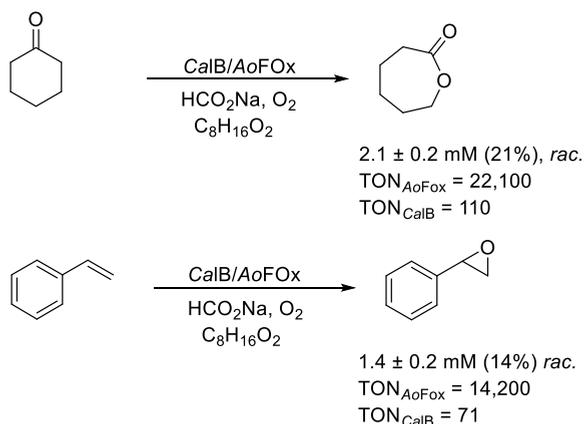
Figure 19. Baeyer-Villiger oxidation of cyclohexanone to caprolactone and epoxidation of styrene to styrene oxide catalysed by *Ca*lB/*Ao*FOx cascade Conditions: 100 mM potassium phosphate buffer (pH 6.5), 30°C, [cyclohexanone] or [styrene] = 10 mM, [*Ca*lB] = 20 µM, [*Ao*FOx] = 100 nM, [octanoic acid] = 10 mM and [NaHCO₂] = 200 mM, 24 h.

Finally, we evaluated *Ao*FOx to promote halogenation reactions catalysed by the V-dependent haloperoxidase from *Curvularia inaequalis*.[29, 30] The halohydroxylation of styrene gave acceptable results in terms of product yield and catalyst performance. Again, the volatility of the reagents impaired the final product concentration and

thereby the catalytic numbers. A completely different picture evolved, however, when using 4-pentenoic acid as starting material. Here, a perfect mass balance was observed and full conversion of the starting material into the desired bromolactone was observed. We also scaled up this reaction to gram scale. Starting from 200 mM 4-pentenoic acid, 150 mM of the desired bromolactone was obtained, which could be separated from the reaction mixture by simple extraction. Thus, 1.6 g of the pure product was obtained. To achieve such a conversion and yield, *Ao*FOx was fed to the reactions several times, 100 nM every 24h approximatively (**Figure 8**). Each fed FOx giving TTN of 100,000 individually.

10.8 mM (54%)
TON_{AoFox} = 1,080,000
TON_{CiVCPO} = 108,000

150 mM
(75%, 45 % isolated, 1.6 g)
TON_{AoFox} = 150,000
TON_{CiVCPO} = 1,500,000
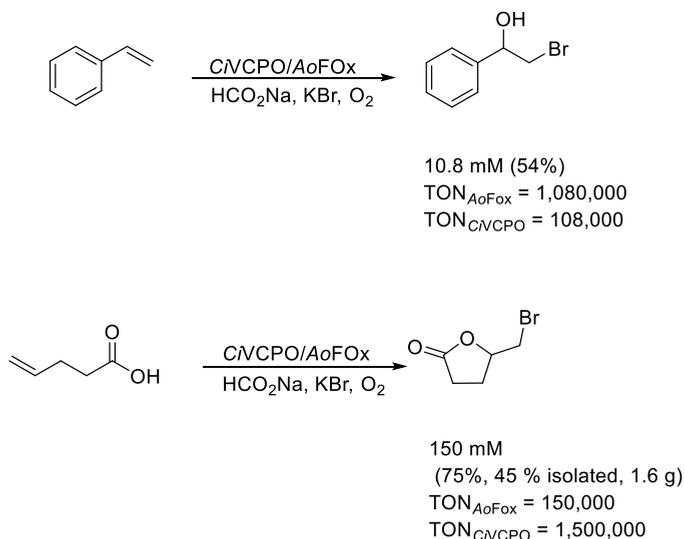
Figure 20. Halohydroxylation of styrene to 2-bromo-1-phenylethanol and halolactonisation of pentenoic acid to 5-(bromomethyl)dihydrofuran-2(3H)-one catalysed by *Ci*VCPO/*Ao*FOx cascade Conditions: 100 mM citrate buffer (pH 6.0), 30°C, [styrene] = 20 mM, [*Ci*VCPO] = 100 nM, [*Ao*FOx] = 10 nM, [octanoic acid] = 10 mM and [NaHCO₂] = 200 mM, overnight see NMR analysis in section 4.5.2. for halohydroxylation conditions and time courses see conditions of halolactonisation on Figure 8.
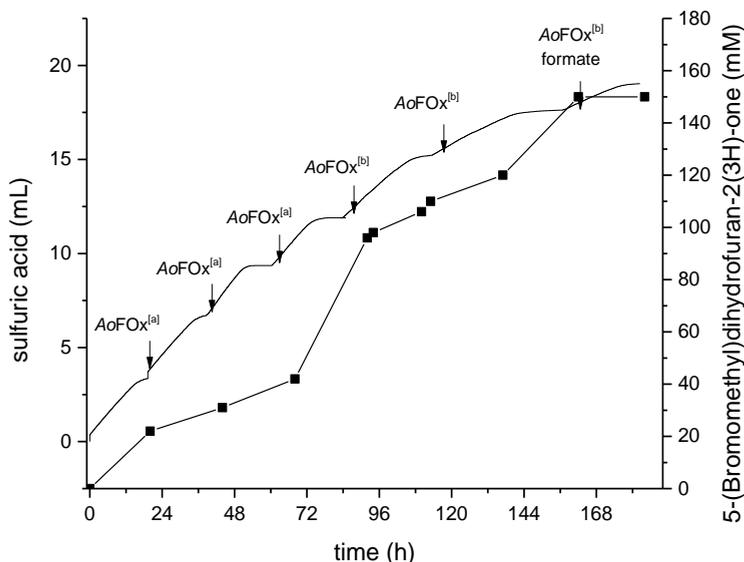
Figure 21. **Time course of halolactonisation catalysed by CiVCPO/AoFOx with the corresponding acid titration to maintain pH 6.0 from Figure 7.** Conditions: Preparative-scale bromolactonisation reactions were performed using a pH STAT titration system (Metrohm). 100 mM potassium phosphate buffer (pH 6.0) 25 °C [4-pentenoic acid] = 200 mM, [*Ci*VCPO] =100 nM, [*Ao*FOx] = 100 nM, [KBr] = 160 mM and [NaHCO₂] = 200 mM. After addition of pentenoic acid, the pH was set to pH 6 by the addition of KOH (100 mM). During the reaction, an acid mixture (1 M sulfuric acid + 200 mM formic acid) was titrated to maintain pH 6. [a] addition of *Ao*FOx (100 nM) [b] addition of *Ao*FOx (200 nM) .

4.4. Conclusion

In conclusion, we present that a simple H_2O_2 generation system based on formate oxidase is not only feasible but viable. This system stands out in terms of practical simplicity and excellent performance, even at this early stage of development. Furthermore, the turnover numbers achieved with *Ao*FOx exceed those of established systems by orders of magnitude (**Table 1**).

Three decades ago, the introduction of formate dehydrogenases as NADH regeneration catalysts ushered in a new era in bioreduction catalysis.[31-34] We are convinced that formate oxidases will have a similar impact for biooxidation/functionalisation catalysis. Further developments in our laboratories will

Chapter 4. Formate oxidase (FOx) from *Aspergillus oryzae*: one catalyst enables diverse H$_2$O$_2$-dependent biocatalytic oxidation reaction

focus on further engineering *Ao*FOx (in particular, a lower K$_M$ value towards formate is highly desirable) and further characterisation and optimisation of the synthetic schemes to fully explore its synthetic potential.

Table 4. Performances of other regeneration systems for peroxizymes

Product	Cosubstrate/ Coproduct	Catalyst: TN	Peroxizyme: TN	Ref
Thioanisole sulfoxide	Glucose/gluconolactone	GOx: 1163	*Cf*CPO: 43100	[35]
(R)-1-phenylethanol	MeOH/CO$_2$	AOx: 245580 FDM: 25400 FDH: 14730 3HB6H: 1330 NAD: 9	r*Aae*UPO: 294700	[2]
Limonene oxide	Choline/betain	ChOx: 350	Lipase <1000	[36]
(R)-1-phenylethanol	HCO$_2$H/CO$_2$	FDH: 39000 NAD: 19 Yqjm: 3600	r*Aae*UPO: 390000	[37]
(R)-1-phenylethanol	Cathode	-	r*Aae*UPO: 140000	[38]
(R)-1-phenylethanol	EDTA/(EDTriA/CH$_2$O/ CO$_2$)	FMN: <1000	r*Aae*UPO: 30000	[39]
(R)-1-phenylethanol	H$_2$O/O$_2$	Au-TiO$_2$ / n.d.	r*Aae*UPO: 38000	[6]

4.5. Supplementary data

4.5.1. Time course Ethylbenzene hydroxylation benchmark
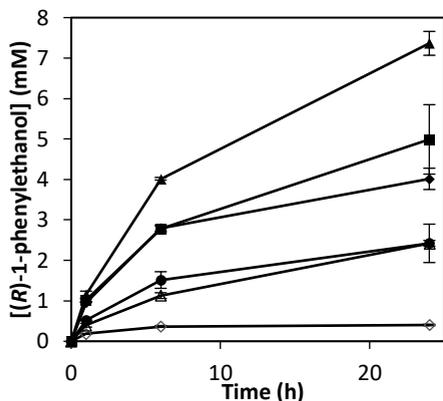
Figure 9. Influence of pH on the *Ao*FOx-driven oxidation of ethylbenzene catalysed by r*Aae*UPO. pH 7.0 (white diamond), pH 6.5 (circle), pH 6.0 (triangle), pH 5.5 (square), pH 4.5 (white triangle).

Conditions: 100 mM acetate buffer acetate buffer (pH 4.5-5.5) or potassium phosphate buffer (pH 6.0-7.0), 25 °C, [ethylbenzene] = 100 mM, [r*Aae*UPO] = 200 nM, [*Ao*FOx] = 20 nM and [NaHCO₂] = 100 mM
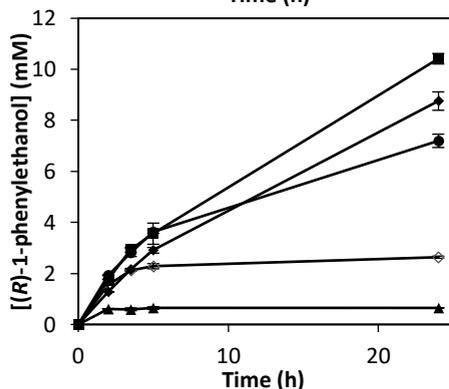
Figure 10. Influence of reaction temperature on the *Ao*FOx-driven oxidation of ethylbenzene catalysed by r*Aae*UPO. 20 °C(diamond), 25 °C(square), 30 °C(circle), 35 °C(white diamond), 40 °C(triangle)

Conditions: 100 mM potassium phosphate buffer (pH 6.0), 20-40 °C, [ethylbenzene] = 100 mM, [r*Aae*UPO] = 200 nM, [*Ao*FOx] = 20 nM and [NaHCO₂] = 100 mM
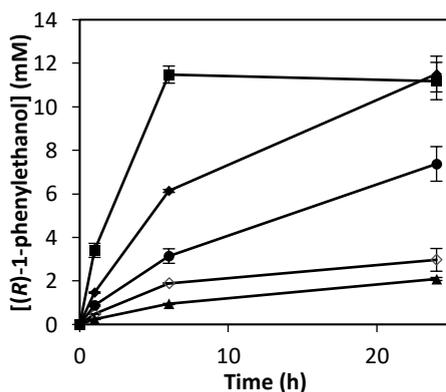
Figure 11. Influence of different enzyme ratios on the *Ao*FOx-driven oxidation of ethylbenzene catalysed by r*Aae*UPO. *Ao*FOx:r*Aae*UPO ratio: 1:40 (triangle), 1:20 (white diamond), 1:10 (circle), 1:5 (diamond), 1:1(square), Conditions: 100 mM potassium phosphate buffer (pH 6.0), 20-40°C, [ethylbenzene] = 100 mM, [r*Aae*UPO] = 100 nM, [*Ao*FOx] = 2.5-100 nM and [NaHCO₂] = 200 mM
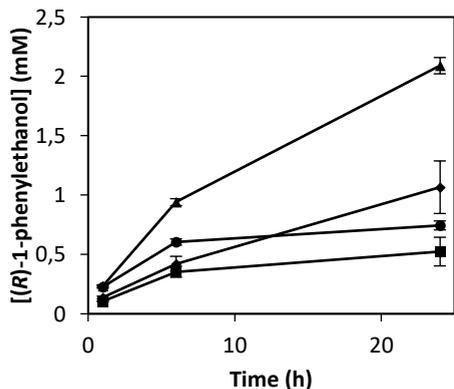
Figure 12. The effect of different sodium formate concentrations on the *Ao*FOx-driven oxidation of ethylbenzene catalysed by r*Aae*UPO. [formate]: 50 mM (square), 200 mM (triangle), 400 mM (circle), 800 mM (diamond),

Conditions: 100 mM potassium phosphate buffer (pH 6.0), 25 °C, [ethylbenzene] = 100 mM, [r*Aae*UPO] = 100 nM, [*Ao*FOx] = 2.5 nM and [NaHCO₂] = 50-800 mM

4.5.2. Time course substrate scope
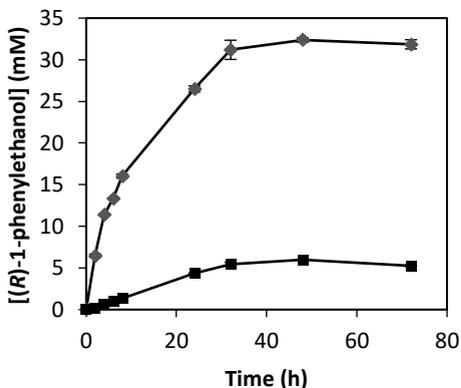
Figure 13. *Ao*FOx-driven oxidation of ethylbenzene to phenylethanol (diamond) and acetophenone (square) catalysed by r*Aae*UPO.

Conditions: 100 mM potassium phosphate buffer (pH 6.0), 25 °C, [ethylbenzene] = 100 mM, [r*Aae*UPO] = 1 μM, [*Ao*FOx] = 100 nM and [NaHCO₂] = 200 mM
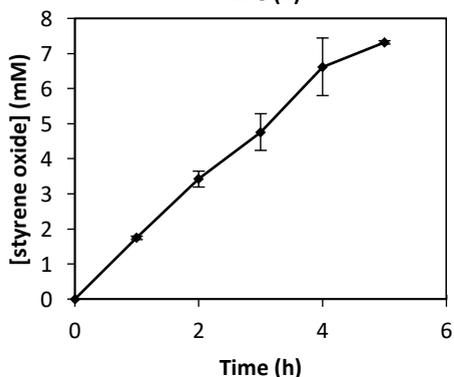
Figure 14. *Ao*FOx-driven oxidation of *cis*-β-methyl styrene (1b) to (1*R*,2*S*)-*cis*-β-methylstyrene (2b) catalysed by r*Aae*UPO.

Conditions: 100 mM potassium phosphate buffer (pH 6.0), 30 °C, [*cis*-β-methyl styrene] = 10 mM, [r*Aae*UPO] = 200 nM, [*Ao*FOx] = 50 nM and [NaHCO₂] = 50 mM
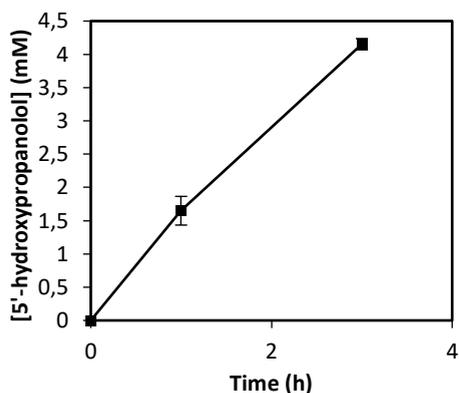
Figure 15. *Ao*FOx-driven oxidation of propranolol (1c) to 5'-hydroxypropranolol (2c) catalysed by SoLo variant.

Conditions: 100 mM potassium phosphate buffer (pH 6.0), 30 °C, [propanolol] = 10 mM, [r*Aae*UPO SoLo] = 50 nM, [*Ao*FOx] = 10 nM and [NaHCO₂] = 75 mM, [ascorbic acid] = 40 mM.

After 3 hours polymerisation product obtained, the reaction has been thus stopped
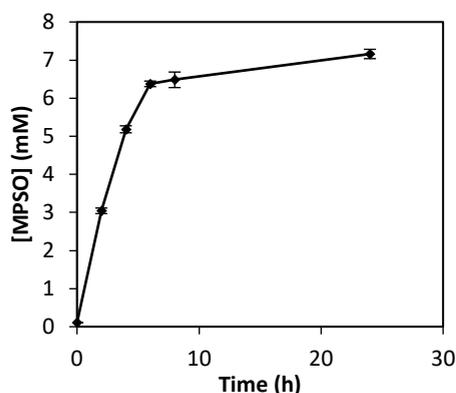
Figure 16. CytC-catalysed sulfoxidation of thioanisole driven by *Ao*FOx

Conditions: 100 mM potassium phosphate buffer (pH 6.0), 25 °C, [thioanisole] = 100 mM, [CytC] = 20 µM, [*Ao*FOx] = 10 nM and [NaHCO₂] = 200 mM, 1%$_{(v/v)}$ DMSO.

4.5.3. Stability AoFOx
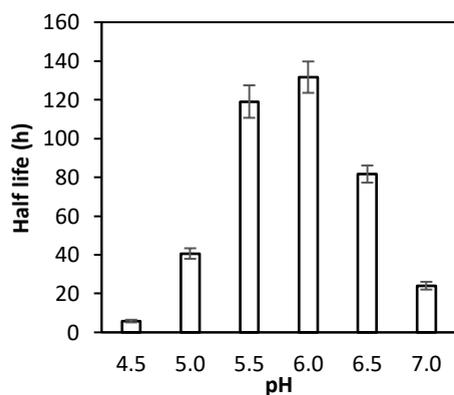
Figure 17. Influence of pH on AoFOx stability Conditions: incubation in 90 mM phosphate buffer (pH 6.0 – 7.0) or acetate buffer (pH 4.5 – 5.5). Residual activities measured with ABTS assay at 420 nm with 1 mM ABTS, 100 mM formate, 10 U mL⁻¹ HRP and 50 µL of enzyme solution in 50 mM acetate buffer (pH 4.5).

Figure 18. Influence of temperature on AoFOx stability Conditions: incubation in 90 mM phosphate buffer (pH 6.0). Residual activities measured with ABTS assay at 420 nm with 1 mM ABTS, 100 mM formate, 10 U mL^{-1} HRP and 50 µL of enzyme solution in 50 mM acetate buffer (pH 4.5).

4.5.4. Semi preparative scale of ethylbenzene hydroxylation

Figure 19. ^{1}H NMR spectrum of isolated (*R*)-1-phenylethanol (400 MHz, DMSO-*d*$_6$) δ 7.39-7.25 (m, 4H), 7.25-7.16 (m, 1H), 5.23 (d, *J* = 4.3 Hz, 1H), 4.71 (dd, *J* = 10.7, 6.3 Hz, 1H), 1.32 (d, *J* = 6.5 Hz, 3H).
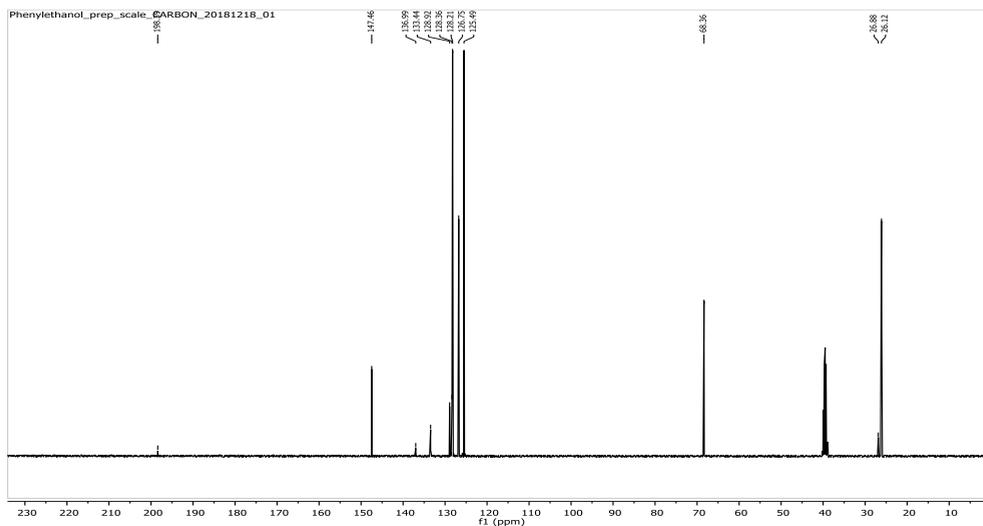
Figure 20. ¹³C NMR spectrum of isolated *(R)*-1-phenlyethanol (101 MHz, DMSO-d$_6$) δ 147.5, 128.2, 126.8, 125.5, 68.4, 26.1.

The semi-preparative scale oxidation of ethylbenzene was performed using a pH STAT titration system (Metrohm). The reaction was performed over 44 h in potassium phosphate buffer (80 mL, 100 mM, pH 6.0, 25 °C) containing ethylbenzene (5 mL), r*Aae*UPO (1.6 μM), *Ao*FOx (166 nM), sodium formate (200 mM). During the reaction, sulfuric acid (1 M) containing sodium formate (200 mM) was titrated to maintain pH 6. After extraction approx. 434 mg (*R*)-1-phenylethanol (containing approx. 13% acetophenone) was obtained. The purity of (*R*)-1-phenylethanol was determined by 1H NMR (97.5% *ee*) (Figure 18).

4.5.5. ¹H and ¹³C NMR spectra of semi preparative scale of bromolactonisation

Figure 21. 5-(Bromomethyl)dihydrofuran-2(3H)-one: ¹H NMR spectrum (400 MHz, Chloroform-*d*) δ 4.68 (tt, *J* = 6.8, 4.9 Hz, 1H), 3.49 (dd, *J* = 4.9, 3.3 Hz, 2H), 2.58-2.42 (m, 2H), 2.35 (m, 1H), 2.02 (m, 1H).

Figure 22. 5-(Bromomethyl)dihydrofuran-2(3H)-one: ¹³C NMR spectrum (101 MHz, Chloroform-*d*) δ 176.4, 77.9, 34.4, 34.4, 28.3, 25.9.

4.6. Materials & Method

100

Chapter 4. Formate oxidase (FOx) from *Aspergillus oryzae*: one catalyst enables diverse H$_2$O$_2$-dependent biocatalytic oxidation reaction

4.6.1. Enzyme preparation

Peroxygenase from *Agrocybe aegerita* (r*Aae*UPO): Two mutants of r*Aae*UPO were used in this study: PaDal (an expression-engineered version of the wild-type enzyme) and SoLo (engineered for the hydroxylation of aromatic substrates). Both mutants were expressed in Pichia pastoris as described previously.[13, 14]

V-dependent haloperoxidase from *Curvularia inaequalis* (*Ci*VCPO): CiVCPO was expressed in *E. coli* as described previously.[40] Cytochrome C (CytC) from Bovine heart and Lipase B from *Candida antarctica* (*Ca*lB) were purchased from Sigma-Aldrich.

Formate oxidase from *Aspergillus oryzae* RIB40 (*Ao*FOx): *Ao*FOx was produced by heterologous expression in *E. coli*, pET21c(+) following a slightly modified protocol.[8, 12] *Ao*FOx was expressed in *E. coli* BL21 (DE3) using TB-media supplemented with ampicillin (100 µg/mL). The main-culture was inoculated to an OD$_{600}$ of approx. 0.05 using the required volume of pre-culture and grown at 37 °C and 180 rpm. When an OD$_{600}$ of 0.6 was reached, IPTG (0.1 mM) was added. After induction, cultures were incubated for an additional 6 h (20 °C, 180 rpm) and afterwards harvested by centrifugation. The obtained cell pellets were washed and suspended in potassium phosphate buffer (50 mM, pH 7.5 with 0.1 mM PMSF). Crude cell extract was obtained by cell disruption using a multi shot cell disruption system. The cleared supernatant was applied onto a HisTrap FF column for further purification of *Ao*FOx using a NGC system (Biorad). An equilibration of the column was performed with potassium phosphate buffer A (50 mM, pH 7.5 with 0.5 M NaCl). A three-step gradient with 5%, 27% and 36% potassium phosphate buffer B (50 mM, pH 8.3 with 0.5 M NaCl and 0.5 M imidazole) was applied for protein elution. Fractions containing *Ao*FOx were pooled and concentrated using Amicon filters (30 kDa cut-off) and desalted using a HiTrap desalting column and potassium phosphate buffer (25 mM, pH 7.5) with a NGC system (Biorad). A protein concentration of 17.3 ± 0.8 mg mL^{-1} was determined by BCA-assay. 67.6% *Ao*FOx purity was determined by SDS-PAGE (**Figure 23**). The absorption spectra showed the characteristic maxima at approx. 360 nm and 472 nm (**Figure 23**). The *Ao*FOx activity was determined via ABTS-

assay using horseradish peroxidase. The ABTS-assay was performed in acetate buffer (50 mM, pH 4.5) containing a diluted sample of purified *Ao*FOx, ABTS (1 mM), horseradish peroxidase (10 U) and sodium formate (100 mM). The absorbance change was followed at 420 nm. Enzyme activity was calculated based on the millimolar extinction coefficient of ABTS at 420 nm (36.0 mM^{-1} cm^{-1}). The *Ao*FOx activity of the preparation was found to be 1642 ± 26 U mL^{-1}, which corresponds to a specific activity of 94.7 U mg^{-1}.
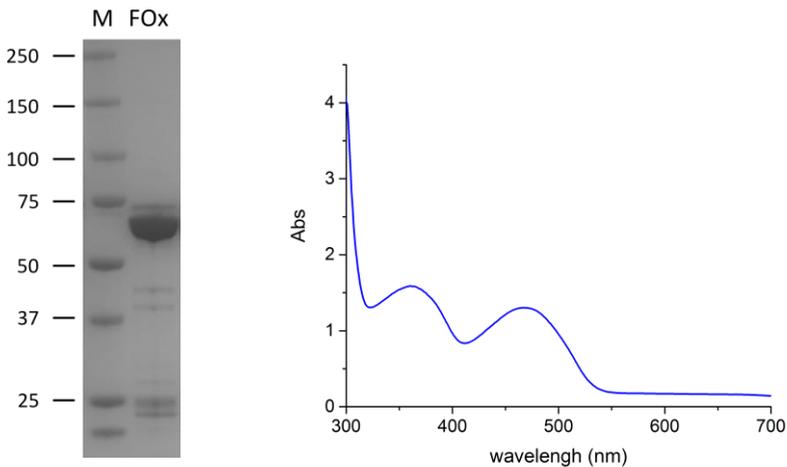
Figure 23. SDS-PAGE (left) and absorption spectra (right) of purified *Ao*FOx. SDS-PAGE was performed in XT MOPS buffer using a Criterion XT 4-12% Bis-Tris precast gel (Biorad). 5 µg total protein after purification (*Ao*FOx) and 5 µl Precision Plus Protein All Blue Standard (M) was loaded after sample pre-treatment. The absorption spectra was recorded of purified *Ao*FOx in potassium phosphate buffer (25 mM, pH 7.5).

4.5.3. Work up and analytical procedures

GC measurements were performed on Shimadzu GC-14A/FID or Shimadzu GC-2010 plus/FID equipped with different columns (**Table 2**). At intervals the reactions were stopped by addition of ethyl acetate containing dodecane (5 mM), 1-octanol (5 mM) or acetophenone (5 mM) as internal standard. After extraction and centrifugation, the organic phase was dried with magnesium sulfate and analysed via gas chromatography (Table S1). All concentrations reported, are based on calibration curves obtained from authentic standards. HPLC measurements were performed on a Shimadzu LC-20 system with a Shimadzu SPD-M20A Photo Diode Array detector using acetonitrile (ACN) and 'water' (containing 5% ACN 0.1% trifluoroacetic acid (TFA)) as mobile phase. The reaction was quantified at 280 nm based on a calibration obtained from authentic standards. NMR spectra were recorded on an Agilent 400 (400 MHz) spectrometer in CDCl3. Chemical shifts are given in ppm with respect to tetramethylsilane. Coupling constants are reported as J-values in Hz.

Chapter 4. Formate oxidase (FOx) from *Aspergillus oryzae*: one catalyst enables diverse H_2O_2-dependent biocatalytic oxidation reaction

Table 5. GC and HPLC analytics

Column	Gradient	Retention time
GC CP-Wax 52 CB (Agilent) (25 m × 0.25 mm × 1.2 μm) carrier gas: N2	150°C hold 2.2 min 25°C/min to 210°C hold 4.2 min 30°C/min to 250°C hold 1.0 min	1.60 min ethylbenzene 7.15 min 1-phenylethanol 5.90 min acetophenone 4.65 min 1-octanol (IS)
GC CP-Wax 52 CB (Agilent) (50 m × 0.53 mm × 2.0 μm) carrier gas: N2	130°C hold 2.2 min 25°C/min to 175°C hold 2.5 min 30°C/min to 250°C hold 1 min	1.48 min ethylbenzene 5.35 min 1-phenylethanol 4.36 min Acetophenone 3.48 min 1-octanol (IS)
GC CP-Chirasil-Dex CB (Agilent) (25 m × 0.32 mm × 0.25 μm) carrier gas: He	120°C hold 2.6 min 15°C/min to 135°C hold 3.3 min 25°C/min to 225°C hold 1.0 min	2.40 min ethylbenzene 6.20 min (R)-1-phenylethanol 6.47 min (S)-1-phenylethanol 4.20 min acetophenone
GC Lipodex E (Macherey-Nagel) (50 m × 0.25 mm × 0.25 μm) carrier gas: He	100°C hold 15.0 min 20°C/min to 220°C hold 1.0 min	5.69 min cis-β-methylstyrene 8.72 min dodecane(IS) 11.23 min (1R,2S)-cis-β-methylstyrene oxide
HPLC Xterra RP18 (Waters) (4.6 × 150 mm, 3.5 μm) flow rate: 1.0 mL/min	isocratic (3-steps): 25%, 4 min hold 50%, 4 min hold 100%, 3 min hold	5.68 min propranolol 4.67 min 5-hydroxy-propranolol
GC Lipodex E (Agilent) (50 m × 0.25 mm × 0.25 μm) carrier gas: He	130°C hold 6.0 min 20°C/min to 200°C hold 5.0 min 25°C/min to 220°C hold 1.0 min	4.2 min thioanisole 4.9 min Dodecane (IS) 11.8 min (S)-methyl phenyl sulfoxide 12.4 min (R)-methyl phenyl sulfoxide
GC CP-Sil 5 CB (50 m × 0.53 mm × 1.0 μm) carrier gas: N2	90°C 2 min hold 25°C/min to 115°C hold 3.5 min 30°C/min to 190°C hold 0.7 min 30°C/min to 320°C hold 0.7 min	2.22 min 4-pentenoic acid 7.59 min Bromolactone 4.19 min acetophenone (IS)
GC CP-Wax 52 CB (Agilent) (25 m × 0.25 mm × 1.2 μm) Carrier gas: N2	110°C hold 3.0 min 20°C/min to 150°C hold 1.0 min 20°C/min to 200°C hold 1.0 min 30°C/min to 250°C hold 3.0 min	8.73 min 1-octanol (IS) 5.75 min styrene 1 0.2 min styrene epoxide
GC CP-Wax 52 CB (Agilent) (50 m × 0.53 mm × 2.0 μm) carrier gas: N2	115°C hold 2 min, 25°C/min to 130°C hold 1.5 min 30°C/min to 150°C hold 0.6 min 30°C/min to 200°C hold 1.4 min 30°C/min to 240°C hold 1.0 min	2.94 min cyclohexanone 4.85 min 1-octanol (IS) 7.64 min ε-caprolactone

4.7. References

1.   Sheldon, R. A.; Pereira, P. C., *Chem. Soc. Rev.* **2017,** *46* (10), 2678-2691.
2.   Ni, Y.; Fernandez-Fueyo, E.; Baraibar, A. G.; Ullrich, R.; Hofrichter, M.; Yanase, H.; Alcalde, M.; van Berkel, W. J. H.; Hollmann, F., *Angew. Chem. Int. Edit.* **2016,** *55* (2), 798-801.
3.   Hollmann, F.; Schmid, A., *J. Inorg. Biochem.* **2009,** *103* (3), 313-315.
4.   Rocha-Martin, J.; Velasco-Lozano, S.; Guisan, J. M.; Lopez-Gallego, F., *Green Chem.* **2014,** *16* (1), 303-311.
5.   Zhang, W. Y.; Burek, B. O.; Fernandez-Fueyo, E.; Alcalde, M.; Bloh, J. Z.; Hollmann, F., *Angew. Chem. Int. Edit.* **2017,** *56* (48), 15451-15455.
6.   Zhang, W. Y.; Fernandez-Fueyo, E.; Ni, Y.; van Schie, M.; Gacs, J.; Renirie, R.; Wever, R.; Mutti, F. G.; Rother, D.; Alcalde, M.; Hollmann, F., *Nat. Catal.* **2018,** *1* (1), 55-62.
7.   Maeda, Y.; Doubayashi, D.; Oki, M.; Nose, H.; Fujii, Y.; Uchida, H., *J. Biosci. Bioeng.* **2009,** *108*, S106-S106.
8.   Maeda, Y.; Doubayashi, D.; Oki, M.; Nose, H.; Sakurai, A.; Isa, K.; Fujii, Y.; Uchida, H., *Biosci. Biotech. Bioch.* **2009,** *73* (12), 2645-2649.
9.   Doubayashi, D.; Ootake, T.; Maeda, Y.; Oki, M.; Tokunaga, Y.; Sakurai, A.; Nagaosa, Y.; Mikami, B.; Uchida, H., *Biosci. Biotech. Bioch.* **2011,** *75* (9), 1662-1667.
10.   Robbins, J. M.; Bommarius, A. S.; Gadda, G., *Arch. Biochem. Biophys.* **2018,** *643*, 24-31.
11.   Robbins, J. M.; Geng, J. F.; Barry, B. A.; Gadda, G.; Bommarius, A. S., *Biochem.* **2018,** *57* (40), 5818-5826.
12.   Robbins, J. M.; Souffrant, M. G.; Hamelberg, D.; Gadda, G.; Bommarius, A. S., *Biochem.* **2017,** *56* (29), 3800-3807.
13.   Molina-Espeja, P.; Garcia-Ruiz, E.; Gonzalez-Perez, D.; Ullrich, R.; Hofrichter, M.; Alcalde, M., *Appl. Environ. Microbiol.* **2014,** *80* (11), 3496-3507.
14.   Molina-Espeja, P.; Ma, S.; Mate, D. M.; Ludwig, R.; Alcalde, M., *Enz. Microb. Tech.* **2015,** *73-74*, 29-33.
15.   de Santos, P. G.; Canellas, M.; Tieves, F.; Younes, S. H. H.; Molina-Espeja, P.; Hofrichter, M.; Hollmann, F.; Guallar, V.; Alcalde, M., *ACS Cat.* **2018,** *8* (6), 4789-4799.
16.   Ullrich, R.; Nuske, J.; Scheibner, K.; Spantzel, J.; Hofrichter, M., *Appl. Environ. Microbiol.* **2004,** *70* (8), 4575-81.
17.   Perez, D. I.; Grau, M. M.; Arends, I. W. C. E.; Hollmann, F., *Chem. Commun.* **2009,** (44), 6848-6850.
18.   Pouvreau, L. A. M.; Strampraad, M. J. F.; Van Berloo, S.; Kattenberg, J. H.; de Vries, S., *Globins and Other Nitric Oxide-Reactive Proteins, Pt A* **2008,** *436*, 97-112.
19.   Zhang, W.; Fernandez-Fueyo, E.; Ni, Y.; van Schie, M.; Gacs, J.; Renirie, R.; Wever, R.; Mutti, F. G.; Rother, D.; Alcalde, M.; Hollmann, F., *Nat. Catal.* **2018,** *1* (1), 55-62.
20.   Zhang, W.; Burek, B. O.; Fernandez-Fueyo, E.; Alcalde, M.; Bloh, J. Z.; Hollmann, F., *Angew. Chem. Int. Edit.* **2017,** *56* (48), 15451-15455.

21.	Peter, S.; Kinne, M.; Ullrich, R.; Kayser, G.; Hofrichter, M., *Enz. Microb. Tech.* **2013,** *52* (6-7), 370-376.

22.	Kluge, M.; Ullrich, R.; Scheibner, K.; Hofrichter, M., *Green Chem.* **2012,** *14* (2), 440-446.

23.	Hollmann, F.; Schmid, A., *J. Inorg. Biochem.* **2009,** *103* (3), 313-315.

24.	Dong, J.; Fernandez-Fueyo, E.; Hollmann, F.; Paul, C. E.; Pesic, M.; Schmidt, S.; Wang, Y.; Younes, S.; Zhang, W., *Angew. Chem. Int. Edit.* **2018,** *57* (30), 9238-9261.

25.	Bjorkling, F.; Frykman, H.; Godtfredsen, S. E.; Kirk, O., *Tetrahedron* **1992,** *48* (22), 4587-4592.

26.	Ma, Y.; Li, P.; Li, Y.; Willot, S. J. P.; Zhang, W.; Ribitsch, D.; Choi, Y. H.; Verpoorte, R.; Zhang, T.; Hollmann, F.; Wang, Y., *ChemSusChem* **2019,** *12* (7), 1310-1315.

27.	Zhou, P.; Wang, X.; Yang, B.; Hollmann, F.; Wang, Y., *RSC Adv.* **2017,** *7* (21), 12518-12523.

28.	Zhou, P.; Lan, D.; Popowicz, G. M.; Wang, X.; Yang, B.; Wang, Y., *Appl. Microbiol. Biotechnol.* **2017,** *101* (14), 5689-5697.

29.	Dong, J. J.; Fernández-Fueyo, E.; Li, J.; Guo, Z.; Renirie, R.; Wever, R.; Hollmann, F., *Chem. Commun.* **2017,** *53* (46), 6207-6210.

30.	Fernandez-Fueyo, E.; van Wingerden, M.; Renirie, R.; Wever, R.; Ni, Y.; Holtmann, D.; Hollmann, F., *ChemCatChem* **2015,** *7* (24), 4035-4038.

31.	Tishkov, V. I.; Popov, V. O., *Biochem.* **2004,** *69* (11), 1252-+.

32.	Bommarius, A. S.; Schwarm, M.; Stingl, K.; Kottenhahn, M.; Huthmacher, K.; Drauz, K., *Tetrahedron: Asymmetry* **1995,** *6* (12), 2851-2888.

33.	Popov, V. O.; Lamzin, V. S., *Biochem. J.* **1994,** *301*, 625-643.

34.	Shaked, Z.; Whitesides, G. M., *J. Am. Chem. Soc.* **1980,** *102* (23), 7104-7105.

35.	Pereira, P. C.; Arends, I. W. C. E.; Sheldon, R. A., *Process Biochem.* **2015,** *50* (5), 746-751.

36.	Ma, Y. J.; Li, P. L.; Li, Y. R.; Willot, S. J. P.; Zhang, W. Y.; Ribitsch, D.; Choi, Y. H.; Verpoorte, R.; Zhang, T. Y.; Hollmann, F.; Wang, Y. H., *ChemSusChem* **2019,** *12* (7), 1310-1315.

37.	Pesic, M.; Willot, S. J. P.; Fernandez-Fueyo, E.; Tieves, F.; Alcalde, M.; Hollmann, F., *Z. Naturforsch., C: J. Biosci.* **2019,** *74* (3-4), 100-103.

38.	Choi, D. S.; Ni, Y.; Fernandez-Fueyo, E.; Lee, M.; Hollmann, F.; Park, C. B., *ACS Cat.* **2017,** *7* (3), 1563-1567.

39.	Churakova, E.; Kluge, M.; Ullrich, R.; Arends, I.; Hofrichter, M.; Hollmann, F., *Angew. Chem. Int. Edit.* **2011,** *50* (45), 10716-10719.

40.	Hasan, Z.; Renirie, R.; Kerkman, R.; Ruijssenaars, H. J.; Hartog, A. F.; Wever, R., *J. Biol. Chem.* **2006,** *281* (14), 9738-9744.

Chapter 5. Formate oxidase (FOx) towards methanol-driven biocatalytic oxyfunctionalisation reactions

Chapter submitted

Chapter 5. Formate oxidase (FOx) towards methanol-driven biocatalytic oxyfunctionalisation reactions

5.1. Introduction

Selective oxyfunctionalisation of C-H-bonds is one of the most challenging reactions in organic chemistry. In recent years, peroxygenases have emerged as promising catalysts for this reaction enabling a broad range of regio- and stereoselective oxyfunctionalisation reactions.[1] Like the well-known P450 monooxygenases[2, 3] peroxygenases utilise a highly oxidised heme-Fe-oxo complex (Compound I) to electrophilically insert an oxygen atom into the starting material. Whereas P450 monooxygenases depend on molecular oxygen and rather complicated electron transport chains to attain the reductive activation of O_2 (yielding Compound I) peroxygenases directly use H_2O_2 for the same goal. Hence, peroxygenases appear as simpler, easier applicable alternatives to P450 monooxygenases. However, as for all heme enzymes, peroxygenases are rapidly inactivated by H_2O_2, necessitating controlled provision with H_2O_2 to balance the H_2O_2-dependent catalytic activity and the (likewise H_2O_2-dependent) inactivation reaction.[4] *In situ* generation of H_2O_2 through catalytic reduction of O_2 is one of the most promising approaches, which, however, also necessitates a sacrificial co-substrate to provide the reducing equivalents needed for the reductive activation of O_2. Envisioning large-scale preparative applications, those H_2O_2 generation systems producing no or innocuous wastes are preferred. Electrochemical generation of H_2O_2, for example, is an attractive means to drive peroxygenase reactions.[5, 6] Simple reductants such as H_2 [7, 8] or H_2O [9] also appear promising. Methanol would be a suitable sacrificial electron donor as it is readily available, easy to handle and, in principle, can be fully oxidised to CO_2 to provide reducing equivalents for 3 equivalents of H_2O_2 per equivalent of MeOH.[10, 11]

5.2. *Ao*FOx oxidation promiscuity applied to r*Aae*UPO oxyfunctionalisation

In the previous chapter, we reported that the formate oxidase from *Aspergillus oryzae* (*Ao*FOx) is an efficient catalyst for the *in situ* generation of H_2O_2 to drive peroxygenase-catalysed oxyfunctionalisation reactions. Encouraged by the very promising results, we originally aimed at a further characterisation of *Ao*FOx. To our surprise, while evaluating methanol as potential co-solvent, we found that *Ao*FOx

also exhibited a methanol oxidase activity. We therefore further investigated *Ao*FOx to drive peroxygenase-catalysed oxyfunctionalisation reactions using either methanol, formaldehyde or formic acid as sacrificial electron donor (**Figure 1**). As production enzyme we chose the recombinant, evolved peroxygenase from *Agrocybe aegerita* (r*Aae*UPO).[12-14]
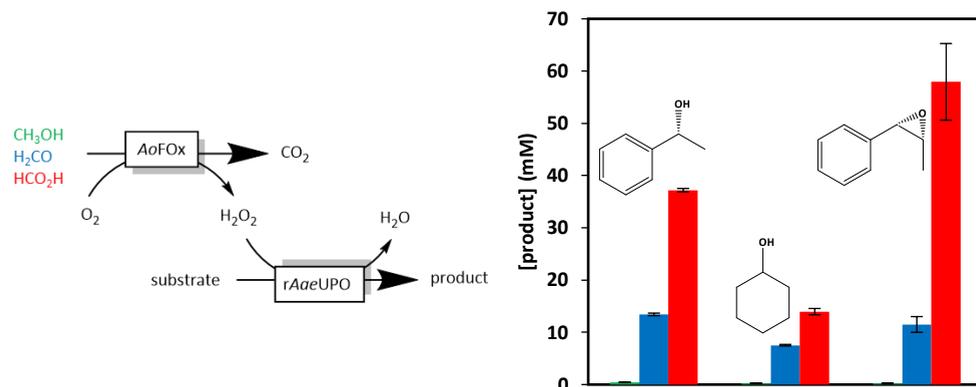
Figure 22. Comparison of r*Aae*UPO formation of (*R*)-phenylethanol, cyclohexanol or cys-β-methylstyrene oxide when either 250 mM methanol, formaldehyde or formate is applied. Conditions: [substrate] = 100 mM, [r*Aae*UPO] = 1 μM, [*Ao*FOx] = 200 nM, 25 °C, 100 mM potassium phosphate buffer (pH 6.0), 600 rpm, 24 h.

For all model reactions investigated (i.e. the hydroxylation of cyclohexane or ethyl benzene as well as the epoxidation of *cis*-ß-methyl styrene) some product accumulation (0.22 mM, 0.21 mM and 0.43 mM of (*R*)-1-phenyl ethanol, cyclohexanol and (1*R,2S)-cis*-ß-methyl styrene oxide, respectively, **Figure 1**) was observed after 24h of incubation of in the presence of 250 mM methanol. Substituting methanol with the same concentration of either formaldehyde of formic acid under otherwise identical conditions resulted in significantly higher product accumulation (**Figure 1**). Apparently, *Ao*FOx exhibits a low, but detectable methanol oxidase activity. Interestingly, *Ao*FOx appeared to be promiscuous with respect to the oxidation state of the C1-substrate but accepted no other starting material such as ethanol or propanol (see 5.8.3).

Chapter 5. Formate oxidase (FOx) towards methanol-driven biocatalytic oxyfunctionalisation reactions

5.3. *Ao*FOx kinetic limitations

Next, we determined the kinetic parameters of *Ao*FOx for the oxidation of methanol and formaldehyde (**Table 1**). Indeed, the catalytic performance of *Ao*FOx on formaldehyde and especially methanol falls back significantly behind its natural formate oxidation activity. Instead of interpreting this as a disadvantage, we rather see the advantage of this relative activity as it, in principle, results in low in situ concentrations of harmful (HCHO) or acidifying (HCO$_2$H) intermediate oxidation states of the sacrificial cosubstrate. However, even the comparably low methanol oxidase activity under saturation conditions corresponds to a specific activity of 0.43 U mg^{-1}, which appeared to us sufficient to evaluate *Ao*FOx with methanol to drive peroxygenase-reactions.

Table 1. Kinetic parameters for the *Ao*FOx-catalyzed oxidation of methanol, formaldehyde and formic acid.
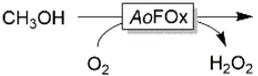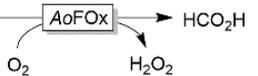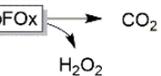
	CH$_3$OH oxidation	H$_2$CO oxidation	HCO$_2$H oxidation[15, 16]
k_{cat} (s^{-1})	0.46 ± 0.02	8.28 ± 0.12	82
K_M (mM)	3300 ± 400	380 ± 16	160

Experimental conditions: [*Ao*FOx] = 42 nM, 25 °C, 50 mM KPi buffer (pH 6.0), [O$_2$] = 0.25 mM (1 atm air), 10 U horseradish peroxidase, [ABTS] = 1 mM (see SI for further details).

5.4. Methanol/*Ao*FOx/r*Aae*UPO robustness

Envisaging robust reaction schemes (i.e. avoiding the *in situ* accumulation of H$_2$O$_2$), we aimed at controlling the *Ao*FOx/r*Aae*UPO activity ratio. Of particular interest were the concentration of methanol and the relative ratio of *Ao*FOx and r*Aae*UPO (**Figure 2**). As expected from the kinetic measurements, increasing the methanol concentration increased the overall product formation, which we attribute to the increasing methanol oxidation rate (**Figure 2**). A methanol concentration around 10% (vol/vol, approx. 2.5 M) appeared optimal. We attribute the decreasing product formation at higher methanol concentrations to a decreasing long-term stability of either *Ao*FOx or r*Aae*UPO (or both) in aqueous methanol solutions. Accumulation of HCHO may also contribute to this observation. We therefore used this methanol

concentration of 2.5 M for further experiments. Under these conditions, *Ao*FOx-catalysed H_2O_2 generation appeared to be still the overall rate-limiting step as further increase of the concentration of *Ao*FOx also lead to increasing product formation rates (**Figure 2**). Equimolar concentrations of *Ao*FOx and r*Aae*UPO gave the highest product concentration after 24 h; time courses of all the reactions were linear highlighting *Ao*FOx rate limitation (**Figure 13**).
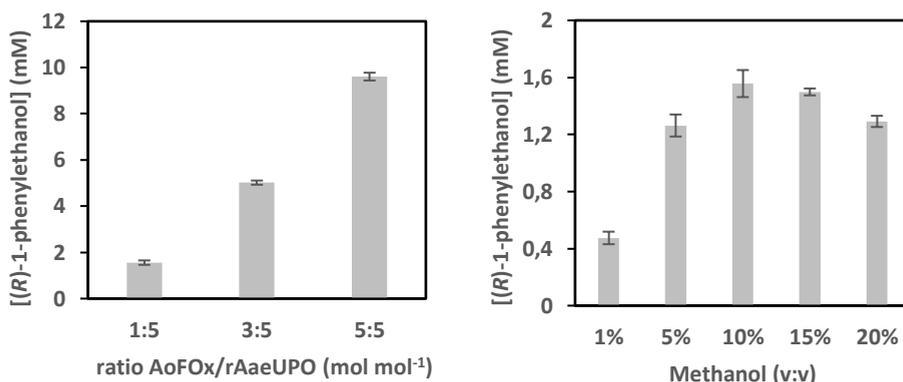
Figure 23. Influence of (left) methanol concentration on product formation over 24 h and (right) *Ao*FOx: r*Aae*UPO ratio on product formation rate. Conditions (unless mention otherwise): 10% (v/v) methanol, [ethylbenzene] = 100 mM, [r*Aae*UPO] = 1 µM, [*Ao*FOx] = 200 nM, 25 °C, 100 mM KPi buffer (pH 6.0), 600 rpm.

As shown in **Figure 3**, robust oxyfunctionalisation of all three model starting materials over at least 5 days could be achieved using methanol as sacrificial electron donor. Very promising turnover numbers for r*Aae*UPO and *Ao*FOx of up to 49,000 were observed (equimolar concentrations of biocatalysts used).
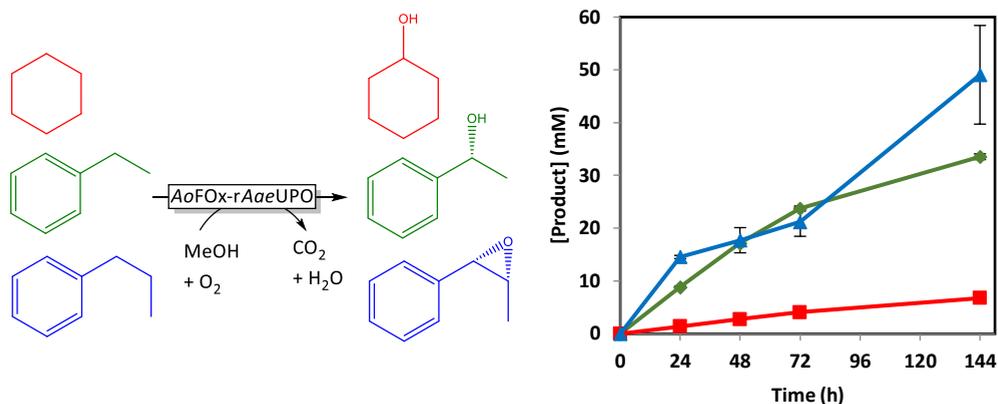
Figure 24. Time-courses of the selective oxyfunctionalization of (●) ethyl benzene, (▲) *cis*-β-methylstyrene and (■) cyclohexane using the MeOH/*Ao*FOx/r*Aae*UPO cascade. Conditions: 10% (v/v) methanol, [substrate] = 100 mM, [r*Aae*UPO] = 1 µM, [*Ao*FOx]= 1 µM, 25 °C, 100 mM KPi (pH 6.0), 600 rpm.

Despite the excellent product formation and catalyst performance, the current, bienzymatic system necessitates rather high methanol concentrations. As a consequence, the overall yield in methanol was only 0.7% (assuming triple oxidation of MeOH).

5.5. Methanol full oxidation to drive r*Aae*UPO hydroxylation

To demonstrate that full oxidation of methanol to CO_2 is feasible we propose that accelerating the first oxidation step may be necessary. In the long-term, improved *Ao*FOx mutants will be used. But for now, we envision that co-catalysis by wild-type alcohol oxidase and *Ao*FOx may be sufficient to provide the proof-of-concept. Therefore, we applied the commercially available alcohol oxidase from *Pichia pastoris* (*Pp*AOx) as co-catalyst to accelerate the first oxidation step (methanol to formaldehyde). Compared to *Ao*FOx, *Pp*AOx exhibited a much lower K_M value for MeOH,[17, 18] which is why high rates for the first oxidation step could be achieved.

As shown in **Figure 4**, under MeOH limiting conditions, using either *Ao*FOx or *Pp*AOx alone lead to the conversion of 0.3 and 1.3 eq. of MeOH, respectively. In the first case, the above-described low activity of *Ao*FOx in the presence of low MeOH concentrations limits the conversion, while in the second case, full conversion of

MeOH does. However, upon combination of both, close to 2.5 eq of MeOH were productively used for the peroxygenase reaction. In other words, using only 5 mM MeOH, more than 12.5 mM of (*R*)-1-phenyl ethanol were produced. This finding corresponds to a 82% yield in methanol.
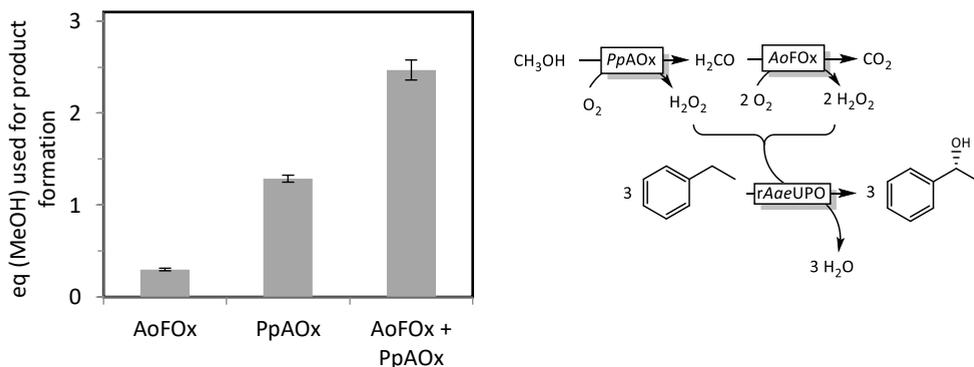
Figure 25. (*R*)-1-phenylethanol formation from 5 mM methanol applying *Pp*AOx, *Ao*FOx, r*Aae*UPO cascade. Conditions: [ethylbenzene] = 100 mM, [r*Aae*UPO] = 100 nM, [*Ao*FOx] = 4 µM, [*Pp*AOx] = 500 nM, 25 °C, 50 mM KPi buffer (pH 6.0), 600 rpm, 64 h.

5.6. Conclusion

Overall, with the current contribution we have demonstrated that methanol-driven peroxygenase reactions are principally possible using just one biocatalyst (*Ao*FOx). At present, the major limitation of this approach is the comparably high K_M value of the wild-type *Ao*FOx for MeOH, which may be addressable through protein engineering. Envisioning preparative-scale applications, further issues are likely to occur such as the poor solubility of O_2 in aqueous media, which we will address by either using non-aqueous reaction media[19, 20] and/or innovative reactor concepts such as the bubble column[21] or flow-chemistry[22] to attain higher k_L values for O_2.

Nevertheless, already at present stage, the catalytic performance of the biocatalysts points towards economically feasible reaction schemes!

5.7. Materials and Methods

5.7.1. Chemicals

Chapter 5. Formate oxidase (FOx) towards methanol-driven biocatalytic oxyfunctionalisation reactions

Ethylbenzene, (*R*)-1-phenylethanol, *cis*-ß-methylstyrene oxide, 1-octanol and dodecane were purchased from Sigma Aldrich. Cyclohexane and cyclohexanol were purchased from Merck KGaA and *cis*-ß-methylstyrene was purchased from TCI Europe. All chemicals were in the highest purity available and used without further purification.

5.7.2. Enzymes

Recombinant evolved unspecific peroxygenase from *Agrocybe aegerita* (r*Aae*UPO) was expressed in *Pichia pastoris* as described previously.[12, 13]

Formate oxidase from *A. oryzae* RIB40 (*Ao*FOx) was produced recombinantly in *E. coli* BL21(DE3) as reported before (Chapter 4)[23] with slight modifications. During the desalting step with HiTrap, an additional buffer exchange was applied by using a phosphate potassium buffer (25 mM, pH 6.0) for elution of the target enzyme of the column. A final protein concentration of 2.16 ± 0.06 mg mL^{-1} was measured by BCA assay. *Ao*FOx purity of approximately 60% was determined by SDS-PAGE (Figure S1). With consideration of the absorption at 472 nm (during measurement of the absorption spectrum) a molar protein concentration of 21 μM was calculated (Figure S1). Enzyme solution in a glass cuvette was measured with an UV-Vis spectrometer (Cary 60 UV-Vis) from 550 to 300 nm with a scan rate of 600 nm min^{-1}. The final concentration was calculated by using the Lambert-Beer equation with an extinction coefficient ε_{420nm} of 10 200 M^{-1}cm^{-1}
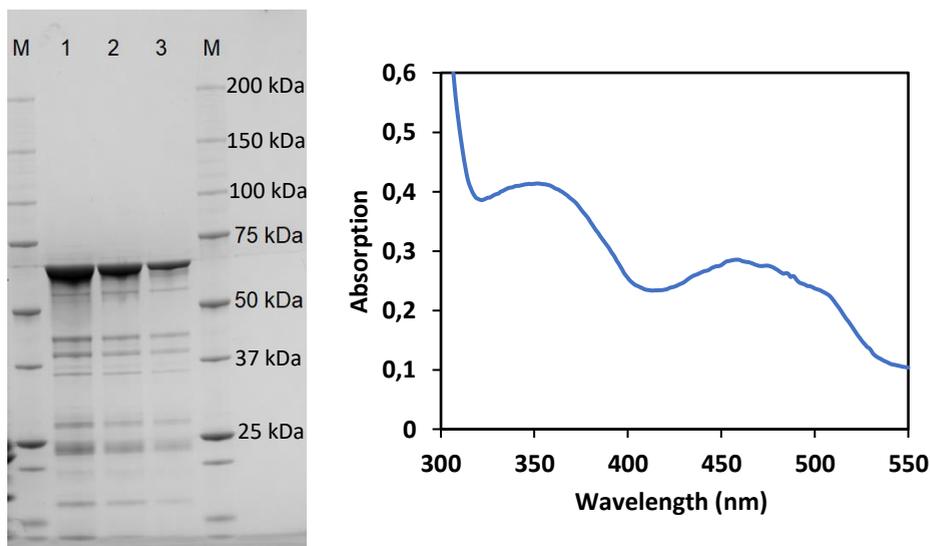
Figure 26. SDS PAGE (left) of purified enzyme solution (lane 1 to 3) and absorption spectrum of purified enzyme solution from 300 to 550 nm (right). M is the reference ladder for the proteins.

5.7.3. Analytics

5.7.3.1. Activity assays

ABTS assays were performed with 50 mM of acetate buffer at pH 4.5 or phosphate buffer at pH 6.0, respectively. A final concentration of 1 mM of ABTS, 10 U mL^{-1} of horseradish peroxidase (HRP) and 100 mM of formate. HRP was stored in 25 mM phosphate buffer (pH 7.5). The reactions were measured with an UV-Vis spectrometer at 420 nm for 1 min at a temperature of 25 °C. For calculation, an extinction coefficient of 36 000 M^{-1}cm^{-1} was used. 1 U of HRP corresponds to the oxidation of 1 µmol ABTS per minute at pH 6.0 and 25 °C.

5.7.3.2. SDS PAGE

Protein samples were diluted with distilled water and mixed with 25 µL staining agent (XT sample buffer 4x) and 5 µL reducing agent (XT reducing agent 20x) to a final volume of 100 µL. After heat incubation the samples were loaded onto the gel. A precast gel was used (XT Criterion 4-12% Bis-Tris) with 1x MOPS buffer as a running

solution. 5 µL of marker solution (Precision Plus ProteinTM Unstained Standard) was applied for every run. As running conditions, a constant voltage of 200 V and a starting current of 165 mA per gel with a running time of 1 h were applied

5.7.3.3. Gas chromatography

Table 2 Applied GC methods

Column	Temperature program	Retention times
CP-Wax 52 CB (Agilent) 25 m – 0.53 mm – 2.0 µm Carrier gas: N_2 Splitless	130 °C hold 2.2 min 25 °C min^{-1} to 175 °C 175 °C hold 2.5 min 30 °C min^{-1} to 250 °C 250 °C hold 1 min	1.8 min ethylbenzene 3.8 min 1-octanol (IS) 4.8 min acetophenone 6.0 min (R)-1-phenylethanol
CP-Chirasil-Dex CB (Agilent) 25 m – 0.32 mm – 0.25 µm Carrier gas: He Split 75	120 °C hold 2.6 min 15 °C min^{-1} to 135 °C 135 °C hold 3.3 min 25 °C min^{-1} to 225 °C 225 °C hold 1 min	6.8 min (R)-1-phenylethanol 7.1 min (S)-1-phenylethanol
CP-Wax 52 CB (Agilent) 25 m – 0.53 mm – 2.0 µm Carrier gas: N_2 Splitless	80 °C hold 3.0 min 5 °C min^{-1} to 90 °C 90 °C hold 2.0 min 20 °C min^{-1} to 140 °C 140 °C hold 2.0 min 30 °C min^{-1} to 230 °C 230 °C hold 1.0 min	7.6 min cyclohexanone 9.2 min cyclohexanol 11.2 min 1-octanol (IS)
Lipodex E (Macherey-Nagel) 50 m – 0.25 mm – 0.25 µm Carrier gas: He Split 100	100 °C hold 15.0 min 20 °C min^{-1} to 220 °C 220 °C hold 1.0 min	5.7 min cis-ß-methylstyrene 8.7 min dodecane (IS) 11.2 min cis-ß-methylstyrene oxide

Gas chromatographs (GCs) from Shimadzu GC-14A/FID or Shimadzu GC-2010 were used for separation of organic compounds in the reaction mixture. Each GC was equipped with an auto injector (AOC-20i) and a FID as a detector. Either nitrogen or helium was used as a carrier gas. For the preparation of the samples, extraction was done with ethyl acetate and 5 mM 1-octanol or dodecane as an internal standard. After centrifugation at 13 000 rpm for 1 min, the organic phase was transferred and dried with $MgSO_4$. For every compound, a calibration curve with 6 points was made.

5.8. Supplementary data

5.8.1. Negative controls

To verify that *Ao*FOx solely catalysed the conversion of methanol, fermentation procedure was repeated as described before with *E. coli* BL21(DE3) with pET22b(+) as an empty vector. After fermentation, cells were disrupted and supernatant and cell debris were collected for negative controls (Figure 6). These were performed using the ABTS assay with acetate buffer (50 mM, pH 4.5) and 10% methanol (v/v) with 50 µL of proteins solution (Figure 6). Additionally, the absorption spectrum from 300 to 800 nm was measured (Figure 7). During the assay, white precipitate was formed over time, probably protein precipitation.
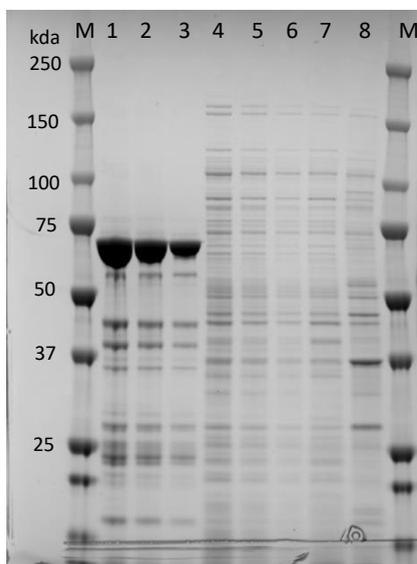
Figure 27. SDS-PAGE with purified *Ao*FOx solution (lane 1 to 3), supernatant of disrupted cells with empty vector (lane 4 to 6) and disrupted cells (lane 7 and 8). M is the reference ladder in kda
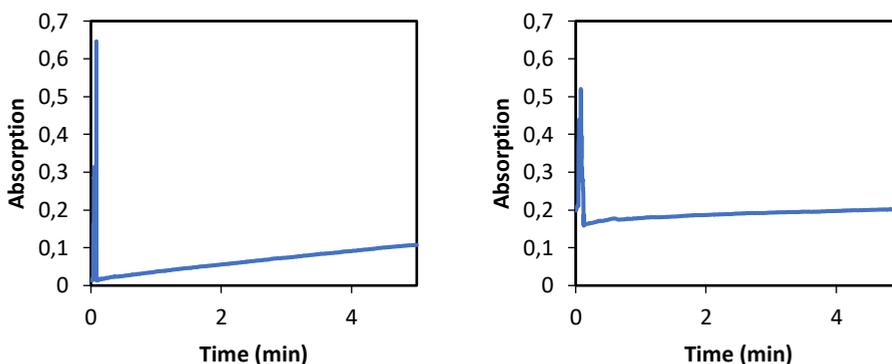
Figure 28. Activity assay supernatant of disrupted cells (A) and cell debris (B) of E. coli pET22b(+). Absorption was measured at 420 nm. Conditions: [ABTS] = 1 mM, 10 U mL^{-1} HRP 10% methanol (v/v) and 50 µL of solution (dilution x4) in acetate buffer (50 mM, pH 4.5). Peaks at the beginning are due to solution mixing.
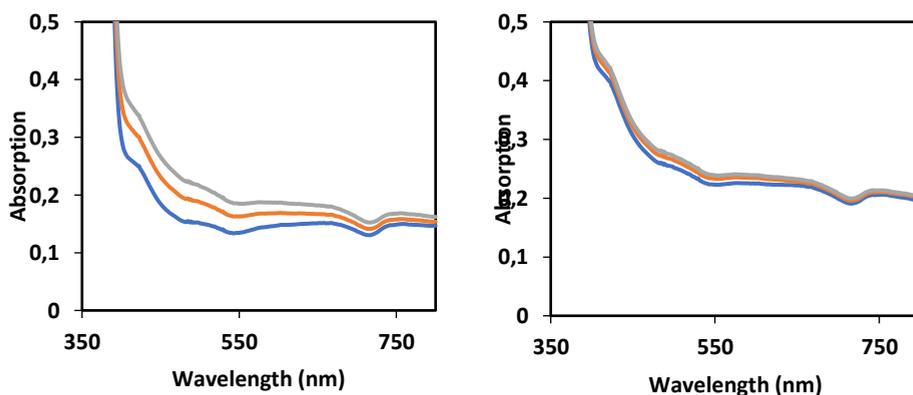
Figure 29. Absorption spectrum from 350 to 800 nm with supernatant of broken cells (A) and cell debris (B) of *E. coli* pET22b(+). Absorption was measured at 420 nm. Conditions: [ABTS] = 1 mM, 10 U mL^{-1} HRP, 10 % methanol (v/v) and 50 µL of solution (dilution 4x) in acetate buffer (50 mM, pH 4.5) at different time points (0 min blue, 2.5 min orange, 5 min grey).

A cascade UPO/supernatant of *E. coli* BL21(DE3) with pET22b(+) empty vector has been also performed. The reaction was carried out with total volume of 200 µL containing 100 mM phosphate buffer (pH 6), 100 mM ethylbenzene, 62.5 mM formate or 2.5 M methanol or 250 mM formaldehyde, 40 µL of supernatant, 1 µM r*Aae*UPO at 25 °C and 600 rpm during 64 h. The (*R*)-1-phenylethanol concentrations

118

obtained from these reactions were 0.12 mM for methanol, 0.03 mM for formaldehyde and 0.05 mM for formate.

5.8.2. Michaelis Menten kinetics
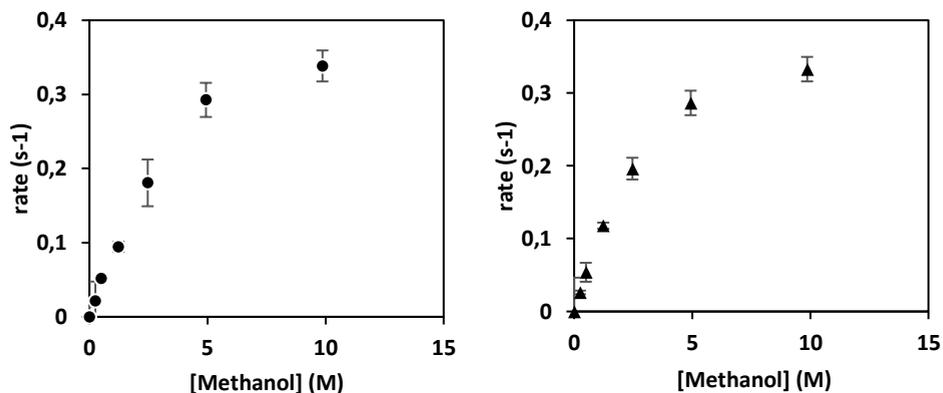
Figure 30. Michaelis Menten kinetics with *Ao*FOx using methanol as a substrate at pH 4.5 (●) and 6.0 (▲). The initial reaction rates were measured at 420 nm using ABTS-assay. Conditions: with 1 mM ABTS, 10 U mL^{-1} HRP and 42 nM of *Ao*FOx, 50 mM sodium acetate pH 4.5 or potassium phosphate pH 6.0 buffer.

.
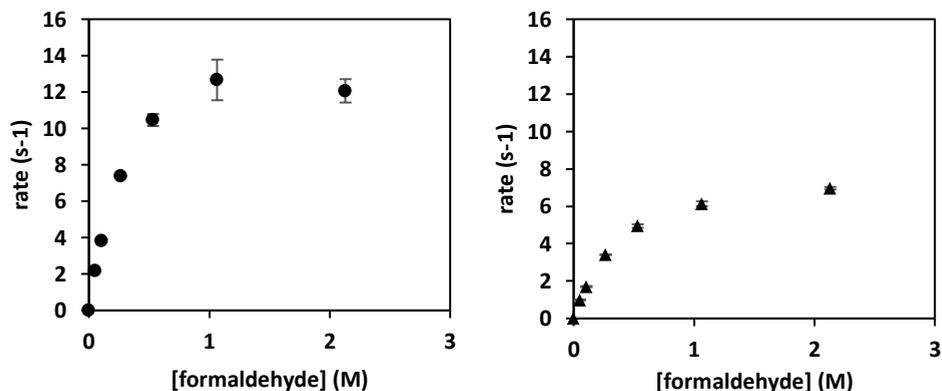
Figure 31. Michaelis Menten kinetics with *Ao*FOx using formaldehyde as a substrate at pH 4.5 (●) and 6.0 (▲). The initial reaction rates were measured at 420 nm using the ABTS Conditions: [ABTS] = 1 mM, 10 U mL^{-1} HRP, [*Ao*FOx] = 42 nM, 50 mM sodium acetate pH 4.5 or phosphate pH 6.0 buffer.

Chapter 5. Formate oxidase (FOx) towards methanol-driven biocatalytic oxyfunctionalisation reactions

Michaelis Menten kinetics were measured for methanol and formaldehyde at two different pH conditions 4.5 and 6.0 using ABTS assay (Figure 9 for methanol and Figure 10 for formaldehyde).

5.8.3. Activity C1-C3 primary alcohol
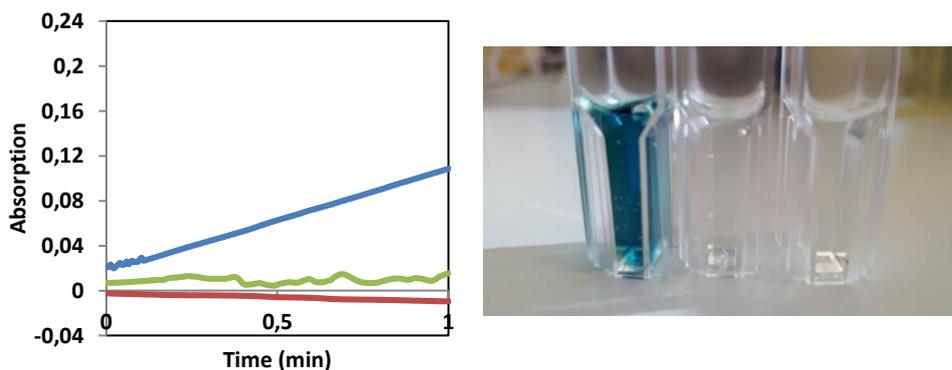
Figure. 32 ABTS activity assay of *Ao*FOx. initial rate measured at 420 nm with methanol (blue), ethanol (red), *n*-propanol (green). On the right picture of 1 h incubation of these activity assays: methanol (left), ethanol (middle), *n*-propanol (right). Conditions: [ABTS] = 1 mM, 10 U mL^{-1} HRP, room temperature (*circa* 20 °C), [*Ao*FOx] = 320 nM, 10% (v/v) alcohol

5.8.4. Time courses of different reaction conditions

For optimization of the two enzymes system with *Ao*FOx and r*Aae*UPO using methanol as a sacrificial donor, temperature, methanol concentration and enzymes ratio were tested. The effect of different methanol concentrations (**Figure 12**) and enzymes ratios (**Figure 13**) were tested directly in 24 h batch reactions in analytical scale.
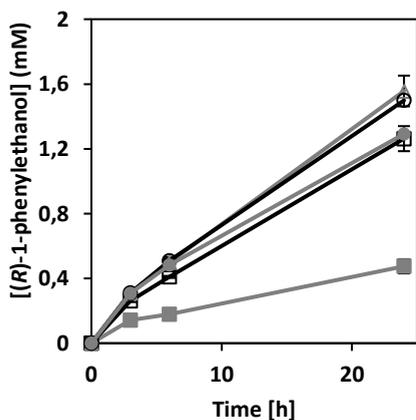
Figure 33. Reaction with AoFOx and rAaeUPO for the conversion of ethylbenzene to (*R*)-1-phenylethanol with different methanol concentrations: 1 (■), 5 (□), 10 (△), 15 (○) or 20 (●) % of methanol (v/v). Conditions: 100 mM phosphate buffer (pH 6.0), [ethylbenzene] = 100 mM, 1-20% (v/v) methanol, [*Ao*FOx] = 200 nM and [r*Aae*UPO] = 1 µM, 25 °C, 600 rpm.
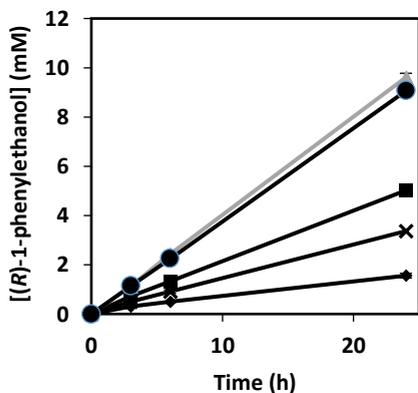
Figure 34. Hydroxylation of ethylbenzene with different *Ao*FOx: r*Aae*UPO ratio: 1 to 5 (♦),3 to 5 (■) and 5 to 5 (▲) as well as 2 to 1 (×) and 5 to 1 (●) (*Ao*FOx to r*Aae*UPO) with lower concentrations. Conditions: 100 mM phosphate buffer (pH 6), [ethylbenzene] = 100 mM, 10% (v/v) methanol, [*Ao*FOx] = 200,600,1000 µM with [r*Aae*UPO] = 1 µM (1:5, 3:5 and 5:5) or [*Ao*FOx] = 600,1 µM and [r*Aae*UPO] = 200 nM (2:1 and 5:1 reactions), 25 °C, 600 rpm.

Chapter 5. Formate oxidase (FOx) towards methanol-driven biocatalytic oxyfunctionalisation reactions

5.9. References

1.   Wang, Y. H.; Lan, D. M.; Durrani, R.; Hollmann, F., *Curr. Opin. Chem. Biol.* **2017,** *37*, 1-9.
2.   Urlacher, V. B.; Girhard, M., *Trends Biotechnol.* **2019,** *37* (8), 882-897.
3.   Fasan, R., *ACS Cat.* **2012,** *2* (4), 647-666.
4.   Burek, B. O.; Bormann, S.; Hollmann, F.; Bloh, J. Z.; Holtmann, D., *Green Chem.* **2019,** *21* (12), 3232-3249.
5.   Lutz, S.; Steckhan, E.; Liese, A., *Electrochem. Commun.* **2004,** *6* (6), 583-587.
6.   Getrey, L.; Krieg, T.; Hollmann, F.; Schrader, J.; Holtmann, D., *Green Chem.* **2014,** *16* (3), 1104-1108.
7.   Karmee, S. K.; Roosen, C.; Kohlmann, C.; Lutz, S.; Greiner, L.; Leitner, W., *Green Chem.* **2009,** *11* (7), 1052-1055.
8.   Freakley, S. J.; Kochius, S.; van Marwijk, J.; Fenner, C.; Lewis, R. J.; Baldenius, K.; Marais, S. S.; Opperman, D. J.; Harrison, S. T. L.; Alcalde, M.; Smit, M. S.; Hutchings, G. J., *Nat. Commun.* **2019,** *10*.
9.   Kim, H. W.; Ross, M. B.; Kornienko, N.; Zhang, L.; Guo, J. H.; Yang, P. D.; McCloskey, B. D., *Nat. Catal.* **2018,** *1* (4), 282-290.
10.   Zhang, W. Y.; Burek, B. O.; Fernandez-Fueyo, E.; Alcalde, M.; Bloh, J. Z.; Hollmann, F., *Angew. Chem. Int. Edit.* **2017,** *56* (48), 15451-15455.
11.   Ni, Y.; Fernandez-Fueyo, E.; Baraibar, A. G.; Ullrich, R.; Hofrichter, M.; Yanase, H.; Alcalde, M.; van Berkel, W. J. H.; Hollmann, F., *Angew. Chem. Int. Edit.* **2016,** *55* (2), 798-801.
12.   Molina-Espeja, P.; Ma, S.; Mate, D. M.; Ludwig, R.; Alcalde, M., *Enz. Microb. Tech.* **2015,** *73-74*, 29-33.
13.   Molina-Espeja, P.; Garcia-Ruiz, E.; Gonzalez-Perez, D.; Ullrich, R.; Hofrichter, M.; Alcalde, M., *Appl. Environ. Microbiol.* **2014,** *80* (11), 3496-3507.
14.   Ulrich, R.; Nuske, J.; Scheibner, K.; Spantzel, J.; Hofrichter, M., *Appl. Environ. Microbiol.* **2004,** *70* (8), 4575-4581.
15.   Robbins, J. M.; Bommarius, A. S.; Gadda, G., *Arch. Biochem. Biophys.* **2018,** *643*, 24-31.
16.   Robbins, J. M.; Souffrant, M. G.; Hamelberg, D.; Gadda, G.; Bommarius, A. S., *Biochemistry* **2017,** *56* (29), 3800-3807.
17.   Liu, Y. P.; Pan, J. F.; Wei, P. L.; Zhu, J. Z.; Huang, L.; Cai, J.; Xu, Z. N., *Biotechnol. Bioprocess Eng.* **2012,** *17* (4), 693-702.
18.   Couderc, R.; Baratti, J., *Agr Biol Chem Tokyo* **1980,** *44* (10), 2279-2289.
19.   Rauch, M. C. R.; Tieves, F.; Paul, C. E.; Arends, I. W. C. E.; Alcalde, M.; Hollmann, F., *ChemCatChem* **2019,** *11* (18), 4519-4523.
20.   Fernandez-Fueyo, E.; Ni, Y.; Baraibar, A. G.; Alcalde, M.; van Langen, L. M.; Hollmann, F., *J. Mol. Catal. B.: Enzym.* **2016,** *134*, 347-352.
21.   Gomes, M. D.; Bommarius, B. R.; Anderson, S. R.; Feske, B. D.; Woodley, J. M.; Bommarius, A. S., *Adv. Synth. Catal.* **2019,** *361* (11), 2574-2581.
22.   van Schie, M. M. C. H.; de Almeida, T. P.; Laudadio, G.; Tieves, F.; Fernandez-Fueyo, E.; Noel, T.; Arends, I. W. C. E.; Hollmann, F., *Beilstein J. Org. Chem.* **2018,** *14*, 697-703.

23.   Tieves, F.; Willot, S. J. P.; van Schie, M. M. C. H.; Rauch, M. C. R.; Younes, S. H. H.; Zhang, W. Y.; Dong, J. J.; de Santos, P. G.; Robbins, J. M.; Bommarius, B.; Alcalde, M.; Bommarius, A. S.; Hollmann, F., *Angew. Chem. Int. Edit.* **2019,** *58* (23), 7873-7877.

Chapter 6. Conclusion

Chapter 6. Conclusion

The use of enzymes as catalysts for selective oxidation, is entering a new area with the availability of active and robust peroxizymes such as unspecific peroxygenases (UPOs) and Vanadium dependent peroxidase (VCPOs).[1] These enzymes can be conveniently stored and produced and only depend on hydrogen peroxide as the oxidant. They are therewith simple and straightforward to be used on large scale. UPOs are very attractive enzymes because they can introduce an oxygen atom selectively in one step in non-activated C-H bonds. A reaction for which still very few selective methods are available.[2-6] The topic of this thesis is finding the best method to supply these promising peroxygenase enzymes with hydrogen peroxide *in-situ* in such a way that it makes them attractive to be used on a large scale.

In enzymatic cascades commonly glucose is used to supply the electrons needed to convert oxygen to hydrogen peroxide. However, we wanted to move from glucose because it is a large molecule that produces gluconic acid as by product. Alternatives such as choline[7] or direct use of a cathode[8, 9] (see chapter 1) have been studied, however in this thesis the focus lies on formic acid as sacrificial reductant because it has high potential to become a cheap and widely available electron carrier. It can act as electron reservoir, simply by coupling sustainable electrons from sun and wind to carbon dioxide.

1. Production of hydrogen peroxide from formic acid

In this thesis, two different strategies to produce peroxide from formic acid for r*Aae*UPO have been explored. Our strategies are compared with similar reported systems,[10-12] and listed in **Figure 1**. The majority of the systems employ formate dehydrogenase from *Candida boidinii* (*Cb*FDH) to produce peroxide, either using flavoenzymes with promiscuous NADH-oxidase activity (**Figure 1 A** and **1 B**) or applying photocatalysts (**Figure 1 C**). Two other systems propose the use of a single catalyst, either a biocatalyst with the formate oxidase from *Aspergillus oryzae* (*Ao*FOx, **Figure 2 A**) or a heterogeneous photocatalyst with graphitic carbonitrile (g-C_3N_4, **Figure 2 B**).

All the systems with *Cb*FDH are suffering from the use of NAD^+. This nicotinamide cofactor is expensive when applied *in vitro* and thus needs to be regenerated *in situ*

by another catalyst and oxidant. Only up to 23 total turnover number (TTN) for NAD^+ could be achieved with these systems. Moreover, the TTN of the biocatalytic partners, *Cb*FDH + NADH-oxidase, are not excelling and lower than that of r*Aae*UPO (**Figure 1 A** and **B**). The replacement of the NADH-oxidase with photocatalysts could not enhance the catalytic performances of the system (**Figure 1 C**). Using a low molecular weight photocatalysts mix came at the cost of low enzymatic stability (chapter 3). Overall, the complexity of these systems, comparable to P450-monooxygenase redox systems found in nature,[13] is not counteracted by outstanding catalytic performances

The last two systems, studied in this thesis, involve a single catalyst to produce H_2O_2 and consequently lead to a simpler system. The g-C_3N_4 photocatalytic system is promising because of the accessibility and simplicity of the catalyst: the calcination of urea is the only step required to produce it. In essence, urine can be used as renewable material.[14] The catalytic performances of r*Aae*UPO are up to 100,000 TTN in both cases. One disadvantage of both systems is the poor conversion of the added formic acid (200 mM formate to obtain 10 to 5 mM of product). However, we foresee that the upscaling of light-driven reaction might be tedious, especially considering light penetration through highly concentrated and dense solutions. The conclusion from this overall comparison is that currently *Ao*FOx represents the best solution for formate driven *in situ* hydrogen peroxide formation in a cascade with peroxizymes.
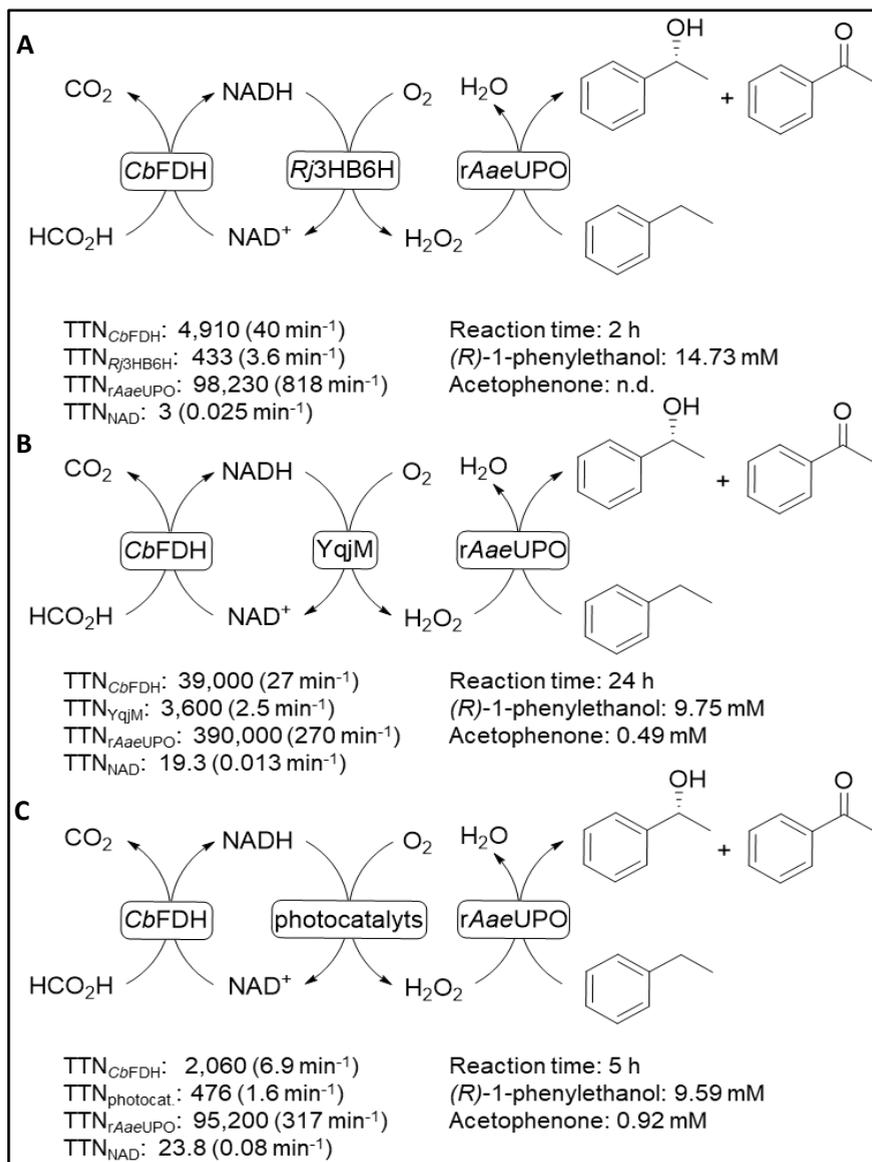
Figure 35 Formic acid driven ethylbenzene hydroxylation reactions by different biocascades comprising *Cb*FDH and NAD⁺ to oxidise formic acid with either (A) *Rj*3HB6H [11] or (B) YqjM [12] or (C) photocatalysts (FMN + methylene blue + phenosafranin) to produce peroxide for r*Aae*UPO from NADH (chapter 3)

Figure 36 Formic acid driven ethylbenzene hydroxylation reactions by different biocascades comprising (A) _Ao_FOx to produce the peroxide for r_Aae_UPO (chapter 4) (B) g-C₃N₄ activated by light to produce the peroxide for r_Aae_UPO[10]

2. _Ao_FOx as the enzyme of choice.

_Ao_FOx shows outstanding performances to promote H_2O_2-dependent enzymes (some examples with TTN>1,000,000) with formate. _Ao_FOx was particularly interesting when coupled with _Cv_CPO and r_Aae_UPO. Initial semi preparative scale experiments already gave significant catalytic performances. _Ao_FOx also catalyses the oxidation of methanol and formaldehyde. Thanks to this promiscuity, the cascade proposed by Ni _et al._[11] for methanol driven oxyfunctionalisation can be greatly simplified, going from 6 components to 3 (Scheme 2). The numbers obtained are promising and raise the question of applicability.

Scheme 3 *Ao*FOx enables simpler cascade for methanol driven oxyfunctionalisation

In order to assess the applicability of formic acid/*Ao*FOX couple to drive oxidations with peroxygenases, various aspects need to be considered. The concept of sustainability generally comprises three different aspects: society, environment and economy (people, planet, profit).[15, 16] The different parameters to be considered in order to perform a full assessment of these three aspects are bountiful. For instance, to correctly assess the environmental impact, a full life-cycle analysis should be done.[17] In this section we will perform a preliminary analysis by evaluating the industrial and green aspects, using the tools available in literature.

3. Assessment of the industrial potential of the formic acid/*Ao*FOX driven biocatalytic oxidation

For a preliminary economic assessment, the reaction performance of the semi preparative scale synthesis from chapter 4 will be evaluated according to the methodology of Tufvesson *et al.* regardless the market.[18, 19] They approximate the requirements needed for a biocatalytic process depending on the type of industry aimed.

Several numbers are encouraging but not all parameters meet the requirements for application yet. In terms of enzyme productivity, *Cl*VCPO and r*Aae*UPO systems meet requirements for pharmaceuticals (**Table 1**). Both are only 2 to 5 fold away

130

from fine chemistry requirements. In these reactions, the conditions were set to be in favour AoFOx to obtain high TTN. On an analytical scale, by simply changing rAaeUPO: AoFOx ratio to equimolar concentration, up to 125 $kg_{product}kg^{-1}_{enzyme}$ could be obtained (**Table 2**).

Table 6 Performances of semi preparative scale synthesis of 5-(bromomethyl)dihydrofuran-2(3H)-one catalysed by AoFOx/CiVCPO system and (R)-1-phenylethanol catalysed by AoFOx/rAaeUPO from chapter 4 compared to industrial requirements[17, 18]

	CiVCPO AoFOx	rAaeUPO AoFOx	Requirements pharma	Requirements fine chemistry
Biocatalytic yield ($kg_{product}$ kg^{-1}_{enzyme})	23.6	48.4	10-100	100-1000
Reaction yield (%)	75 (a) 50 (b)	7.6	> 90	> 80
Product concentration (g L^{-1})	26.9	4.4 (c)	50-100	100-200

(a) GC yield (b) isolated yield (c) considering total volume organic and aqueous phase

In the case of CiVCPO, the reaction yield and product concentration are close to meet all requirements of pharmaceutical industry. An isolated yield of 50% could be obtained with a product concentration of 26.9 g L^{-1}. To improve the reaction, substrate and product inhibitions have to be considered.[20] By applying a two-phase-system, product concentration is increased while minimising enzyme inhibition to fulfil high yield/conversion.

For rAaeUPO, the numbers are not as satisfying as with CiVCPO. The product concentration is rather low. The system applied was already a two-phase system with the substrate as the organic phase. The product concentration can be increased by increasing enzyme concentration. The low conversion (and consequently yield) is due to the direct application of the substrate as the organic phase. The low conversion can be easily circumvented by reusing the substrate after its distillation.

Overall, the system is not meeting all the industrial requirements yet. However, no extensive optimisation has been performed. Further optimisation, discussed later, can improve the system.

4. Is the formic acid/AoFOx driven biocatalytic oxidation green?

Chapter 6. Conclusion

The following question remains "Is it actually green chemistry?" The production of enzymes is a demanding fermentation process. Tieves *et al.* have calculated the E factor for *Ao*FOx and r*Aae*UPO and Hoefler *et al.* for *Civ*CPO productions.[20, 21] The E factors obtained are tremendously high, over tens of tonnes per kilogram of enzyme produced. This is mainly caused by considering water as waste. And even though these enzymes are highly catalytically active, their impact on the E factor remains important.

When looking at the reactions (**Figure 3**), water from the reaction and from the fermentation constitutes by far the greatest part of the E factor. In the reactions studied, the enzyme concentrations applied were low and working with non-diluted reaction will highly decrease the impact of water on the E factor. Because of poor binding capacity, *Ao*FOx is not fully converting formic acid to carbon dioxide, creating consequently waste. The other components represent only a small part of the E factor. Ethylbenzene, as previously said, can be easily recovered (phase separation + distillation) and reused for the following reaction. Its implication on the E factor can hence be decreased.

The E factor of biocatalysis is highly affected by the enzyme's production. A rather large part of the raw materials applied during the fermentation (carbon and nitrogen source from yeast extract for example) are not ending in the overexpressed enzyme but in the biomass that produce this biocatalyst. This fact highlights the need of applying performant biocatalysts that their TTN will greatly decreased the fermentation impact on the E factor.

However, the E factor is only one indicator. It is lacking the concept of chemical properties of the different waste generated: risk; hazard, etc. Moreover, biomass waste can be reused as feed for other bioprocesses or burnt to retrieve energy. The obtained ashes can be used as fertiliser and a circular process system can be envisaged. Here, the high E factor highlights the need for better enzyme production processes and enhanced catalytic activity to decrease the waste generated.
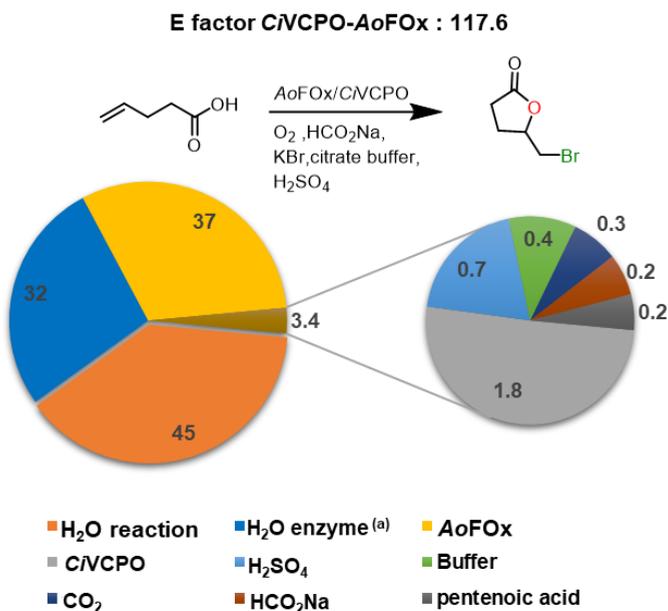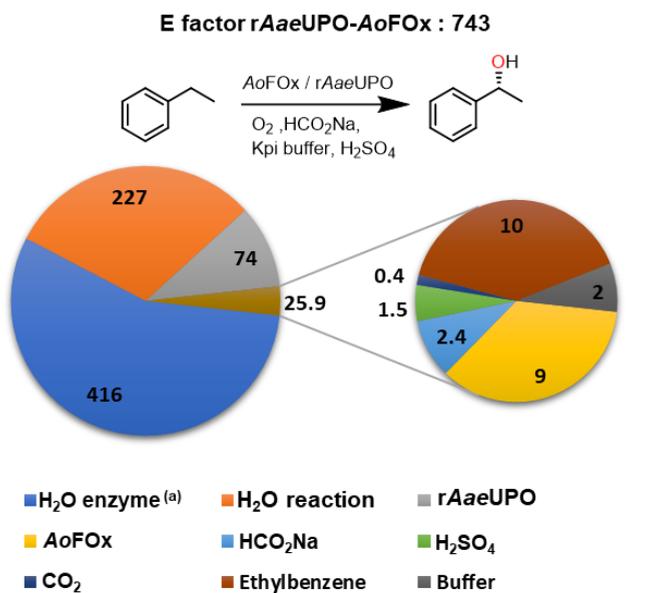
Figure 37 E factor contributions on semi preparative scale reactions of ethylbenzene hydroxylation by *Ao*FOx-r*Aae*UPO and pentenoic acid bromolactonisation by *Ao*FOx-*Ci*VCPO from chapter 4 (a) water waste produced by fermentation and purification (heat purification for *Ci*VCPO and His-trap purification for *Ao*FOx)

Chapter 6. Conclusion

During the reactions, CO_2 as greenhouse gas, is directly produced. These questions the inherent sustainability of our method. The connected impact on the environment will depend on the source of formic acid. Only when the CO_2 comes from a renewable resource, can the cycle be closed. In case formic acid comes from fossil sources it will contribute to the increase of atmospheric CO_2. Moreover, the CO_2 released by the direct formic acid oxidation is lower than the increase of atmospheric CO_2 released by energy consumption.[21] Starting from methanol will also diminish the equivalent of CO_2 produced per synthesised product.

To sum up, *Ao*FOx-*Ci*VCPO/r*Aae*UPO biocascades are on their way to be industrially applicable. By working on optimisation and engineering their productivity and environmental impact could be greatly improved.

4. Future studies

From our preliminary catalytic studies, it can be concluded that *Ao*FOx shows great promise. However, further engineering studies are needed to improve its performance and practical applicability

4.1. Enzyme engineering

The major limitation of *Ao*FOx, on a molecular scale, is its poor binding capacity of the substrates. From pH 4 to 7, the K_M is increasing from 8 mM to over 3 M. The catalytic performances are highly impacted by the pH of the reaction and the initial rates obtained in batch reactors applying formate are 2 to 5 times lower than k_{cat}. Moreover, a large part of formate is not converted during the reaction (only up to 30% conversion). Improving its binding will lead to a more efficient use of this sacrificial reductant while increasing the catalytic performances.

Additionally, if the binding capacity of *Ao*FOx was also improved towards formaldehyde and methanol, ideally only one biocatalyst would be needed for the full oxidation of methanol (**Scheme 1**). By applying methanol as reductant, the pH shift due to formate oxidation will be minimised, consequently ensuring better *Ao*FOx catalytic performance. A slight acidification occurs due to carbonate accumulation.

A rationally evolved *Ao*FOx library is highly needed. Thus, successful mutants of *Ao*FOx could become standards for the formate driven oxidation with peroxizymes.

4.2. Reaction and process engineering

Even with its current poor binding efficiency, AoFOx-r*Aae*UPO/*Cl*VCPO performances are sufficient to be scalable. The catalysed reaction rates are such that the overall system is mass transfer controlled. Mass transfer limitations, especially considering O_2, thus has to be considered and can be tackled. In **Table 2** differently reaction set-ups are compared. In the first case, a round bottom flask was used with a small stirring bar that could not ensure an intensive mixing and the reaction rates and performances where thus lower than at analytical scale. Moreover, the K_M of *Ao*FOx for O_2 is 240 µM, which corresponds approximately to the concentration present in water at room temperature and in presence of 1 atmosphere of air. By switching from air to O_2 gas, the initial production rates could also be increased (**Table 2**).

Table 7 *Ao***FOx-r***Aae***UPO ethylbenzene hydroxylation performances depending on the set up applied**

	Product (g.L^{-1})	Space time yield (g L^{-1} d^{-1})	*Ao*FOx TTN (TF min^{-1})	r*Aae*UPO TTN (TF min^{-1})	Biocatalytic yield (kg$_{product}$ kg^{-1}$_{enzyme}$)
Semi preparative scale (air)	4.4	2.4	219,296 (83)	21,930 (8.3)	48.4
Analytical Scale (air)	0.9	0.9	737,000 (512)	73,200 (51)	158
Autoclave (air)	0.5	6.0	40,800 (340)	4,080 (34)	8.7
Autoclave (2 bar O_2)	1.7	20	136,800 (1140)	13,680 (114)	29.3
Segmented flow (O_2)	3.8	271	61,000 (3000)	30,500 (1500)	46.2

A segmented flow reactor ensures high mass transfer rates thanks to a high interface: volume ratio in combination with an increased O_2 concentration because pure O_2 is applied. In this way up to 50 s^{-1} for *Ao*FOx has been obtained, getting close to k_{cat}. Moreover, the reaction times (less than 1 hour) are such that conditions

applied are focused on rates more than robustness, i.e. pH conditions applied are more acidic to ensure better formate binding. Oher promising reactors that will ensure oxygen mass transfer with no denaturation of enzyme could also be applied.[22-24] In the case of high *Ao*FOx activity, it might not be necessary to purify it to avoid catalase activity of crude extract. The use of crude extract will inherently decrease the E factor and price of *Ao*FOx application.

5. Final conclusion

Decades of researches on FDH prove that it is feasible to drive NADH-dependent redox bio-reactions with formate.[25-27] In this thesis, we especially found one enzyme that is close to enable the formate driven biocatalytic oxidations with peroxizymes, *Ao*FOx. The scope of formate driven biocatalysis is consequently expended. Further research from enzyme engineering to reaction engineering is required to promote *Ao*FOx to industrial application.

Both formic acid as well as methanol can then be used as sacrificial reductants to drive oxyfunctionalisation. *Ao*FOx can then become the enzyme of choice for the highly important and robust peroxygenase enzyme UPO and thus enable the selective biocatalytic production of a wealth of oxidation products within research and industry.

6. References

1.   Burek, B. O.; Bormann, S.; Hollmann, F.; Bloh, J. Z.; Holtmann, D., *Green Chem.* **2019,** *21* (12), 3232-3249.
2.   Trammell, R., *Abstr. Pap. Am. Chem. Soc.* **2017,** *254*.
3.   Dantignana, V.; Milan, M.; Cusso, O.; Company, A.; Bietti, M.; Costas, M., *Acs Central Sci* **2017,** *3* (12), 1350-1358.
4.   Shilov, A. E.; Shul'pin, G. B., *Chem. Rev.* **1997,** *97* (8), 2879-2932.
5.   Wender, P. A.; Hilinski, M. K.; Mayweg, A. V. W., *Org. Lett.* **2005,** *7* (1), 79-82.
6.   Newhouse, T.; Baran, P. S., *Angew. Chem. Int. Edit.* **2011,** *50* (15), 3362-3374.
7.   Ma, Y. J.; Li, P. L.; Li, Y. R.; Willot, S. J. P.; Zhang, W. Y.; Ribitsch, D.; Choi, Y. H.; Verpoorte, R.; Zhang, T. Y.; Hollmann, F.; Wang, Y. H., *ChemSusChem* **2019,** *12* (7), 1310-1315.

8.   Holtmann, D.; Krieg, T.; Getrey, L.; Schrader, J., *Catal. Commun.* **2014,** *51*, 82-85.

9.   Krieg, T.; Huttmann, S.; Mangold, K. M.; Schrader, J.; Holtmann, D., *Green Chem.* **2011,** *13*, 2686.

10.   van Schie, M. M. C. H.; Zhang, W. Y.; Tieves, F.; Choi, D. S.; Park, C. B.; Burek, B. O.; Bloh, J. Z.; Arends, I. W. C. E.; Paul, C. E.; Alcalde, M.; Hollmann, F., *ACS Cat.* **2019,** *9* (8), 7409-7417.

11.   Ni, Y.; Fernandez-Fueyo, E.; Baraibar, A. G.; Ullrich, R.; Hofrichter, M.; Yanase, H.; Alcalde, M.; van Berkel, W. J. H.; Hollmann, F., *Angew. Chem. Int. Edit.* **2016,** *55* (2), 798-801.

12.   Pesic, M.; Willot, S. J. P.; Fernandez-Fueyo, E.; Tieves, F.; Alcalde, M.; Hollmann, F., *Z. Naturforsch. C* **2019,** *74* (3-4), 100-103.

13.   McLean, K. J.; Luciakova, D.; Belcher, J.; Tee, K. L.; Munro, A. W., *Biological Diversity of Cytochrome P450 Redox Partner Systems*. Springer: 2015; Vol. 851, p 299-317.

14.   Zhuang, Q. F.; Guo, P.; Zheng, S.; Lin, Q.; Lin, Y. Y.; Wang, Y.; Ni, Y. N., *Talanta* **2018,** *188*, 35-40.

15.   Sheldon, R. A., *Green Chem.* **2017,** *19* (1), 18-43.

16.   Sikdar, S. K., *AIChE J.* **2003,** *49* (8), 1928-1932.

17.   Tufvesson, L. M.; Tufvesson, P.; Woodley, J. M.; Borjesson, P., *Int J Life Cycle Ass* **2013,** *18* (2), 431-444.

18.   Tufvesson, P.; Lima-Ramos, J.; Nordblad, M.; Woodley, J. M., *Org. Process Res. Dev.* **2011,** *15* (1), 266-274.

19.   Tufvesson, P.; Lima-Ramos, J.; Al Haque, N.; Gernaey, K. V.; Woodley, J. M., *Org. Process Res. Dev.* **2013,** *17* (10), 1233-1238.

20.   Höfler, G. T.; But, A.; Younes, S. H. H.; Wever, R.; Paul, C. E.; Arends, I. W. C. E.; Hollmann, F., *Manuscript submitted* **2019**.

21.   Tieves, F.; Tonin, F.; Fernandez-Fueyo, E.; Robbins, J. M.; Bommarius, B.; Bommarius, A. S.; Alcalde, M.; Hollmann, F., *Tetrahedron* **2019,** *75* (10), 1311-1314.

22.   Gomes, M. D.; Bommarius, B. R.; Anderson, S. R.; Feske, B. D.; Woodley, J. M.; Bommarius, A. S., *Adv. Synth. Catal.* **2019,** *361* (11), 2574-2581.

23.   Zhu, Y.; Chen, Q.; Shao, L.; Jia, Y.; Zhang, X., *Reaction Chemistry & Engineering* **2019**.

24.   Pedersen, A. T.; de Carvalho, T. M.; Sutherland, E.; Rehn, G.; Ashe, R.; Woodley, J. M., *Biotechnol. Bioeng.* **2017,** *114* (6), 1222-1230.

25.   Shaked, Z.; Whitesides, G. M., *J. Am. Chem. Soc.* **1980,** *102* (23), 7104-7105.

26.   Binay, B.; Alagoz, D.; Yildirim, D.; Celik, A.; Tukel, S. S., *Beilstein J. Org. Chem.* **2016,** *12*, 271-277.

27.   Gröger, H.; Borchert, S.; Marina Kraußer , M.; Hummel, W., Enzyme-Catalyzed Asymmetric Reduction of Ketones. In *Encyclopedia of Industrial Biotechnology*, 2010; pp 1-16.

Acknowledgments

Acknowledgments

The final piece of my thesis and my journey in TU Delft, the acknowledgments. There will be no order as I am writing with the flow, on the spot. It will also be a strange mix of French and English so don't be afraid if at some points you are not able to understand anymore.

Firstly, I would like to thank Frank who had the crazy idea to hire me while having first hired my girlfriend. We had been through a painful first year but then we managed to complete finish? awesome projects. You show me the excitement of doing research and I hope you will keep this precise excitement all your carees. I hope that one day we could challenge ourselves on Command and Conquer. I would like also to thank Isabel that despite her agendas could always help through her guidance and positivity.

I would like also to acknowledge my student Dat, that gave his best to finish a project within a short amount of time. I wish him the best for his current PhD in the dark city of "Monaco di Bavaria".

Time to thank the metal people. What would have been my PhD without the master of darkness, Maarten. You made my first year of PhD looks like a Waaaaagh! I hope everything is going fine in Scotland and hope to see you soon around a whiskey bottle. Lloyd, you were an amazing lab mate. I had so much fun with you. I hope I will be able to hear a second album soon. Don't forget our fight against the doors!

What would have been my PhD without the technician of the year, Remco. It is true that you were a bit noisy in the office but making it alive and at the end that's how we love you. Take care of yourself and your heart.

The permanent staff Marc, Linda and Laura, not only it was great with you but also outside of work it was always a pleasure to share a beer (or two or three…). Also, many thanks to Stephen that brings his stories and shares a good laugh with. I would like to thank a lot Mieke van der Kooij. You are doing an amazing job and you are also so kind, you are the heart of Biocatalysis. Without you, we are lost.

Luuk and Stefan, it was always a pleasure to talk with you and help each other. It was also great to share time together in USA. Good luck with the end of your thesis and I hope to see you soon. Tiago don't change a bit of you, your energy and smile, our "fight" around money was a life changer in our office. I hope to be able to visit you in Brazil one day, cheers!

Many thanks to the Post-Docs Carolin, Mieke, Sabry, Wuyuan, Elena, Milja, JiaJia, Yan Ni for their help and the moments shared with them (notably during the group weekend). One Italian apart I would like to thank Fabio. We have been through stress together but at the end we hate foam! As for Maarten, what would have been my first year without Jonathan. I am still laughing just by imaging you imitating Marine's laugh or complaining when people are drinking the wrong drink at the wrong time.

It was also great to share moments with Albert, Sam, Xiaomin, Yinqi, Alexandra, Gaurav, Retna, José, Alice. Wish you the best for the time left in Biocatalysis. Many thanks to Hanna, we shared pain and glory through our PhD. Always have a good laugh with you and I hope that we will meet one day with our own doggos!

Without the great living students, it would be not possible to have a good time in the lab.

I would like to acknowledge Pati that more than being a guest or a colleague, is a friend. Talking about quokas, dogs or just freezing 60 litres of enzymes, I had and still have amazing laugh with you. Hopefully we will see each other again. Starting to talk about Iberian Peninsula, thanks to Carmen and Andreas the magician that always bring energy around, even sometimes too much I could take. See you around! Finally, our Queen Laura, I hope I will be able to see you in Basel.

Through her kindness and friendship, Andrada was an amazing colleague and friend. You are always there even if you don't need to. I will always remember our rush on the German highway. See you soon! One major game changer in my PhD was my angry beard, mon chéri, Florian. You taught me a lot; we have been through so many things together. See you in Dusseldorf around a Kölsch or a glass of wine.

142

Curriculum Vitae

Sébastien Jean-Paul Willot was born the 19th of July 1992 in Mulhouse, France where he spent most of his life. He grew up in a small village in the surroundings of Mulhouse and followed general science courses in high school. After passing his "Baccalauréat Générale Scientifique", he decided to stay in Mulhouse to follow bachelor studies specially created for students willing to enter French Engineering School, considered as a better alternative than University cursus to find a job in industry. During the two years of bachelor, the courses were multidisciplinary, from chemistry to mathematics and physics. After two years, he passed a competitive exam to enter one of these engineering schools, he decided to stay again in Mulhouse and enter the chemical engineering school (ENSCMu) to stay close to the great industrial area of Saint-Louis-Basel-Weil am Rhein. In this school he mainly focused on engineering, chemical safety and green chemistry courses. After having discovered pharmaceutical and fine chemistry companies by doing internship for DSM and Roche, he knew he wanted to continue in this direction. Therefore, betting on biocatalysis to grow exponentially in chemical industries, he decided to follow his companion in life and do a PhD with Dr. Hollmann in the Netherlands.

List of publications

S.J.-P. Willot, M.D. Hoang, C.E. Paul, M. Alcalde, I.W.C.E. Arends, A.S. Bommarius, B. Bommarius, F. Hollmann, FOx News: Towards Methanol-driven Biocatalytic Oxyfunctionalisation Reactions. ChemCatChem. **2020**; doi:10.1002/cctc.202000197

Y.Ma, Y. Li, S. Ali, P. Li, W. Zhang, M.C.R. Rauch, S.J.-P. Willot, D. Ribitsch, Y.H. Choi, M. Alcalde, F. Hollmann, Y. Wang. Natural Deep Eutectic Solvents as Performance Additives for Peroxygenase Catalysis. *ChemCatChem*. **2019**, doi:10.1002/cctc.201901842 .

F. Tieves, S. J.-P. Willot, M. M. C. H. van Schie, M. C. R. Rauch, S. H. H. Younes, W. Zhang, J. Dong, P. Gomez de Santos, J. M. Robbins, B. Bommarius, M. Alcalde, A. S. Bommarius, F. Hollmann. Formate Oxidase (FOx) from Aspergillus oryzae: One Catalyst Enables Diverse H2O2-Dependent Biocatalytic Oxidation Reactions. *Angew. Chem. Int. Ed.* **2019**, *58*, 7873.

Y. Ma, P. Li, Y. Li, S. J.-P. Willot, W. Zhang, D. Ribitsch, Y. H. Choi, R. Verpoorte, T. Zhang, F. Hollmann, Y. Wang. Natural Deep Eutectic Solvents as Multifunctional Media for the Valorization of Agricultural Wastes. *ChemSusChem,* **2019**, *12*, 1310.

S.J.-P. Willot, E. Fernández-Fueyo, F. Tieves, M. Pesic, M. Alcalde, I.W.C.E. Arends, C.B. Park, Frank Hollmann Expanding the Spectrum of Light-Driven Peroxygenase Reactions. *ACS Catalysis,* **2019** *9* (2), 890-894.

S.J.-P. Willot, F. Tieves, M. Girhard, V.B. Urlacher, F. Hollmann, G. de Gonzalo, P450BM3-Catalyzed Oxidations Employing Dual Functional Small Molecules. *Catalysts,* **2019**, *9*, 567.

M. Pesic, S.J.-P. Willot, E. Fernández-Fueyo, F. Tieves, M. Alcalde, F. Hollmann. Multienzymatic in situ hydrogen peroxide generation cascade for peroxygenase-catalysed oxyfunctionalisation reactions. Zeitschrift für Naturforschung C, **2018**, 74(3-4), 101-104.